University of Alberta

Molecular Characterization of Human Adult Anterior Segment Expressed Genes

by

James Samuel Friedman

A thesis submitted to the Faculty of Graduate Studies and Research in partial fulfillment

of the requirements for the degree of Doctor of Philosophy

in

Medical Sciences- Ophthalmology

Edmonton, Alberta

Fall 2002

National Library of Canada
Acquisitions and Bibliographic Services
395 Wellington Street
Ottawa ON K1A 0N4
Canada

Bibliothèque nationale du Canada
Acquisitions et services bibliographiques
395, rue Wellington
Ottawa ON K1A 0N4
Canada

Your file Votre référence

Our file Notre référence

The author has granted a non-exclusive licence allowing the National Library of Canada to reproduce, loan, distribute or sell copies of this thesis in microform, paper or electronic formats.

L'auteur a accordé une licence non exclusive permettant à la Bibliothèque nationale du Canada de reproduire, prêter, distribuer ou vendre des copies de cette thèse sous la forme de microfiche/film, de reproduction sur papier ou sur format électronique.

The author retains ownership of the copyright in this thesis. Neither the thesis nor substantial extracts from it may be printed or otherwise reproduced without the author's permission.

L'auteur conserve la propriété du droit d'auteur qui protège cette thèse. Ni la thèse ni des extraits substantiels de celle-ci ne doivent être imprimés ou autrement reproduits sans son autorisation.

0-612-81190-5

Canada

University of Alberta

Library Release Form

Name of Author: James Samuel Friedman

Title of Thesis: Molecular Characterization of Human Adult Anterior Segment Expressed Genes

Degree: Doctor of Philosophy

Year this Degree Granted: 2002

Permission is hereby granted to the University of Alberta Library to reproduce single copies of this thesis and to lend or sell such copies for private, scholarly or scientific research purposes only.

The author reserves all other publication and other rights in association with the copyright in the thesis, and except as herein before provided, neither the thesis nor any substantial portion thereof may be printed or otherwise reproduced in any material form whatever without the author's prior written permission.

James Friedman

95 Quesnell Cres.
Edmonton, Alberta
Canada
T5R-5N8

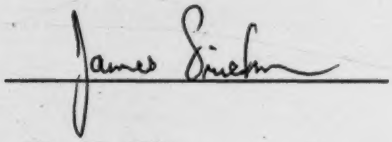

May 29, 2002

What is a scientist after all? It is a curious [person] looking through a keyhole, the keyhole of nature, trying to know what's going on.

--Jacques Cousteau, Christian Science Monitor 21 Jul 71

University of Alberta

Faculty of Graduate Studies and Research

The undersigned certify that they have read, and recommend to the Faculty of Graduate Studies and Research for acceptance, a thesis entitled Molecular Characterization of Human Adult Anterior Segment Expressed Genes submitted by James Samuel Friedman in partial fulfillment of the requirements for the degree of Doctor of Philosophy in **Medical Sciences- Ophthalmology**.

Dr. Michael A. Walter, Supervisor

Dr. Roseline Godbout

Dr. Rachel Wevrick

Dr. D. Alan Underhill

Dr. Stanislav I. Tomarev, External

Date: May 22, 2002

Abstract:

Overall, my work has been to identify novel genes expressed in the iris of the human eye and to characterize them. As a starting point, I was able to use human adult iris total RNA obtained from our collaborator, Dr. Vincent Raymond. I made a cDNA library from this material. The iris cDNA library is a collection of DNA that may be considered a representation of the expressed genes in that particular tissue. To identify genes that may be important for eye structure or function, I performed two different types of screens on my iris library.

In my first analysis, I performed a differential selection screen searching for cDNAs that were either more highly expressed in iris than lymphoblast or, alternatively, more highly expressed in trabecular meshwork than either iris or lymphoblast. Of the ten novel sequences I identified, I focussed on one cDNA that we named Oculoglycan, now named Opticin. I have characterized the Opticin gene and determined where Opticin protein localizes in the human eye. In association with our collaborators, we have screened Opticin as a candidate gene for glaucoma and age-related macular degeneration. Of the alterations observed, one potentially causes a more severe phenotype in an age-related macular degeneration patient than his siblings. I further tested one alteration isolated in this screen for gross changes in migration on polyacrylamide gels.

The second screen I performed was to identify genes both highly expressed in the iris and conserved between species. From this work I isolated a novel ubiquitin-like gene,

UBL5 and characterized it. Although UBL5 may be considered a ubiquitin-like gene, I determined that it did not appear to function in the same manner as other ubiquitin-like genes.

As a whole, my work has expanded the number of characterized genes expressed in the anterior segment of the eye. One gene I characterized, Opticin, is potentially a modifier of age-related macular degeneration.

Acknowledgements:

I would like to thank many people for their help and assistance throughout my degree. I would first like to thank my supervisor, Dr. Michael Walter, and the Chair of Ophthalmology, Dr. Ian MacDonald, for their constant encouragement and support. The 'warm and friendly' lab environment that exists in the Ocular Genetics Lab is very much influenced by their example. Thanks also go to my committee members for their critical comments and advice. I would like to thank members of the Ocular Genetics lab, past and present, for their camaraderie and advice on things both work-related and not so work-related. I would also like to thank members of the Department of Medical Genetics for their friendship and assistance. I'd lastly like to thank my family, immediate and extended, for their love and encouragement. My journey was more easily travelled because of them.

Table of Contents:

CHAPTER I: INTRODUCTION 1

CHAPTER 1A: EYE STRUCTURE AND FUNCTION- A BRIEF OVERVIEW 2

CHAPTER 1B: GLAUCOMA- ONE EXAMPLE OF OCULAR DISEASE 10

PRIMARY GLAUCOMAS: 15

GLC1A (TIGR/MYOC) 15

TIGR AND METABOLIC INTERFERENCE 20

TIGR and Phenotypic Variability 21

GLC1B 22

GLC1C 22

GLC1D 23

GLC1E (OPTN) 24

GLC1F 26

CONGENITAL GLAUCOMAS: 28

GLC3A (CYP1B1) 28

GLC3B 32

SECONDARY GLAUCOMA/DEVELOPMENTAL GLAUCOMA 34

PAX-6 34

Axenfeld-Rieger Malformations 36

Axenfeld-Rieger Syndrome, additional locus 38

Pigment Dispersion Syndrome (PDS) 39

Pseudoexfoliation of the Lens 41

CHAPTER 1C: AGE-RELATED MACULAR DEGENERATION (AMD)- A SECOND EXAMPLE OF OCULAR DISEASE....44

VMD2 as a candidate gene for AMD....45

ARMD1....46

AMD Susceptibility Loci....46

ABCR/ABCA4....47

ABCR/ABCA4 and AMD, Discovery and Controversy....48

RESEARCH PROJECT DESCRIPTION....52

OUTLINE OF EXPERIMENTS PERFORMED I....52

OUTLINE OF EXPERIMENTS PERFORMED II....53

CHAPTER II: CHARACTERIZATION AND GENETIC SCREEN OF A NOVEL IRIS SPECIFIC AND LEUCINE-RICH REPEAT PROTEIN (OCULOGLYCAN/OPTICIN) ISOLATED USING DIFFERENTIAL SELECTION....55

INTRODUCTION:....56

MATERIALS AND METHODS:....58

Preparation of human iris, trabecular meshwork, retina and lymphoblast RNA and construction of adult iris cDNA library:....58

Differential Screen:....59

Polymerase Chain Reaction (PCR) primers:....60

Northern Blot hybridization:....60

Radiation Hybrid (RH) mapping:....61

Computer Based (in silico) Searches:....62

Rapid Amplification of cDNA Ends (RACE):....63

Mouse Sequence cDNA: *63*

Porcine Sequence cDNA: *64*

Reverse Transcriptase-PCR (RT-PCR): *64*

Intron/Exon Boundaries: *65*

Antibody Generation: *66*

Opticin Constructs: *67*

Immunoblot Analysis: *68*

Immunohistochemical Experiments: *70*

RESULTS: 71

DISCUSSION: 109

CHAPTER III: ISOLATION OF A UBIQUITIN-LIKE (UBL5) GENE FROM A SCREEN IDENTIFYING HIGHLY EXPRESSED AND CONSERVED IRIS GENES **118**

INTRODUCTION: 119

MATERIALS AND METHODS: 121

Identification of Iris cDNAs Which Hybridize at High Stringency to a Porcine Anterior Segment Angle Probe: *121*

Elimination of Elongation factor 1-alpha from selected cDNAs: *122*

Northern Blot hybridization: *123*

Computer Based (in silico) Searches: *123*

Intracellular Localization: *124*

Immunoblot Analysis: *125*

RESULTS: 126

DISCUSSION: 143

CHAPTER IV: DISCUSSION AND CONCLUSIONS: **148**

FUTURE DIRECTIONS 153

LAST REMARKS 154

REFERENCES: **156**

APPENDIX A: GENETIC SCREEN OF OPTICIN IN A FRENCH-CANADIAN POPULATION **184**

MATERIALS AND METHODS: 185

Mutational Screening of OPTC: *185*

Polymerase Chain Reaction and DNA sequencing: *186*

AciI restriction enzyme test: *189*

RESULTS: 190

DISCUSSION: 201

CURRICULUM VITAE: **202**

EDUCATION: 202

TRAINING: 202

AWARDS: 203

STUDENTS TRAINED: 203

REFEREED PUBLICATIONS: 204

PUBLICATIONS: CHAPTERS/REVIEWS 204

PUBLICATIONS: ABSTRACTS 205

PUBLICATIONS: ABSTRACTS CON'T 206

List of Tables:

TABLE 1-1: PRIMARY OPEN ANGLE GLAUCOMAS 27

TABLE 1-2: CONGENITAL GLAUCOMAS 33

TABLE 1-3: SECONDARY GLAUCOMAS 42

TABLE 1-4: AGE-RELATED MACULAR DEGENERATION (AMD) LOCI 51

TABLE 2-2: IDENTITY AND PUTATIVE FUNCTION OF TEN NOVEL ISOLATED GENES 78

TABLE 2-3: CHROMOSOMAL LOCALIZATION AND *IN SILICO* EXPRESSION OF KNOWN ISOLATED GENES 79

TABLE 2-4: INTRON/EXON BOUNDARY SEQUENCE OF THE IR185 (OCULOGLYCAN/OPTICIN) GENE 94

TABLE 3-1: GENES ISOLATED FROM A HUMAN ADULT IRIS LIBRARY 131

TABLE 3- 2 INTRON/ EXON BOUNDARY SEQUENCES OF THE UBIQUITIN- LIKE 5 (UBL5) GENE 139

TABLE A-1: SUMMARY OF OPTICIN VARIATIONS DETECTED AMONG VARIOUS PHENOTYPIC GROUPS. 193

TABLE A-2: GENOTYPE/PHENOTYPE CORRELATION FOR OPTICIN ARG229CYS IN AN AMD-AFFECTED FAMILY 199

TABLE A-3: GENOTYPE/PHENOTYPE CORRELATION FOR OPTICIN ARG229CYS IN AN AMD-AFFECTED FAMILY CON'T. 200

List of Figures:

FIGURE 1-1: ANATOMY OF THE EYE. 4

FIGURE 1-2: ANATOMY OF THE ANTERIOR CHAMBER 6

FIGURE 1-3: ANATOMY OF THE RETINA. 8

FIGURE 1-4: SCHEMATIC DIAGRAM OF OPEN-ANGLE AND CLOSED-ANGLE GLAUCOMAS 13

FIGURE 1-5: FREQUENCY AND LOCATION OF TIGR MUTATIONS. 16

FIGURE 1-6: SCHEMATIC DIAGRAM OF THE CYP1B1 GENE. 30

FIGURE 2-1: SCHEMATIC DIAGRAM OF THE DIFFERENTIAL SCREEN USING A HUMAN ADULT IRIS LIBRARY ... 73

FIGURE 2-2: EXAMPLE AUTORADIOGRAPHS FROM THE IRIS DIFFERENTIAL SCREEN 75

FIGURE 2-3: IR185 LOCUS ON HUMAN CHROMOSOME 1 82

FIGURE 2-4: REVERSE TRANSCRIPTASE PCR ANALYSIS OF IR185 (OCULOGLYCAN/OPTICIN) 84

FIGURE 2-5: MULTIPLE TISSUE NORTHERN BLOT ANALYSIS OF IR185 (OCULOGLYCAN/OPTICIN) 86

FIGURE 2-6: EYE NORTHERN BLOT ANALYSIS OF IR185 (OCULOGLYCAN/OPTICIN) 88

FIGURE 2-7: DNA SEQUENCE OF IR185 (OCULOGLYCAN/OPTICIN) 92

FIGURE 2-8: AMINO ACID ALIGNMENT OF OPTICIN WITH CLASS III SLRPS 95

FIGURE 2-9: FOUR SPECIES AMINO ACID ALIGNMENT OF OPTICIN WITH ITS ORTHOLOGS 99

FIGURE 2-10: IMMUNOBLOT ANALYSIS OF OPTICIN 102

FIGURE 2-11: IMMUNOHISTOCHEMISTRY OF THE HUMAN EYE WITH ANTI-OPTICIN ANTIBODY 105

FIGURE 3-1: SCHEMATIC DIAGRAM OF SCREEN FOR HIGHLY EXPRESSED AND CONSERVED GENES 127

FIGURE 3-2: EXAMPLE AUTORADIOGRAPH FROM THE HIGHLY EXPRESSED AND CONSERVED IRIS SCREEN .. 129

FIGURE 3-3: DNA SEQUENCE AND AMINO ACID ALIGNMENT OF UBIQUITIN-LIKE 5 (UBL5) 133

FIGURE 3-4: NORTHERN BLOT ANALYSIS OF UBIQUITIN-LIKE 5 (UBL5) 137

FIGURE 3-5: INTRACELLULAR LOCALIZATION AND IMMUNOBLOT ANALYSIS OF UBIQUITIN-LIKE 5 (UBL5) 141

FIGURE A-1: A SCHEMATIC OF THE HUMAN OPTICIN GENE 191

FIGURE A-2: PEDIGREE OF THE BN FAMILY AFFECTED WITH FOVEOMACULAR DYSTROPHY AND AMD 197

List of Abbreviations:

^{32}P dCTP	radioactive phosphorous isotope 32, deoxycytosine triphosphate
^{33}P dCTP	radioactive phosphorous isotope 33, deoxycytosine triphosphate
ABCA-G	ATP binding cassette subfamily A through G
ABCR	retina specific ABC transporter gene
ADK	autosomal dominant keratitis
AEC	9-amino-3-ethylcarbamazole
ALDH	aldehyde dehydrogenase
AMD	age-related macular degeneration
Apg12	autophagy defective 12
AR	Axenfeld Rieger
ARA	Axenfeld Rieger anomaly
Arg	arginine
ARMD	age-related macular degeneration
arRP	autosomal recessive retinitis pigmentosa
ARS	Axenfeld Rieger syndrome
At	adipose tissue
ATP	adenosine triphosphate
AXPC1	posterior column ataxia with retinitis pigmentosa locus

BAC	bacteria artificial chromosome
BCM	Baylor College of Medicine
BLAST	Basic Local Alignment Search Tool
Bm	bone marrow stroma
Bn	bone
bp	base pairs of DNA
Br	brain
Bs	breast
BSA	bovine serum albumin
CALM2	calmodulin 2
Cb	ciliary body
cDNA	complementary DNA
CHUL	Centre Hospitalier de l'Université Laval
Chx10	ceh-10 homeo domain containing homolog
cM	centiMorgans
cm	centimeters
Co	colon
COT-1	first fraction of reannealed genomic DNA
CYP1B1	cytochrome P450 1B1
Cys	cysteine

DAPI	4',6-diamidino-2-phenylindole/propidium iodide
DEPC	diethylpyrocarbonate
DMEM	Dulbecco's Modified Eagle's Medium
DNA	deoxyribonucleic acid
dpc	days post-coitum
E	glutamate
E	epididymus
EFEMP1	EGF-containing fibulin-like extracellular matrix protein 1
EGR-α	epidermal growth factor-alpha
ELOVL4	elongation of very long chain fatty acids-like 4
EST	expressed sequence tag
F	phenylalanine
F	fibroblast
FBr	fetal brain
FBS	fetal bovine serum
FC	fetal cochlea
Fhe	fetal heart
FK	fetal kidney
FKHL7	forkhead homolog-like 7
FKHR	forkhead in rhabdomyosarcoma

FLS	fetal liver and spleen
Flu	fetal lung
FLv	fetal liver
FOXC1	forkhead box C1
FR	fetal retina
FS	fetal skin
FSp	fetal spleen
Gb	gall bladder
GFP	green fluorescent protein
GLC1	primary open-angle glaucoma loci A-F
GLC2	primary closed-angle glaucoma loci
GLC3	primary congenital glaucoma loci
Gln	glutamine
Glu	glutamate
Go	greater omentum
GPI	glycosylphosphatidyl
GPNMB	glycoprotein (transmembrane) nmb
H_2O	water
H_2O_2	hydrogen peroxide
HBT1	Hub1 target

HCl	hydrochloric acid
He	heart
HEPES	4-(2-hydroxyethyl)-1-piperazineethane sulfonic acid
HIS	histidine
HPE3	holoprosencephaly type three
HRP	horseradish peroxidase
HTM	human trabecular meshwork
I	isoleucine
IGDA	iridogoniodysgenesis anomaly
IGDS	iridogoniodysgenesis syndrome
Ile	isoleucine
IOP	intra-ocular pressure
IPD	iris pigment dispersion
IPTG	isopropylthio-B(beta)-D-galactoside
IRID2	Iridogoniodysgenesis type 2
ISA	iris stromal atrophy
JOAG	juvenile open-angle glaucoma
K	lysine
K	kidney
kb	kilobase

kDa	kilodalton
Ke	keratinoctye
L	leucine
Le	lens
Leu	leucine
LGALS3BP	lectin, galactoside-binding, soluble 3 binding protein
Ll	lymphocytes and lymphokines
LOD	Log of odds
Lu	lung
Lv	liver
Lys	lysine
M	methionine
Met	methionine
ml	milliliter
mm	millimeter
Mm	millimolar
MPS	metallopanstimulin
mRNA	messenger RNA
Mt	mitochondria
Mu	muscle

MYOC	myocillin
N	asparagine
NaCl	sodium chloride
NaOH	sodium hydroxide
NCBI	National Center for Biotechnology Information
Ne	neuroepithelium
NEDD8	neural precursor cell expressed, developmentally down-regulated 8
ng	nanogram
Nr	neuron
NTG	normal tension glaucoma
O	ovary
OD	oculus dexter (right eye)
OHT	ocular hypertension
OPTC	opticin
OPTN	optineurin
OS	oculus sinister (left eye)
OU	oculus uterque (both eyes)
P	proline
Pa	pancreas
PAGE	polyacrylamide gel electrophoresis

PAX-6	paired box 6
PBS	phosphate-buffered saline
PCAG	primary closed-angle glaucoma
PCR	polymerase chain reaction
PDS	pigment dispersion syndrome
pfu	plaque forming units
PIC1	PML (promyelocytic leukemia)-interacting clone 1 (UBL-1)
PITX2	pituitary transcription factor 2
Pl	placenta
pmol	picomoles
POAG	primary open-angle glaucoma
Pr	prostate
PRELP	proline arginine-rich end leucine-rich repeat protein
Pro	proline
PSORT	Prediction of Protein Sorting and Localization Sites
PST	proline/serine/threonine
R	arginine
R	retina
RACE	rapid amplification of cDNA ends
RAGE	rapid amplification of genomic ends

REP-1	rab escort protein 1
RGS-r	retina-specific regulator of G protein signaling
RH	radiation hybrid
Ribo	ribonuclear
RIEG	Rieger
RNA	ribonucleic acid
Rom1	retinal outer segment membrane protein 1
RPE	retina pigment epithelium
RT-PCR	reverse transcriptase polymerase chain reaction
SDS	sodium dodecyl sulfate
Si	small intestine
Sk	skin
SLRP	small leucine-rich repeat proteoglycan
Sm	skeletal muscle
Sp	spleen
SSC	sodium chloride, sodium citrate
STGD	Stargart
SUMO-1	small ubiquitin-related modifier 1
SYDN2	syndecan 2
T	testis

TBST	tris-buffered saline with 0.05% Tween-20
TC	tentative consensus
TCDD	2,3,7,8-tetrachlorodibenzo-p-dioxin
Th	thyroid
Thr	threonine
TIGR	The Institute for Genomic Research
TIGR	trabecular meshwork-induced glucocorticoid response
TIMP2	tissue inhibitor of matrix-metalloproteinase 2
TIMP3	tissue inhibitor of matrix-metalloproteinase 3
TM	trabecular meshwork
TPT1	translationally controlled tumor protein 1
Trp	tryptophan
Ty	thymus
tyrp1	tyrosinase-related protein 1
U	units
U	uterus
UBL	ubiquitin-like
UCRP	ubiquitin cross-reactive protein
Urm1	ubiquitin related modifier
V	valine

VMD2	vitelliform macular dystrophy
WAGR	Wilms tumor--aniridia--genitourinary anomalies--mental retardation syndrome
WT	wild type
x	any amino acid
x-gal	5-bromo-4-chloro-3-indolyl-beta-D-galactoside

Chapter I: Introduction

Portions of this chapter have been published in:

Friedman, J.S. and Walter, M.A. Glaucoma Genetics, Present and Future. (1999) Clinical Genetics. 55:71-79.

Friedman, J.S. and Walter, M.A. Biomedicine. Under Pressure. (2002) Science. 295(5557):983-4.

Sight is probably the most valued of the five senses. The loss of vision through disease affects countless millions worldwide and will become an increasing problem as the world ages. It has been estimated that by the year 2020, the number worldwide of people who are blind will have doubled (1). Two eye-related diseases that are associated with age are glaucoma and age-related macular degeneration (AMD). Both of these diseases have known hereditary components, although not all of the genes involved are currently known. To better understand how these two diseases affect the eye, it is first necessary to briefly describe the tissues of the eye prior to reviewing what is known of the genetics of glaucoma and AMD.

Chapter 1A: Eye Structure and Function- A Brief Overview

The eye can be separated into two parts, the anterior and posterior chambers (Figure 1-1). The anterior chamber comprises several important tissues, which include the cornea, lens and iridocorneal angle of the eye. The cornea is the first and main refractive surface encountered by light. The lens is the next refractive element and a major component of it is made up of crystallin proteins. The iridocorneal angle contains the iris and trabecular meshwork (Figure 1-2). The iris covers part of the lens and, depending on the amount of light required, the iris sphincter opens or closes the pupil of the eye. Adjacent to the iris is the trabecular meshwork, the tressle-like structure through which the aqueous humor passes prior to exiting the eye through Schlemm's canal.

Beside the trabecular meshwork is the ciliary body, which produces the aqueous humor. The largest part of the posterior chamber is taken up by the vitreous, which is made up of several components including hyaluronic acid and several types of collagens. Along the back of the eye is the retina. The retina consists of several layers and many different cell types including rod and cone photoreceptors and retinal ganglion cells (Figure 1-3). The greatest number of cone photoreceptors is located in the macula of the eye, where central vision acuity is located. Age-related macular degeneration first affects this region and can potentially spread to other parts of the retina. Lastly, at the back of the eye is the optic nerve. The optic nerve contains the greatest number of retinal ganglion axons, from which the neuronal signals generated by the retina are passed to the brain. Retinal ganglion cell death is part of the damage caused to the optic nerve from glaucoma.

Figure 1-1: Anatomy of the Eye.

Anatomy of the eye. Adapted from (2).

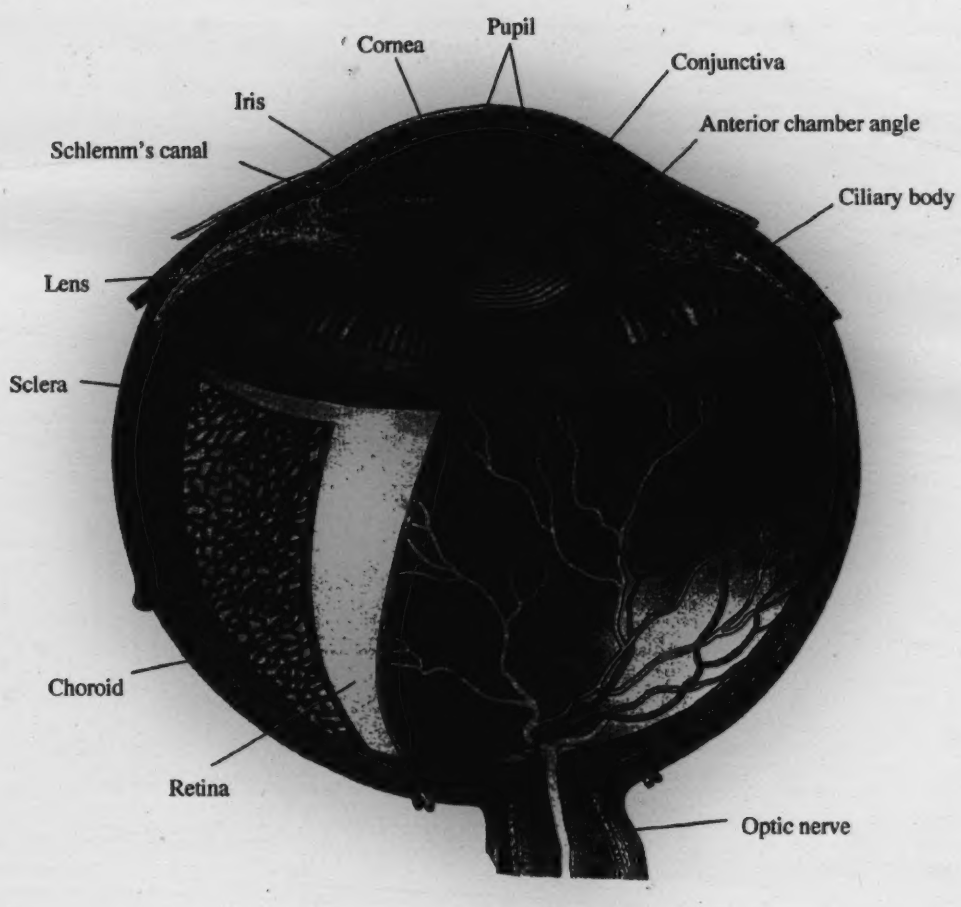
Pupil
Cornea
Conjunctiva
Iris
Anterior chamber angle
Schlemm's canal
Ciliary body
Lens
Sclera
Choroid
Retina
Optic nerve

Figure 1-2: Anatomy of the Anterior Chamber.

Anatomy of the anterior chamber. Adapted from (2).

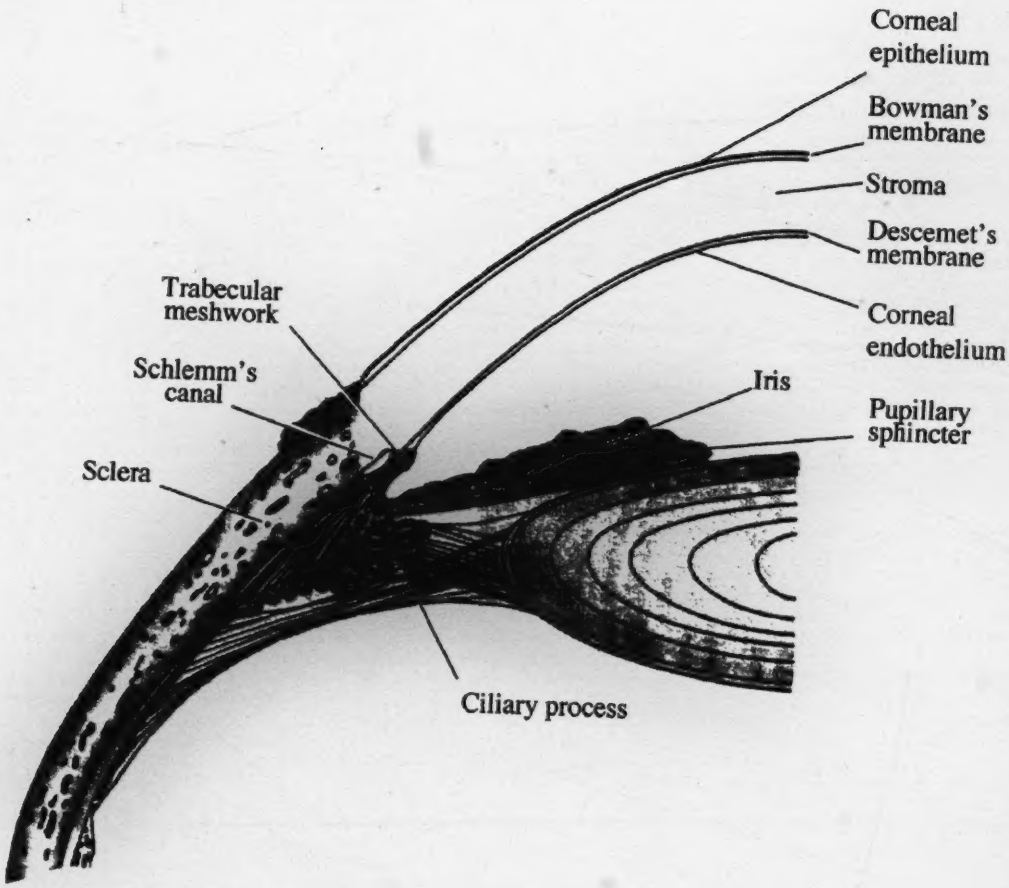
Corneal epithelium
Bowman's membrane
Stroma
Descemet's membrane
Corneal endothelium
Trabecular meshwork
Schlemm's canal
Iris
Pupillary sphincter
Sclera
Ciliary process

Figure 1-3: Anatomy of the Retina.

Anatomy of the retina. Adapted from (3).

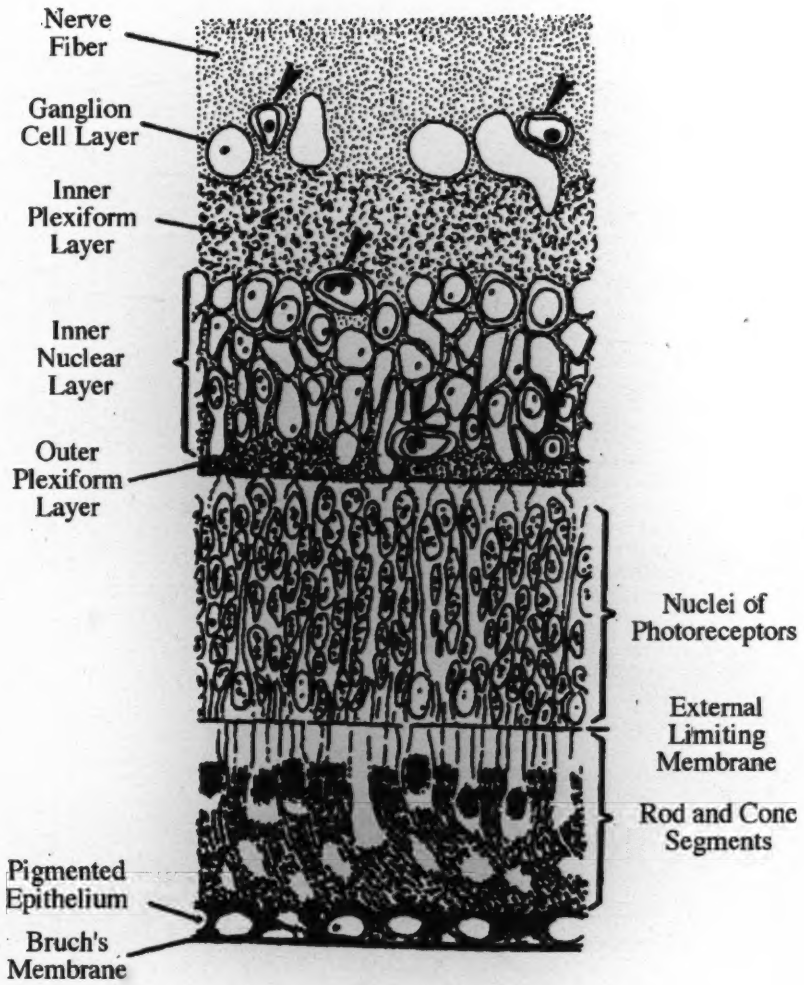
Nerve Fiber
Ganglion Cell Layer
Inner Plexiform Layer
Inner Nuclear Layer
Outer Plexiform Layer
Nuclei of Photoreceptors
External Limiting Membrane
Rod and Cone Segments
Pigmented Epithelium
Bruch's Membrane

Chapter 1B: Glaucoma- One example of ocular disease

Glaucoma is a group of neurodegenerative disorders characterized by the death of retinal ganglion cells and a specific deformation of the optic nerve head, known as glaucomatous cupping. The Canadian National Institute for the Blind has identified glaucoma and macular degeneration as the two leading causes of blindness in Canada. Glaucoma is the primary cause of blindness in Canadians of African descent and the second leading cause in Caucasians. It is predicted that there are at least 67 million people with glaucoma and nearly 6.7 million cases of bilateral blindness caused by glaucoma worldwide (4).

Blindness from glaucoma begins with loss of peripheral vision. Central vision is often maintained until the late stages. By the time the patient notices visual loss, damage to the optic nerve is advanced. In most cases vision loss could have been prevented had glaucoma been detected and treated in time. Although glaucoma is as common as high blood pressure and diabetes, the widespread general public lack of familiarity with it results in thousands of blind patients annually, in whom blindness could have been prevented in many cases. Glaucoma can be successfully treated in the majority of cases with existing drugs or surgery. The key to successful treatment lies in early detection of glaucoma before irreversible optic nerve damage has occurred.

Glaucoma arises as a result of hereditary or non-hereditary means (e.g. trauma). Hereditary forms of glaucoma are grouped into three broad categories: primary, secondary and congenital glaucomas. All three types may in turn be classified as open or closed (narrow-angle), based on the structure of the iridocorneal angle of the eye (Figure 1-4). The iridocorneal angle is comprised of the iris and trabecular meshwork through which the aqueous humor of the eye travels before leaving the eye. Clinical examination of the angle is necessary to determine whether the angle is open or closed. Secondary glaucomas are usually caused by developmental malformations in the eye. The malformations decrease the aqueous outflow of the eye and result in increases of intraocular pressure (IOP) usually associated with glaucoma. The changes seen in secondary glaucomas can also be part of a syndrome with other clinical features. Congenital glaucomas present before three years of age and have been traditionally categorized separately from primary or secondary glaucomas.

The primary method by which glaucoma loci have been identified is through a 'top down' approach. Researchers using this method would first collect families with glaucoma and then examine the association of glaucoma with polymorphic markers through linkage analysis. Once this is complete, the genes within the genetic region associated with glaucoma may be examined as candidate genes for the disorder.

Glaucoma loci have been grouped into three categories for the purposes of genetic nomenclature. GLC1, GLC2 and GLC3 are the prefixes used to refer to primary open

angle glaucomas (POAG), primary closed angle glaucomas (PCAG) and congenital glaucomas, respectively. Each locus discovered is given an alphabetical letter after the GLC prefix. For example, GLC1A and GLC1B were the names assigned to the first two genetic loci identified for POAG.

There are currently eight genes or genetic regions assigned with the GLC nomenclature. Six of these loci are associated with open angle glaucoma (GLC1A-F), while two are of the congenital type (GLC3A and GLC3B). Tables 1-1, 1-2 and 1-3 summarize the primary, secondary and congenital forms of glaucoma, list the genes involved, and give the mapping locations known for these forms of glaucoma.

Figure 1-4: Schematic Diagram of Open-Angle and Closed-Angle Glaucomas.

In open-angle glaucoma the iridocorneal angle appears normal, but adhesions block aqueous flow (arrow). In angle-closure glaucoma, the iridocorneal angle is closed, obstructing the aqueous flow (arrow).

Diagram by Dr. Ian MacDonald (Department of Ophthalmology, University of Alberta. Published in: Glaucoma genetics, present and future. Friedman, J.S. and Walter M.A. (1999) Clin. Genet. 55:71-79.

Open-angle glaucoma

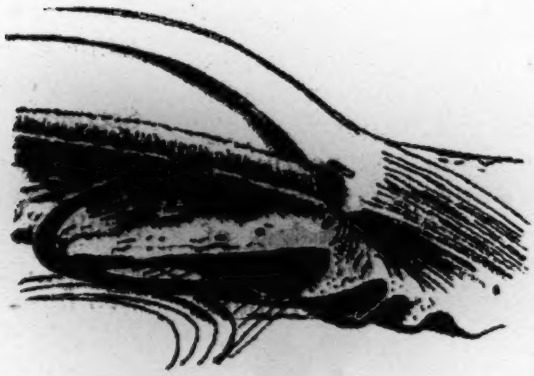

Closed-angle glaucoma

Primary Glaucomas:

GLC1A (TIGR/MYOC)

Juvenile open angle glaucoma (JOAG), an aggressive form of glaucoma, is inherited in an autosomal dominant fashion with an age of onset of less than 40 years. The GLC1A region was originally mapped by Sheffield and co-workers to chromosome 1q21-q31 through linkage analysis (5). The genetic region was later narrowed to a 3 cM region between markers D1S3665 and D1S3664 using additional JOAG families (6). Stone and colleagues identified *myocilin* as the gene mutated in this disorder (7). *Myocilin* (MYOC), also known as trabecular meshwork induced glucocorticoid response protein (*TIGR*) was first isolated by Escribano and co-workers from an ocular ciliary body subtractive cDNA library (8). *TIGR/MYOC* has since been fine-mapped to 1q24.3-q25.2 (9). Mutations in *TIGR/MYOC* constitute about 2-4% of all POAG patients, with the vast majority of changes located in the third exon (Figure 1-5) (10).

The *TIGR/MYOC* gene encodes a 504 amino acid protein. TIGR/MYOC domains consist of a leucine-zipper and an olfactomedin-like domain, at the N and C terminal regions of TIGR/MYOC respectively.

Figure 1-5: Frequency and Location of TIGR Mutations.

Frequency and location of TIGR mutations. Adjusted from (10).

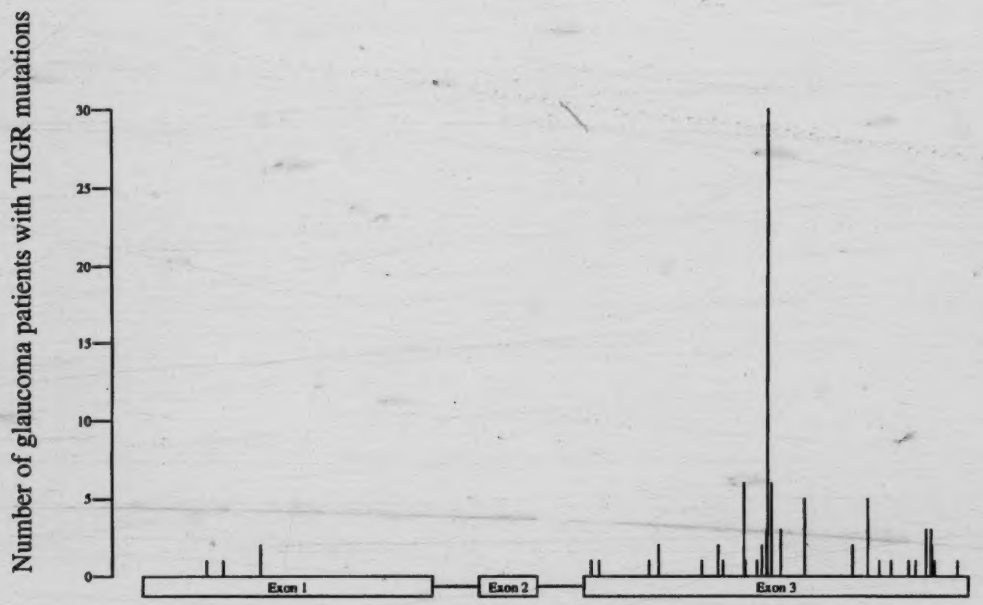

Location of Mutations in TIGR

Within the myosin-like domain is a leucine zipper motif believed to be involved in protein-protein interactions (11,12). The amino acid sequence in the olfactomedin-like domain is homologous to the frog olfactomedin gene (13) and other olfactomedin-related proteins (14) with about 50% similarity (15). Frog olfactomedin has been hypothesized to be involved as an intermediary between odorants and olfactory receptors (13).

TIGR/MYOC gene expression has been observed in a variety of tissues including: trabecular meshwork, iris, ciliary muscle, retina, Schlemm's canal and optic nerve (16-19). TIGR protein has been detected through immunoblot analysis as a 52-57 kDa protein in human iris, ciliary body, trabecular meshwork, cornea, aqueous humor, vitreous and optic nerve (20-23). In trabecular meshwork cell culture and aqueous humor, myocilin was observed as both a 65 kDa and a 55 kDa band (12,24). In cultured trabecular meshwork (TM) or Schlemm's canal (SC) cells, TIGR has been observed in golgi, mitochondria, cytoplasmic filaments, vesicles and golgi (25-27). Additionally, in ascorbate and dexamethasone treated human trabecular meshwork (HTM) cell cultures, TIGR/MYOC protein was determined to be outside of the cells, in the extracellular matrix (28).

The observation that recombinant TIGR protein can be isolated through columns or detected by immunoblot at sizes greater than its known protein size, suggest that the TIGR protein, like olfactomedin, can also form multimers (12,29-31). Recent work with

two hybrid experiments has demonstrated that TIGR/MYOC can bind to itself (31,32) as well as to fibronectin and the myosin regulatory light chain (28,32).

How TIGR/MYOC is involved in the pathogenesis of glaucoma is still unknown. TIGR/MYOC has been observed to be expressed at high levels in anterior segment organ cultures, when these cultures were grown under high pressure conditions (33). The environment used in these experiments was thought to mimic the high intraocular pressure seen in glaucomatous eyes. As TIGR/MYOC was expressed after these organs were treated in this way for an extended time, it led to the suggestion that TIGR/MYOC may be involved in a protective response (33).

Other data can also appear somewhat contradictory. As mentioned above, TIGR protein has been observed in a wide variety of intracellular locations, including mitochondria (27). In another example, overexpressed TIGR/MYOC in organ cultures was reported to generate an increase in outflow (lowering IOP), while bacterially expressed and purified TIGR/MYOC decreased outflow (raising IOP) when injected into organ culture systems (30,34). Recent experiments have suggested that mutant forms of TIGR/MYOC are retained in TM cells, while normal TIGR/MYOC is secreted (30,35). Further work has demonstrated that a truncated version of TIGR/MYOC is present in the detergent insoluble fraction of cell lysates, suggesting that there is a defect in mutant TIGR/MYOC folding (36). Further work will be needed to fully unravel how TIGR/MYOC alterations lead to disease.

TIGR and Metabolic Interference

Morissette and colleagues examined a very large French Canadian pedigree linked to the GLC1A locus and identified the *TIGR* mutation that caused POAG in this family. In one branch of the pedigree, two affected second cousins married and had ten children. Assuming the parents were each heterozygous for the mutation, 75% of their children would, on average, be expected to harbour at least one copy of the mutated *TIGR* gene while 25% would have two copies of the normal *TIGR* allele. If one or more copies of the altered *TIGR* gene causes POAG, then about seven or eight (~75%) of the children would develop POAG, on average. Only two siblings (20%) however, developed glaucoma. A PCR-based test determined that these two siblings and a third sibling all had one normal *TIGR* allele and the mutant *TIGR* allele. The siblings with two mutant *TIGR* alleles did not develop glaucoma (29).

To explain how two mutant alleles may still generate a phenotypically normal product, Morissette and co-workers hypothesized that the *TIGR* gene product may be involved in "metabolic interference" (37). Assuming TIGR protein exists in multimers, homozygous mutant copies of the TIGR protein may still generate a functional product depending on the mutation. Heterozygote copies, on the other hand, may differ in such a way that the activity or structure of the multimeric product is not functional enzymatically or structurally. Further examination of this mutation may lead to a better

understanding of TIGR's activity, as the previously mentioned observations suggest that TIGR protein functions as homodimers or homotetramers.

TIGR and Phenotypic Variability

The family examined by Morissette and colleagues was also reported to have both primary open angle glaucoma (POAG) and JOAG. As mentioned previously, adult onset glaucoma is generally observed in patients after 40 years of age, while juvenile onset is seen before 40 years of age. Using polymorphic markers in the 1q23-q25 region, Morissette and co-workers first examined whether the JOAG/COAG locus was in the same location as the GLC1A. Most of the markers in this region demonstrated linkage with the disorder in a significant manner (LOD > 3). A greater number of markers were used to examine the genetic recombination of this region to find the common interval within the affected individuals. The recombination data was also consistent with the GLC1A locus being the locus responsible for the disease phenotype in this family. The authors concluded that a single mutation in the *TIGR* gene may cause a variety of phenotypes from ocular hypertension (OHT) to JOAG to COAG. They further argued that the variable expressivity between the JOAG and COAG patients may simply be a result of the age at which these two conditions are distinguished from one another (40 years) (38).

The above finding has been controversial as Wiggs and colleagues have argued that the findings of Morissette and co-workers may be due to the variable expressivity of only JOAG and that the GLC1A locus is not a locus for COAG (39). Variable phenotypic expression in glaucoma patients with mutations in the same gene is not limited to the GLC1A locus and has been shown in other genes related to glaucoma including *PAX-6* (40-43) and *PITX2* (44-46). Recent work by Vincent et al. has uncovered that the CYP1B1 gene is a potential modifier of TIGR/MYOC as shall be discussed below.

GLC1B

The GLC1B locus was identified by Stoilova and co-workers in 1996. Affected individuals from six families had adult onset (>40 years of age) glaucoma and low to moderate IOP (low/normal tension). These patients were reported to respond well to medical treatment. The GLC1B locus was restricted to chromosome 2 cen-q13, an 8.5 cM region defined by markers D2S2161 and D2S2264. No gene has yet been identified for this condition (47).

GLC1C

Wirtz and colleagues localized the GLC1C region by linkage analysis of a Caucasian Oregon family. Clinical features included increased intraocular pressure (high tension), visual field loss and/or a cup to disk ratio greater than normal. The average age

of onset was over 40 years therefore classifying GLC1C as an adult onset glaucoma. The GLC1C locus is within an 11.1 cM region on chromosome 3q21-q24, flanked by markers D3S3637 and D3S1744 (48). A novel type I procollagen C-proteinase enhancer protein gene was isolated from the critical region and tested as a candidate gene. However, no mutations were identified (49). A second family, of Greek origin, has recently been linked to this region (50).

GLC1D

Trifan and co-workers used a four generation family to identify the fourth GLC1 locus. The ocular findings in this family included a moderate elevation of IOP with visual field loss occurring past 40 years of age. The GLC1D locus is located within a 6.3 cM region bounded by markers D8S1830 and D8S592. Two candidate genes are *Syndecan2* (*SYDN2*) and *Early Growth Response Gene Alpha* (*EGR-α*). *SYND2* is the core protein of heparin sulphate proteoglycan and is associated with cell surface interactions. *EGR-α* protein may have the potential to regulate transcription levels of some cytrochrome P450 genes. As mutations in a cytochrome P450 gene at the GLC3A locus cause glaucoma (see below), *EGR-α* protein is a potential transcriptional regulator of a glaucoma causing gene. Mutations in *EGR-α* may therefore disrupt the transcription of this gene or a related gene and trigger glaucoma (51). However, to date, no mutations have been found.

GLC1E (*OPTN*)

Sarfarazi and co-workers have reported the GLC1E locus, an adult onset POAG identified from a single large family. The age of diagnosis ranged from 23-65 years of age. Patients were seen with normal ocular tension, high cup to disk ratios, visual field loss and changes of the optic nerve head. The GLC1E locus has been linked to chromosome 10p14-p15, within a 21 cM region defined by markers D10S1729 and D10S1664. After reducing the GLC1E critical region to a length of 5 cM and excluding four other genes, Rezaie and colleagues selected optineurin (*OPTN*) as a candidate gene (52). They found that in members of their pedigree the *OPTN* gene contained a missense mutation that resulted in a Glu50Lys (E50K) amino acid change in the optineurin protein. A broader search of 54 additional adult-onset families with normal to moderately elevated eye pressure uncovered several additional *OPTN* mutations. Alterations observed included an insertion in *OPTN* resulting in a premature stop codon and an Arg545Gln residue change. A "risk associated" Met98Lys change was present in 12.1% of individuals without a family history of glaucoma and in 17.8% of the author's kindreds with glaucoma. The high frequency of the Met98Lys mutation in glaucoma patients was statistically significant, even though the risk-associated change is present in the normal population at a frequency of about 2%. The authors detected expression of *OPTN* mRNA and protein in the tissues of healthy individuals. With Northern blot analysis, they found *OPTN* mRNA expression in the trabecular meshwork and non-pigmented ciliary

epithelium of the human eye. In addition, human optineurin is expressed in retina neuroepithelial cells, fibroblasts, skeletal muscle and kidney. Immunoblotting experiments revealed that optineurin is a secreted protein localized in the Golgi apparatus of cells. Cultured dermal fibroblasts derived from a patient with an E50K missense mutation in OPTN produced less optineurin than fibroblasts from a healthy control. This suggests that haploinsufficiency of the *OPTN* gene through mutation could be the underlying cause of glaucoma.

Optineurin is known to interact with several important proteins including huntingtin, the protein mutated in Huntington's disease (53). In addition, optineurin may be a component of the tumor necrosis factor-α signaling pathway, which regulates programmed cell death (54). Li and co-workers identified FIP-2 (Optineurin) in a two-hybrid screen searching for proteins which interacted with the adenovirus E3-14.7K protein (54). The E3-14.7K protein prevents tumor necrosis factor-α cytolysis. Rezaie and colleagues speculate that optineurin's normal protective task in this pathway may be disrupted in glaucoma patients carrying *OPTN* mutations (52). Interestingly, TIGR/MYOC may also be part of a neuroprotective response (33). The identification of more genes implicated in glaucoma increased the possibility that I may elucidate a common pathway that is disrupted in different forms of the disease.

GLC1F

Wirtz and co-workers identified the GLC1F locus from linkage analysis of a large family. The GLC1F region is flanked by markers D7S2442 and D7S483 on chromosome 7q35-q36 and is 5.3 cM in size. The authors noted that the individuals involved in their study did not display pigmentory problems associated with pigment dispersion syndrome (see below), which is also located at 7q35-q36. Although no disease causing mutations have been identified to date, the authors included nitric oxide synthase as a candidate gene for this condition (55).

Table 1-1: Primary Open Angle Glaucomas

Glaucoma Subtype	Gene	Location	Transmission	Age of Onset (years)	References
JOAG/early onset COAG (aggressive) GLC1A	*TIGR/MYOC*	1q21-q23	Autosomal dominant	5-45	(5)
COAG (normal/moderate tension) GLC1B	No gene identified	2cen-q13	Autosomal dominant	>40	(47)
COAG (high tension) GLC1C	No gene identified	3q21-q24	Autosomal dominant	>40	(48)
POAG (moderate tension) GLC1D	No gene identified	8q23	Autosomal dominant	>40	(51)
POAG (normal tension) GLC1E	*OPTN*	10p14-p15	Autosomal dominant	23-65	(56)
POAG (moderate tension) GLC1F	No gene identified	7q35-q36	Autosomal dominant	25-70	(55)

Congenital Glaucomas:

GLC3A (*CYP1B1*)

Buphthalmos ('ox eye' or 'big eye') is the term used to describe eyes which are unusually large due to the increased intraocular pressure, sometimes during intrauterine growth. Buphthalmos also refers to the enlarged eye as seen in any congenital glaucoma. Patients with this disorder usually present with glaucoma prior to three years of age. The condition is believed to be due to a maldevelopment of the anterior chamber. The maldevelopment is hypothesized to block the aqueous outflow through the trabecular meshwork and lead to increased ocular pressure (57).

Sarfarazi and colleagues isolated the GLC3A loci using linkage analysis on 11 of 17 Turkish families. Six of the 17 families did not map to this locus indicating that there is at least one more congenital glaucoma locus. The GLC3A region is on chromosome 2p21 between markers D2S1788/D2S1325 and D2S1356. Stoilov and co-workers identified mutations in the human *cytochrome P4501B1* gene (*CYP1B1*) in patients with GLC3A (57). Human *CYP1B1* was first isolated in 1991 by Sutter and colleagues. *CYP1B1* was one of five genes isolated in a differential hybridization screen to identify dioxin (2,3,7,8-tetrachlorodibenzo-p-dioxin, TCDD) induced genes. Dioxin was known to cause chloracne in humans, a disorder affecting the growth and differentiation of the epidermis (58).

As a member of the cytochrome P450 superfamily, *CYP1B1* is expected to add an atmospheric oxygen to its substrate. It is hypothesized that the oxygenation of the CYP1B1 substrate would allow the proper functioning of signal transduction pathways involved in eye growth and differentiation. The CYP1B1 substrate(s) are still unknown.

The *CYP1B1* gene is comprised of three exons and produces a 5.1kb transcript. CYP1B1 also contains multiple amino acid domains which have been conserved between cytochrome P450 molecules. The disease causing mutations identified to date either truncated the CYP1B1 protein product or caused missense mutations in highly conserved regions, some of which are predicted to alter the structure and/or function of CYP1B1 (Figure 1-6) (57,59-62). One mutation, leading to a truncation of CYP1B1, was identified in a patient with Peters' anomaly (63). Of two other CYP1B1 alterations examined, one was reported to have lower stability and activity while a second tested had lowered function (64).

Bejjani and co-workers have suggested that CYP1B1 may be modified by another gene (60,61). Recently, Vincent and colleagues uncovered a potential modifying effect of CYP1B1 on TIGR/MYOC. Individuals with mutations in both genes developed glaucoma at a significantly younger age than did family members in TIGR/MYOC alone (65). Whether TIGR/MYOC modifies CYP1B1 remains to be tested.

Figure 1-6: Schematic Diagram of the CYP1B1 Gene.

Protein encoding segments of the gene are enclosed in a black border. Filled coding regions represent amino acid residues conserved among CYP family members. Letters "a-p" denote mutations identified in CYP1B1. Open arrows mark missense changes while closed arrows show truncations. Mutation "f" is a splice site alteration. Adjusted from (57).

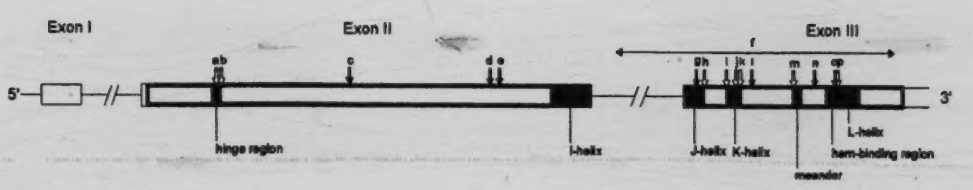
Exon I
Exon II
Exon III
5'
3'
hinge region
I-helix
J-helix
K-helix
meander
L-helix
hem-binding region

GLC3B

Akarsu and co-workers identified the GLC3A locus from 11 of 17 Turkish GLC3 families. The remaining six families and two other families were used in linkage analysis experiments to identify a second GLC3 region. Four of these eight families mapped to 1p36.2-p36.1 and place GLC3B between markers (D1S1597/D1S489/D1S228) and markers (D1S1176/D1S507/D1S407). No candidate genes have been reported. The authors note that as the remaining four GLC3 families were not linked to GLC3A or GLC3B, there must be at least one more GLC3 region (66).

Table 1-2: Congenital Glaucomas

Glaucoma Subtype	Gene	Location	Transmission	Age of Onset (years)	References
Primary Congenital Glaucoma (Buphthalmos) GLC3A	*CYP1B1*	2p21	Autosomal recessive	<3	(67)
Primary Congenital Glaucoma (Buphthalmos) GLC3B	No gene identified	1p36	Autosomal recessive	<3	(66)

Secondary Glaucoma/Developmental Glaucoma

Secondary glaucomas result from the effects of eye maldevelopment. Occasionally, gene mutations may affect the normal development of the eye and sometimes other tissues as well. The glaucomas usually seen in these situations are observed after, or in addition to, other clinical manifestations. These disorders are referred to as secondary glaucomas as there is a primary event in the development of the iridocorneal angle that can lead to, or contribute to, glaucoma pathogenesis. The glaucomas covered in this section are a selection and are not meant to represent a full list of secondary glaucomas.

PAX-6

The *PAX-6* gene has been implicated in a number of ocular disorders including Peter's anomaly (40), autosomal dominant keratitis (41), congenital cataracts with late onset corneal dystrophy (42) and isolated foveal hypoplasia (43). Aniridia, an autosomal dominant disorder is characterized by absent or hypoplastic irises and has often been associated with the WAGR syndrome on chromosome 11. Peter's anomaly is characterized by corneal abnormalities (iridocorneal adhesions) and bilateral central opacities. Autosomal dominant keratitis (ADK) usually presents with corneal opacification, iris hypoplasia, vascularization and foveal hypoplasia. To date over 180

PAX-6 mutations have been recorded in the Human *PAX-6* Allelic Variant Database (http://www.hgu.mrc.ac.uk/Softdata/PAX6/).

PAX-6 was first associated with aniridia in 1991 by Ton and colleagues. The gene is located on chromosome 11p13 and encodes a paired box, homeobox and a proline/serine/threonine (PST) domain within a 2.7kb transcript (68). The murine *PAX-6* homologue has been shown to be lethal when homozygously mutated while the heterozygous mutant results in microphthalmos, or poor development in the anterior chamber of the eye (40,69,70). Mutations in the eye specific enhancer of the *Drosophila PAX-6* homologue also result in poor or absent eye development depending on the mutation. Halder and co-workers ectopically expressed *Drosophila PAX-6* and murine *PAX-6* in *Drosophila* and produced offspring which developed eyes on their wings, legs and antennae. As the authors were also able to create this phenotype using the murine homologue of *PAX-6*, it suggests that *PAX-6* has been tightly conserved in evolution (71). Recent work repeating the experiment with the squid *PAX-6* homologue suggests that *PAX-6* is a master control gene for eye formation throughout the animal kingdom (72).

The phenotypic variety seen in aniridic patients and the variety of phenotypes observed with *PAX6* mutations makes it difficult for clinicians to categorize eye disorders. One trend which will probably be seen in the future is the further expansion of clinical presentations due to mutations of specific glaucoma causing genes. At the same time, some families with apparently different ocular disorders may be caused by the same

gene, such as in *PAX-6*. These observations are similar to those reported in four clinically distinct corneal dystrophies, which were all found to have mutations in the same gene (73).

Axenfeld-Rieger Malformations

Axenfeld-Rieger malformations encompass a broad spectrum of ocular problems which include iris hypoplasia, Axenfeld-Rieger anomaly (ARA), iridogoniodysgenesis anomaly (IGDA) and the syndromic forms of ARA and IGDA; Axenfeld-Rieger syndrome (ARS), and iridogoniodysgenesis syndrome (IGDS). Two transcription factor encoding genes, PITX2 and FOXC1 were found to be responsible for some of these malformations.

Axenfeld-Rieger anomaly (ARA) was first described by Axenfeld in 1920 (74) and later by Rieger in 1934 (75). Features of ARA include posterior embryotoxon and iris hypoplasia. It was later observed that some patients had non-ocular findings in addition to the ocular changes. The findings included hypodontia, maxillary hypoplasia, failure to involute the periumbilical skin, a broad flat nose and hypertelorism. Patients with Axenfeld-Rieger syndrome (ARS) present with both the ocular and non-ocular features.

Gould and co-workers mapped ARA to 6p25 (76). The gene mutated in ARA patients was cloned by Nishimura and colleagues (77) and Mears and co-workers (78). Both groups identified mutations in the *Forkhead-like 7* (*FKHL7*) gene in ARA patients.

The original *forkhead* gene was identified in *Drosophila* and encodes for a transcription factor protein involved in *Drosophilia* development. Since then mutations in FKHL7, renamed FOXC1, have been reported in individuals with Peters' anomaly, and Axenfeld Rieger syndrome (77,79,80). Additionally, duplications of FOXC1 can also lead to AR malformations (80,81).

A region containing an ARS gene was originally narrowed to 4q25 through examination of deletion and translocation patients (82-84). Murray and co-workers used genetic linkage experiments to confirm the mapping of this ARS gene (85). Mutations were identified in a gene encoding a bicoid class homeobox transcription factor originally named *RIEG* and now called *PITX2*. Homeobox proteins are known to bind to DNA and affect gene transcription. *PITX2* consists of 4 exons and produces a transcript approximately 2 kb in length. The PITX2 protein is predicted to be 271 amino acids long (44). The *PITX2* protein has recently been shown to be involved in a signaling pathway which determines left-right body asymmetry in vertebrates (86,87). Mutations of PITX2 are also responsible for iridogoniodysgenesis syndrome, as discussed below.

The ocular features of iridogoniodysgenesis syndrome are the same as for iridogoniodysgenesis but, in addition, patients present with the non-ocular features of ARS, including dental anomalies and redundant umbilical skin. The *IRID2* locus has been mapped by Heon and colleagues (88) and Walter and co-workers (89) to 4q25, the same genetic location as ARS. The ocular and non-ocular similarities of ARS and *IRID2* led to

the hypothesis that these two conditions were allelic (88). In 1998, Alward and co-workers (45) and Kulak and colleagues (46) demonstrated *IRID2* in two families is caused by mutations in *PITX2*. *PITX2* has also been indicated to be responsible for Peters' anomaly (90). Recent work by Kozlowski and Walter has shown that the range of phenotypes, from mild iris hypoplasia to severe ARS, seen in individuals with PITX2 mutations is directly associated with the level of mutant *PITX2* activity lost (91). Further work has demonstrated that greater than normal amounts of *PITX2* function may also be detrimental and lead to ARS (92).

Axenfeld-Rieger Syndrome, additional locus

Phillips and colleagues identified a second ARS locus (*RIEG2*) on chromosome 13q14, bounded by markers D13S1242 and D13S328. The *RIEG2* critical region encompasses a 26 cM region. The authors note that a human homologue to the *Drosophila forkhead* gene, named *forkhead in rhabdomyosarcoma* (*FKHR*), has been mapped to the same area (93). As *FOXC1* has been shown to be involved with ARA, *FKHR* was a good candidate for RIEG2. However, no mutations have been reported in this gene.

Pigment Dispersion Syndrome (PDS)

Pigment dispersion syndrome (PDS) is an example of an open angle secondary glaucoma. PDS presents with iris transillumination defects and pigment deposition within the anterior chamber of the eye. Using four pedigrees, Anderson and co-workers mapped PDS to a 10 cM region on chromosome 7q35-q36, between markers D7S2462 and D7S2423. As studies have demonstrated that as many as 2-4% of Caucasians may have PDS, finding a gene for this disorder has the potential to benefit a large number of people through early diagnosis. Four candidate genes have been identified in the 7q35-q36 region including the holoprosencephaly type three gene (*HPE3*), the gene for nitric oxide synthase, a homologue for the murine *engrailed* gene, and a muscarinic cholinergic receptor gene (94). A second PDS locus on chromosome 18q11-q21 has also been identified by Andersen and co-workers (95).

Chang and co-workers characterized the mouse strain DBA/2J, which become afflicted with iris atrophy and pigment dispersion prior to generating glaucoma (96). The authors determined through mouse backcross experiments that the phenotypes observed were due to two separate loci, which they named iris pigment dispersion (IPD) and iris stromal atrophy (ISA), respectively. IPD was found to be located on mouse chromosome 6 while ISA was on mouse chromosome 4. IPD was situated in a region with conserved synteny to chromosome 7. Later work by the same group identified the two mouse genes responsible for IPD and ISA. The IPD phenotype was caused by a homozygous R150X

alteration in the Gpnmb gene. Mice heterozygous for the R150X change did not develop IPD (97). GPNMB was previously known to be expressed in human melanoma cell lines and in quail retina (98,99). Although GPNMB was localized to chromosome 7, the human GPNMB was not within the PDS critical region. Sequencing of DNA from patients with PDS did not reveal any mutations.

The tyrosine related protein 1 (tyrp1) gene was known to be associated with melanin production (100) and $Tyrp1^b$ was examined as a candidate for the ISA phenotype by Anderson and co-workers (97). A BAC containing a wild type Tyrp1 gene was used to rescue DBA/2J $Tyrp1^b$ mice from the ISA phenotype, demonstrating that $Tyrp1^b$ was responsible for the ISA in these animals. Interestingly, TYRP1 mutations in humans lead to oculocutaneous albinism, a condition featuring reduced levels of pigmentation (101,102).

Anderson and colleagues hypothesized that the problems stemming from ISA and IPD was due to the generation of cytotoxic intermediates during pigment production. The authors supported this model by not observing either eye phenotype in a hypopigmented mouse background using either homozygous alteration (97). Although GPNMB and TYRP1 may be interesting candidates for PDS in humans, they do not appear to be responsible for the PDS mapped to 7q35-q36.

Pseudoexfoliation of the Lens

Pseudoexfoliation of the lens is associated with high tension glaucoma. Patients with pseudoexfoliation of the lens present with blue-grey on the anterior surface of the lens and usually come to clinical attention past 40 years of age (103). Inheritance of pseudoexfoliation of the lens has been reported as being matrilineal, suggesting mitochondrial inheritance, and as a dominant genetic trait linked to chromosome 2p16. The information to date would suggest that there are at least two loci for this disorder (104,105).

Table 1-3: Secondary Glaucomas

Glaucoma Subtype	Gene	Location	Transmission	Age of Onset (years)	References
Aniridia	*PAX-6*	11p13	Autosomal dominant	<40	(68)
Peter's Anomaly (some cases)	*PAX-6*	11p13	Autosomal dominant	<40	(40)
Autosomal dominant keratitis	*PAX-6*	11p13	Autosomal dominant	<40	(41)
Axenfeld-Rieger Anomaly (ARA)	*FKHL7 (FOXC1)*	6p25	Autosomal dominant	<40	(77,78)
Axenfeld-Rieger syndrome (ARS)	*FOXC1*	6p25	Autosomal dominant	<40	(79)
Iridogoniodysgenesis Type 1 (IRID1)	*FOXC1* duplication	6p25	Autosomal dominant	<15	(80,81)
Axenfeld-Rieger Syndrome (RIEG1)	*PITX2*	4q25	Autosomal dominant	<40	(44)
Iridogoniodysgenesis Type 2 (IRID2)	*PITX2*	4q25	Autosomal dominant	<15	(45,46)
Rieger Syndrome, Additional locus (RIEG2)	No gene identified	13q14	Autosomal dominant	<20	(93)
Pigment Dispersion Syndrome (PDS)	No gene identified	7q35-q36	Autosomal dominant	<40	(94)
Pigment Dispersion Syndrome (PDS)	No gene identified	18q11-q21	Autosomal dominant	<40	(95)
Pseudoexfoliation of the Lens	No gene identified	2p16	Autosomal dominant	>40	(105)
Pseudoexfoliation of the Lens	No gene identified	Mitochom-drial	Matrilineal	>40	(104)

The mapping and cloning of glaucoma-related genes is still in its infancy. However, two trends may be drawn from the existing information. First, the actual number of glaucoma causing genes is most likely much greater than is currently known. The genetic heterogeneity of glaucoma means that the number of glaucoma associated genes may be as high as in retinitis pigmentosa, where at least 22 genes are associated with this condition. Secondly, there is considerable phenotypic variability seen in patients with TIGR, PAX-6 or PITX2 mutations. This variability will make it difficult for clinicians and geneticists to easily associate clinical findings with the genes involved. However, as more genes are identified, the molecular pathogenesis of glaucoma may be better understood. The observation that CYP1B1 may be a modifier of TIGR/MYOC, suggesting that these genes may act through a common pathway, hints that glaucoma genetics may be at the beginning of this pathway.

Chapter 1C: Age-related Macular Degeneration (AMD)- A Second Example of Ocular Disease

Age-related macular degeneration (AMD) is the single largest cause of blindness in the Western world (106-109). AMD is associated with the appearance of drusen, yellowy flecks that can be described as being 'hard' or 'soft'. Later stages of AMD are characterized by geographic atrophy or neovascularization. In geographic atrophy, the retina pigment epithelium (RPE) degenerates. In neovascularization, new blood vessels form under the RPE and damage the retina. Age-related macular degeneration is known to have both environmental and hereditary components. However, although it has been known for some time that AMD has genetic aspects, few loci have been identified for this disorder.

A major stumbling block to identifying the genetic component of AMD is its late age of onset, making the collection of large families for linkage analysis difficult. There have been two AMD loci and one AMD susceptibility locus mapped to date using this method. An alternative method for finding AMD causing genes has been through the candidate gene approach, usually with other genes known to be involved in maculopathies or retinopathies. This 'bottom up' approach used when studying AMD is similar to my methodological approach and contrasts with the 'top down' methods mainly used in glaucoma studies. Examples of genes examined for a role in AMD include the tissue inhibitor of metalloproteinase 3 gene (TIMP3), the EGF-containing fibulin-like

extracellular matrix protein gene (EFEMP1) and the elongation of very long chain fatty acids-like 4 gene (ELOVL4). However, no mutations of these genes have been observed in AMD patients, as reviewed in (110). Two genes have been reported to be altered in individuals with AMD; the vitelliform macular dystrophy gene (VMD2), and the retina specific ABC transporter gene (ABCR). Table 1-4 summarizes the loci and genes containing variations in AMD patients.

VMD2 as a candidate gene for AMD

Mutations in the vitelliform macular dystrophy gene (VMD2), encoding the protein bestrophin, are responsible for Best disease (111,112). Best disease is considered a good model for AMD as both disorders have similar phenotypes, including the collection of yellowy material near the RPE and the subsequent degeneration of the RPE. Several labs investigated whether VMD2 alterations were present in AMD patients. Kramer and co-workers found no mutations in VMD2 within their AMD pool (113). Allikmets and colleagues identified two alterations. One was observed in two AMD patients but was not localized in a highly conserved region. The second change was in a conserved position and was considered more likely to be disease causing (114). Lotery and co-workers found mutations in five AMD patients, two of whom had the same nonsense mutation. However, the frequency of alterations in the authors' AMD patient pool was not significantly different from their control population. This finding suggested

to the authors the possibility that Best disease could be a phenocopy of AMD and that the 'AMD mutations' observed were in misdiagnosed Best patients (115). From the research performed to date, although some alterations have been observed in AMD diagnosed individuals, changes in VMD2 do not appear to cause a significant proportion of AMD.

ARMD1

The ARMD1 locus was identified by Klein and colleagues using linkage analysis on a large U.S. family. The family studied had RPE degeneration (geographic atrophy) and drusen, but did not have neovascularization. The disease segregated in an autosomal dominant manner and was located at chromosome 1q25-q31. The ARMD1 locus is approximately 12 cM in size, bounded by markers D1S446 and D1S413. No putative candidate genes in the region were suggested by the authors (116).

AMD Susceptibility Loci

Weeks and co-workers performed a whole genome screen to identify susceptibility loci for AMD. The authors examined 391 pedigrees using three different clinical stringencies of AMD for their analysis. Two loci at 1q31 and 17q25 were observed to have lod scores of interest. The 1q31 locus was between markers D1S1660 and D1S1647 at a LOD score of 2.46 using the most stringent criteria for diagnosis. The 17q25 locus was at marker D17S928 with a LOD score of 3.16. For both cases the

authors assumed autosomal dominant inheritance. Within the 1q31 region, the authors listed several genes as potential candidates including the retina-specific regulator of G-protein signaling (RGS-r) and phosducin. RGS-r and phosducin are both believed to be involved in the phototransduction cascade (117-119).

At 17q25, the tissue inhibitor of metalloproteinase 2 (TIMP2) gene and the lectin galactose-binding soluble 3 binding protein (LGALS3BP) gene were suggested as candidates. Of these two genes, TIMP2 makes the more intriguing candidate as TIMP3 is known to be mutated in another retinopathy, Sorsby's fundus dystrophy (120).

ABCR/ABCA4

The retina specific ABC transporter (*ABCR*) gene was one of twenty-one novel human ABC genes identified by Allikmets and co-workers and was only observed in retina-expressed transcripts (121). The ABC transporter superfamily consists of seven subfamilies, named ABCA through ABCG, with individual protein activities that include drug resistance, sterol transport and chloride ion movement. (As reviewed in (122)). According to this nomenclature, *ABCR* is also named *ABCA4*. Through radiation hybrid mapping and physical mapping, Allikmets and colleagues determined that the *ABCR/ABCA4* gene was located at 1p13-p21 in the Stargardt disease (STGD) critical region. *ABCR/ABCA4* encodes a 2,235 amino acid protein and the transcript was determined to only be expressed in rod photoreceptors through *in situ* experiments. In 48

Stargardt's pedigrees examined, the authors found 19 mutations including frameshifts, missense changes and alterations affecting splice sites (121). Alterations in *ABCR/ABCA4* have also been observed in autosomal recessive retinitis pigmentosa (arRP) and autosomal recessive cone-rod dystrophy (123,124). These findings suggested that *ABCR/ABCA4* could be responsible for a variety of retinal disorders. As AMD and Stargardt's share common features, the *ABCR/ABCA4* gene was examined by Allikmets and colleagues in AMD affected patients.

ABCR/ABCA4 and AMD. Discovery and Controversy

Allikmets and colleagues examined whether *ABCR/ABCA4* changes were associated with AMD using a panel of 167 AMD patients. The authors detected 13 AMD associated changes including one splice site alteration, two frameshifts and several missense mutations. The two most common mutations were G1961E and D2177N observed in 6 and 7 AMD patients respectively (125).

These first results generated some controversy within the field. Part of the initial criticisms of this study focussed not on the G1961E and D2177N changes but the other missense alterations observed to be associated with AMD. As some of these variants were each seen in single cases, it was thought that there was a lack of statistical evidence that the changes were involved with AMD (126). Further screens performed by other groups concluded that there was no significant association between AMD and

ABCR/ABCA4 (127,128). These researchers and others found that *ABCR/ABCA4* was highly polymorphic and a stricter clinical definition of AMD, relative to the Allikmets study, may have led to no associations being detected (128,129). Additionally, the G1961E alteration was observed at a high frequency in control individuals of Somali ancestry, casting doubt on the hypothesis that the G1961E change is involved in AMD (130).

Allikmets and co-workers responded to these criticisms with an expanded study comprised of over 1200 patients and controls, respectively. Their findings determined that the G1961E and D2177N changes were indeed associated with AMD. However, the authors noted that if the smaller populations examined were tested separately, there would be no significance. A significant result was only determined using large sample sizes (131).

Other lines of biological evidence suggested a role of *ABCR/ABCA4* in AMD. A mouse knockout model of *ABCR/ABCA4* and *in vitro* experiments examining ABCR's ATPase activity elucidated that ABCR's function was to transport all-trans-retinal (132,133). ABCR knockout mice were observed to have delayed rod dark adaptation. Weng and colleagues determined that the levels of all-trans-retinal in the knockout mice were significantly lower in the knockout mice as compared to the normal mice (132,133). Examination of ABCR's transporting activity using normal or mutant ABCR protein

determined that AMD associated missense alterations have an effect on ABCR function (134).

The difficulty of determining a significant link between *ABCR/ABCA4* changes and AMD suggests that for complex diseases like AMD, it is important to either have large numbers of patients and appropriate controls and/or a biological system to examine the effect of any changes identified. Without one or both of these elements, it is challenging to prove that any individual gene has a role in AMD.

Table 1-4: Age-Related Macular Degeneration (AMD) loci

AMD locus	Gene	Location	Transmissio	References
Vitelliform macular dystrophy gene (VMD2)	*VMD2*	1q21-q23	Autosomal dominant	(114)
ARMD1	No gene identified	1q25-q31	Autosomal dominant	(116)
AMD susceptibility	No gene identified	1q31	Autosomal dominant model	(135)
AMD susceptibility	No gene identified	17q25	Autosomal dominant model	(135)
ARMD2 (ABCR/ABCA4)	*ABCR/ABCA4*	1p13-p21	Autosomal recessive	(51)

Research project description

As described above, many genes which cause ocular disease remain to be found. At the start of my studies, Dr. Michael Walter's laboratory was engaged in a 'top down' (or family based) approach to glaucoma research. When we discussed potential projects, a 'bottom up' (or gene based method) was thought to be a good complementary strategy in the search for ocular disease genes. One methodology which may be used to narrow down the search for disease-related genes is to examine genes with an interesting transcript expression pattern. Once isolated, one can examine the candidacy of these genes through physical proximity to known disease loci, or genetic screens of patients with disorders that involve the tissues tested. If none of the genes isolated mapped to known disease loci, they could still be useful in understanding normal eye function. I created an adult iris cDNA library and screened it in two different ways to identify genes which can, in turn, become candidates for ocular disease. From this work, I have characterized two new genes, Oculoglycan/Opticin and UBL5.

Outline of Experiments Performed I

1) Build human adult iris cDNA library.

2) Perform differential screen and isolate novel or uncharacterized cDNAs.

3) Radiation hybrid map any unlocalized cDNAs.

4) Examine isolated cDNA transcript expression profiles through RT-PCR and *in silico* methods.

5) Pick one cDNA for further study (IR185, Oculoglycan/Opticin).

6) Determine the IR185 (Oculoglycan/Opticin) expression profile through Northern analysis.

7) Identify the whole open reading frame for IR185 (Oculoglycan/Opticin).

8) Isolate the mouse and porcine orthologs of Oculoglycan/Opticin.

9) Elucidate Oculoglycan/Opticin's intron/exon structure.

10) Examine the protein localization pattern of Oculoglycan/Opticin in humans through immunoblot and immunohistochemistry experiments.

11) Compare the biochemistry of wild type Oculoglycan/Opticin to the Arg229Cys variant.

Outline of Experiments Performed II

1) Perform screen searching for iris cDNAs that are highly expressed and conserved between species and isolate novel or uncharacterized cDNAs.

2) Determine the chromosomal location for any novel cDNAs identified (Iris Grid 5/ Ubiquitin-like 5).

3) Examine Iris Grid 5/Ubiquitin-like 5's expression profile through Northern analysis.

4) Elucidate Iris Grid 5/Ubiquitin-like 5's intron/exon structure.

5) Test Ubiquitin-like 5's biochemical activity through immunoblot experiments.

6) Identify Ubiquitin-like 5's intracellular location through immunocytochemistry.

Chapter II: Characterization and Genetic Screen of a Novel Iris Specific and Leucine-Rich Repeat Protein (Oculoglycan/Opticin) Isolated Using Differential Selection

Portions of this chapter have been published in:

Friedman, J.S., Ducharme, R., Raymond, V., Walter, M.A. Isolation of a Novel Iris-Specific and Leucine-Rich Repeat Protein (Oculoglycan) Using Differential Selection. (2000) Invest. Ophthal. Vis. Sci. 41(8): 2059-2066.

Friedman, J.S., Faucher, M., Hiscott, P., Biron, V.L., Malenfant, M., Turcotte, P., Raymond, V., and Walter, M.A. Protein Localization in the Human Eye and Genetic Screen of Opticin. (2002) Hum. Mol. Genet. 11(11): 1333-1342.

Introduction:

Age-related macular degeneration (AMD) and glaucoma are two major causes of blindness worldwide. AMD is the single largest cause of blindness in the Western world, while glaucoma is predicted to affect at least 67 million people and cause nearly 6.7 million cases of bilateral blindness worldwide (4,106-109). Methodologies used to search for genes involved in these and other disorders can be separated into two categories. The first, the positional cloning approach (136), uses linkage analysis to identify the genetic region within which lies a disease-causing gene. Once the interval is of a manageable size (less than one Megabase), genes within the minimal region are tested as candidates for the disorder of interest. The second method, the candidate gene approach (136), entails examining individual genes that encode proteins with known functions or have an expression profile that make them candidates for the disorder in question. Both methods are typically used simultaneously to discover genes causing hereditary disorders.

One factor examined when considering the eligibility of any candidate gene is whether the gene is highly or specifically expressed in the tissue affected by the disorder. Genes expressed in this manner can be assumed to be important for the function of that tissue. Once isolated, genes that are highly expressed or tissue specific can become candidate genes for disorders that affect the tissue used for gene isolation. For example, genes expressed in the retina can be candidate genes for retinal disorders. There are a

variety of techniques available to identify genes expressed in some tissues and not in others, including subtractive hybridization (137) and computer based (*in silico*) searches of public databases (138). I have used another technique, differential selection (139), to search for genes expressed in the iris and trabecular meshwork. In a differential selection screen, cDNA pools from different tissues are used as probes against a cDNA library. cDNAs found to be expressed in the tissue of interest and not in the control tissue are selected for further analysis. cDNAs found to be more highly expressed in the tissue of interest than the control tissue may also be chosen for further characterization, as I have done here. Differential selection has been successfully used to isolate new genes involved in retinal function (i.e. Rom1, Chx10) (140,141), but this technique has not been applied previously to the iris. Genes identified using my differential selection screen can be tested as candidates for ocular disorders, including glaucoma.

This chapter describes the screening of an iris cDNA library to identify cDNAs preferentially expressed in the iris or trabecular meshwork. cDNAs were identified through a differential selection screen. One novel cDNA, IR185, (originally named Oculoglycan and subsequently named Opticin) isolated using this method was analyzed in detail and examined as a candidate gene for AMD and glaucoma.

Materials And Methods:

Preparation of human iris, trabecular meshwork, retina and lymphoblast RNA and construction of adult iris cDNA library:

Iris and trabecular meshwork total RNA were obtained though a collaboration with Dr. Vincent Raymond {Molecular Endocrinology and Oncology, Laval University Hospital (CHUL) Research Center}. The RNA was collected from 4 and 8 pairs of human adult donor eyes respectively, less than 24 hours post mortem. The RNA was then precipitated using isopropanol, washed in 70% diethyl pyrocarbonate (DEPC) treated ethanol and resuspended in DEPC treated water. Total lymphoblast RNA was obtained from lymphoblastoid cell lines and isolated using TRIzol reagent (Canadian Life Technologies (Gibco/BRL), Burlington, ON). Poly A+ RNA was isolated from iris using oligo-dT coated Dynabeads (Dynal Oslo, Norway). Five micrograms of iris poly A+ RNA were used as the source material for the iris cDNA library. The iris cDNA library was constructed using the Stratagene cDNA synthesis kit and the Zap-cDNA Gigapack II Gold Cloning kit (Stratagene, La Jolla, CA). The iris cDNA library contained approximately 50,000 primary plaque forming units with an approximate avaerage insert size of 800 base pairs. Trabecular meshwork and lymphoblast cDNA were synthesized using the Stratagene cDNA synthesis kit. Retinal total RNA was donated by Dr. Paul Wong (Department of Biological Sciences, University of Alberta).

Differential Screen:

The iris cDNA library was plated at low density on 245mm square bioassay dishes (Fisher Scientific, Nepean ON). Each dish was plated with either 6,000 or 12,500 plaque forming units (pfu). A total of 72,000 pfu, representing approximately 24,000 recombinant cDNAs, were plated. Triplicate filter lifts were made of each plate using Hybond-N (Amersham Pharmacia Biotech, Baie d'Urfé, Québec). Each filter lift was treated as follows: 5 minutes denaturing in 0.5M NaOH, 1.5M NaCl, followed by 5 minutes neutralizing in 1.5M NaCl, 0.5M Tris-HCl, and 5 minutes rinsing in 2X SSC. (20X SSC is: 175.3g NaCl, 88.2g trisodium citrate, ddH_20 to 1L, pH to 7.0 with NaOH) The filters were then air dried and baked overnight at 80°C in a vacuum oven. Prior to hybridization, each nylon blot was prewashed with 2X SSC before being prehybridized for one hour in Church and Gilbert hybridization solution (142) at 65°C.

Iris, trabecular meshwork or lymphoblast cDNA (50 ng) were radiolabeled with ^{32}P dCTP using the Random Primed Labeling Kit (Roche Diagnostics, Laval, Québec). The radiolabeled probe was denatured at 95°C, cooled rapidly on ice, added to the prehybridized filter lifts and hybridized at 65°C overnight. The filters were washed under low stringency conditions with 2X SSC and 1% SDS for 30 minutes at room temperature. The filters were then washed under high stringency conditions with 0.2X SSC and 0.1% SDS for 45 minutes at 65°C, and were exposed to Biomax film (Kodak, Rochester, NY)

for 1 week at -70°C. Primary cDNA plaques detected with iris cDNA but generated a lower signal with lymphoblast cDNA, or those detected with trabecular meshwork cDNA but generated a lower signal with iris or lymphoblast cDNA, were selected for further analysis.

Plaques of interest were selected and the recombinant cDNAs isolated using the *in vivo* excision protocol as supplied by the manufacturer (Stratagene). Individual cDNAs were manually sequenced using the ^{33}P-radiolabeled terminator ThermoSequenase Cycle Sequencing Kit (Pharmacia Biotech).

Polymerase Chain Reaction (PCR) primers:

cDNA specific PCR primers were designed using the Primer 3 program at the Whitehead Institute for Biomedical Research web page (http://www.genome.wi.mit.edu).

Northern Blot hybridization:

IR185 cDNA (50 ng) was randomly primed and radiolabeled as described above. Radiolabeled IR185 cDNA was hybridized to Clontech multiple tissue northern blots (Human Multiple Tissue Northern Blot, Human Multiple Tissue Northern Blot II and Human Fetal Multiple Tissue Northern Blot II. Each northern blot contained approximately 2 µg of poly A+ RNA per lane.). Hybridization was at 68°C for one hour

using ExpressHyb hybridization solution (Clontech, Palo Alto CA). The Northern blots were first washed under low stringency conditions (2X SSC, 0.05% SDS for 30 minutes at room temperature), followed by higher stringency washes (0.1X SSC, 0.1% SDS for 40 minutes at 50°C), and exposed to Biomax film (Kodak). Northern blots were probed with actin cDNA to control for RNA loading. The actin control hybridization experiment was carried out in an identical manner.

A northern blot containing 3 μg of human iris, human retina and human lymphocyte total RNA was made using standard methods. The Northern blot was probed using actin cDNA as described above. The northern blot was probed with IR185 cDNA at 42°C using UltraHyb hybridization solution (Ambion, Austin, TX). The northern blot was first washed under low stringency conditions (2X SSC, 0.1% SDS for 5 minutes at room temperature), followed by higher stringency washes (0.1X SSC, 0.1% SDS for 30 minutes at 42°C) and exposed to Biomax film.

Radiation Hybrid (RH) mapping:

IR185 primers were used to screen the Genebridge 4 RH panel (Research Genetics, Huntsville, AL). Primers IR185-1F (5'-cccaggtcatcatctcttggacc-3') and IR185-1R (5'-atggagacctttgtccatgc-3') amplified a 142 bp fragment. PCRs were carried out under the following conditions: 94°C for 5 minutes, 30 cycles of 94°C for 30 seconds, 62°C for

30 seconds, and 72°C for 30 seconds, followed by a final extension step at 72°C for 7 minutes. The PCR products from all 93 RH cell lines, HFL121 (human positive control) and A23 (hamster negative control) were separated on agarose gels and scored as positive, negative or ambiguous. The results were electronically submitted to the Whitehead Institute for Biomedical Research web page (http://www.genome.wi.mit.edu) and to the Sanger Centre web page for analysis (http://www.sanger.ac.uk/RHserver).

cDNA specific primers were also used to RH map any unlocalized novel or known cDNAs to chromosomal regions.

Computer Based (in silico) Searches:

The *in silico* expression profile of each cDNA was determined via an electronic search of the cDNA sequence at The Institute for Genomic Research (TIGR) database (http://www.tigr.org/tdb/hgi/hgi.html). The IR185 putative amino acid sequence alignment was performed at the BCM search launcher web site (http://kiwi.imgen.bcm.tmc.edu:8088/search-launcher/launcher.html). The putative protein motifs of IR185 were found through analysis of the predicted amino acid sequence of IR185 with software at the ExPASy-Prosite web site (http://www.expasy.ch/sprot/prosite.html).

Rapid Amplification of cDNA Ends (RACE):

Human anterior segment angles (including iris, trabecular meshwork and ciliary body tissue) were obtained from several donors, less than 24 hours post mortem. Anterior segment angles were collected by the Comprehensive Tissue Centre of the Capital Health Authority with approval from the Research Ethics Board of the Faculty of Medicine of the University of Alberta. Total RNA was isolated using TRIzol reagent (Canadian Life Technologies). Poly A+ RNA was isolated from anterior segment angles (including ciliary body) using oligo-dT coated Dynabeads (Dynal), one microgram of which was used as the substrate for 5' RACE experiments. RACE experiments were carried out using the Marathon cDNA Amplification Kit (Clontech) and the Advantage cDNA Polymerase Mix (Clontech). Amplified DNA was purified using the QIAquick PCR Purification Kit (QIAGEN, Chatsworth, CA) and cloned into pGEM-T Easy vector using the pGEM-T EasyVector System II (Promega, Madison, WI). Cloned cDNAs were sequenced manually as described above.

Mouse Sequence cDNA:

TIGR database (http://www.tigr.org/tdb/) searches using the human *OPTC* cDNA revealed one mouse tentative consensus (TC) sequence (TC207501) and one mouse EST (AA832880), corresponding to the 5' and 3' sections of *Optc* respectively. Primers (5'-ttaagtgaagaaatgagattaggg-3', and 5'-cttgggctacagatgactttc-3') were designed from each

EST and used to amplify the internal mouse *Optc* sequence from mouse eye cDNA generated as described above.

Porcine Sequence cDNA:

Porcine trabecular meshwork/ciliary body RNA collection and RACE cDNA generation was performed in the same manner as described above. Primers specific to human *OPTC* (5'-tcctggctttcctgagtctg-3', 5'-tccaggaactcaatgccac-3') were selected for amplification from pig cDNA. The annealing temperature used was 55°C. A band of expected size (approximately 660 bp) was obtained and cloned into the pGEM-T Easy vector (Promega, Nepean, ON) prior to manual sequencing. 5' and 3' RACE primers were then chosen and RACE was performed to isolate the remaining cDNA sequence. The 5' and 3' RACE fragments were cloned and sequenced as above.

Reverse Transcriptase-PCR (RT-PCR):

Total anterior segment angle (including ciliary body) RNA, total lymphoblast RNA, total trabecular meshwork RNA and total retina RNA were used as a substrate for RT-PCR. First strand cDNA synthesis was performed using Superscript Reverse Transcriptase (Canadian Life Technologies) and oligo-dT using 1 μg of total RNA. cDNA specific PCR primers were used to test whether the cDNAs could be amplified from anterior segment angle, lymphoblast, trabecular meshwork or retina cDNA. PCR

products were separated using agarose gel electrophoresis and visualized with ethidium bromide.

Intron/Exon Boundaries:

To determine the intron/exon boundaries for the coding region of Opticin, primers flanking potential intron/exon boundaries were designed based on the known boundaries of the epiphycan gene (143). The primer sets used are as follows:

AF (5'-ggagaggaagaggagagagg-3'), AR (5'-cgaggctagtcaccttaacc-3')

BF (5'-cgatgaccagacctactacagc-3'), BR (5'-tgtcatcgcaatacacagagg-3')

CF (5'-agaggacattcctcctcttcc-3'), CR (5'-aaatgaggttgttggagagg-3')

DF (5'-ctggatgtcccgctaaatcg-3'), DR (5'-gtctgacaggtaaaggaactgc-3')

EF (5'-ggattctatccggcctttgc-3'), ER (5'-gaagaggctgaggttgatgg-3')

Primer pairs AF/AR, CF/CR and EF/ER were able to amplify from human genomic DNA a product larger than expected from the cDNA. The sizes of the DNA amplified were approximately 900 base pairs, 900 base pairs and 700 base pairs, respectively. The products were extracted and manually sequenced as described above. As primer pairs BF/BR and DF/DR were unable to amplify any product, two introns, with four intron/exon boundaries remained.

Based on discussions with Dr. Michael Walter, a genomic version of RACE was developed, that we have named RAGE, rapid amplification of genomic ends. RAGE was

used to identify the remaining intron/exon boundaries. RAGE involved the digestion of human genomic DNA with the restriction enzyme *Pvu II,* followed by the ligation of RACE adapters. A kit called GenomeWalker, produced by Clontech, performs the same function, but uses several restriction enzymes (Dr. S. Tomarev, personal communication). At the time, PCR was then performed using either BR, BF, DF and DR primers with RACE adapter primers. Intron/exon boundaries close to primers BR and DR were obtained in this manner. The BF associated boundary was elucidated via RAGE through a nested PCR with the external primer BF2 (5'-ctagcctcgctcctgcaacc-3'), followed by a PCR using the more internal BF primer. The last boundary, close to primer DF, was identified through the sequencing of two BACs (0123L07 and 0054P18). The BACs were donated by Dr. Steve Scherer (University of Toronto, Toronto, ON).

Antibody Generation:

A polyclonal chicken antibody was raised against a peptide based on amino acid positions 24 to 42 of human opticin. The polypeptide sequence chosen did not have homology to any other protein besides opticin using BLAST searches. In addition, the region selected included a homology gap of seven amino acids between opticin and its nearest human homologs, epiphycan and osteoglycin (144). Chicken egg IgY was isolated and affinity purified against the peptide (Research Genetics, Huntsville, AL).

Opticin Constructs:

The *OPTC* open reading frame was cloned into the pEGFP vector. Large scale plasmid preparations (Qiagen, Mississauga, ON) of each construct were carried out. Construct DNA (8 μg) was transfected into mammalian COS-7 cells {2 X 10^6 cells per 100 mm plate in 16ml of Dulbecco's modified Eagle's medium (DMEM) + 10% fetal bovine serum} with the FuGENE 6 transfection reagent (24 μl; Roche Molecular Biochemicals, Laval QC). Cells were harvested by scraping 48 hours after transfection and sonicated in lysis buffer (20 mM HEPES pH 7.6, 25% glycerol, 150 mM NaCl, 0.5 mM dithiothreitol with protease inhibitors: aprotinin 5 μg/ml, pepstatin 5 μg/ml, leupeptin 5 μg/ml and phenylmethylsulfonyl fluoride 1 mmol). Soluble and insoluble fractions were collected after a 17,000 x g centrifugation for 10 minutes at 4°C. Fractions were then mixed into 2X SDS sample buffer and boiled for 5 minutes prior to storage. (2X SDS sample buffer is: 3.75 ml 1M Tris-Cl pH 6.8, 6 ml 10% SDS, 3 ml 100% glycerol, 1.5 ml 2X β mercaptoethanol, 0.2 mg bromophenol blue, and ddH_20 to 15 ml) Samples were boiled for 5 minutes prior to loading onto 9% SDS PAGE gels.

Opticin Biochemical Analysis:

To examine any effect of an Arg229Cys variation on the opticin protein, a comparision was made between these two proteins on denaturing, non-reducing SDS

PAGE gels. The opticin cDNA was cloned into a pcDNAc vector lacking the DNA sequence encoding the Xpress™ epitope and the 6-His tag. Primers (5'-agttcctggatgtcTgcctaaatcggctc-3' and 5'-gagccgatttaggcAgacatccaggaact-3') were designed to introduce a cytosine to thymine change that would create the Arg229Cys variant. Mutagenesis was performed using the QuikChange Site-Directed Mutagenesis Kit (Stratagene, La Jolla, CA). Mutagenized plasmid DNA was isolated and sequenced as described above. Denaturing, non-reducing conditions were achieved by extracting the protein without dithiotheitol and using 2X SDS sample buffer without β-mercaptoethanol. Media was collected from normal and Arg229Cys variant transfected cells and tested as described above.

Immunoblot Analysis:

One pair of normal donor eyes (female, age 87 years) was obtained post mortem from the comprehensive tissue centre at the University of Alberta Hospital, Edmonton, AB, Canada. Different ocular tissues (iris, trabecular meshwork/ciliary body, vitreous, retina and optic nerve) were subsequently isolated and frozen at -80^{0}C. All human eye proteins, except for vitreous, were homogenized and extracted in 4 M Guanidine HCl. Human vitreous was extracted in a 50 mM Tris HCl pH 7.4 buffer cocktail containing 1%

NP-40, 0.2% SDS, 1% Triton X, and protease inhibitors: aprotinin 5 μg/ml, pepstatin 5 μg/ml, leupeptin 5 μg/ml and phenylmethylsulfonyl fluoride 1 mM.

Human protein samples of approximately 100 μg were size separated using a 3% stacking and an 11% separating gel. The gels were then transferred to Trans-Blot Transfer Medium (Biorad, Mississauga, ON). The blots were blocked for at least one hour prior to a one hour incubation with the anti-opticin antibody (1:95 dilution). The blots were then washed five times in five minute intervals with TBST before incubation in rabbit anti-chicken antibody (1:2000 dilution) conjugated to horseradish peroxidase (HRP) (Amersham-Pharmacia, Baie d'Urfé, QC) for one hour. (TBST is: 100 ml 1M Tris-Cl pH 7.5, 30 ml 5M NaCl, 0.5 ml Tween-20, dH_20 to 1L) Blots were washed again in TBST before detection using chemiluminescent substrate (Pierce, Rockford, IL) and exposure to Biomax film (Kodak, Rochester, NY). Anti-GFP antibody was kindly provided to us by Dr. Luc Berthiaume (Department of Cell Biology, University of Alberta) and was used at a 1:3333 dilution. The anti-GFP antibody was detected using an anti-rabbit antibody (1:3333 dilution) conjugated to HRP (Amersham-Pharmacia, Baie d'Urfé, QC).

Immunohistochemical Experiments:

Paraffin embedded eye sections of a normal male eye used in immunohistochemistry analysis were obtained as a generous gift from Dr. Ian MacDonald (Department of Ophthalmology, University of Alberta). Slides were first dewaxed in xylene and rehydrated in gradual changes of ethanol. The slides were further rehydrated in PBS for 30 minutes before blocking with 10% FBS. (PBS is: 10 ml Na_2HPO_4/NaH_2PO_4, 7.6 g NaCl, 990 ml dH_20) Endogenous peroxidase activity was then removed by placing the cells in a 3% H_2O_2/methanol solution for 20 minutes. Slides were washed in PBS prior to antibody incubation at 37°C in a humidity chamber. The anti-opticin Ab (1:5 dilution) was used as the primary antibody and incubated overnight at 4°C. A HRP labeled anti-chicken antibody (1:100 dilution) was used as the secondary antibody and incubated for 1.5 hours at 37 °C. The tertiary antibody was incubated for 1.5 hours at 37 °C using a HRP labeled donkey anti-rabbit antibody (1:100 dilution). Antibody staining was observed using the red chromagen 9-amino-3-ethylcarbamazole (AEC) in acetate buffer with H_2O_2.

Results:

Twenty-four cDNAs were isolated from the differential selection screen of the iris library. A schematic diagram outlining the screen is shown in Figure 2-1. Two sample autoradiographs from the screen are shown in Figure 2-2. All twenty-four cDNAs were partially sequenced and the sequences were used in BLAST analyses to determine their identity. Fourteen cDNAs corresponded to known genes, while ten were novel cDNAs. cDNAs selected from the iris cDNA probe screen were designated 'IR', while those identified using the trabecular meshwork probe were named 'TM'. The following numbers indicate the miniprep generated from the *in vivo* excision of cDNA from selected plaques. For example, IR185 was the 185th miniprep performed and its corresponding plaque was originally selected from the iris screen. The chromosomal localization, *in silico* expression profile, gene name and function of the novel and known cDNAs are summarized in Tables 2-1 and 2-2. Known cDNA gene names, chromosomal localization and *in silico* expression profile are shown in Table 2-3. Three of the novel cDNAs (IR108, TM258, TM267) corresponded to uncharacterized ESTs. The remaining novel cDNAs have since been characterized as hypothetical proteins or cloned genes. Ron Ducharme, a summer student I trained, radiation hybrid mapped one known cDNA (IR404) and I mapped four novel cDNAs (IR108, IR185, TM267, IR355). IR185, a novel

cDNA, mapped between markers D1S306 and D1S2727, within the 1q31-q32 chromosomal region.

Figure 2-1: Schematic Diagram of the Differential Screen using a Human Adult Iris Library

Schematic diagram of the differential screen used to identify cDNAs that were more highly expressed in iris rather than lymphoblast, or were more highly expressed in trabecular meshwork than in iris or lymphoblast tissue

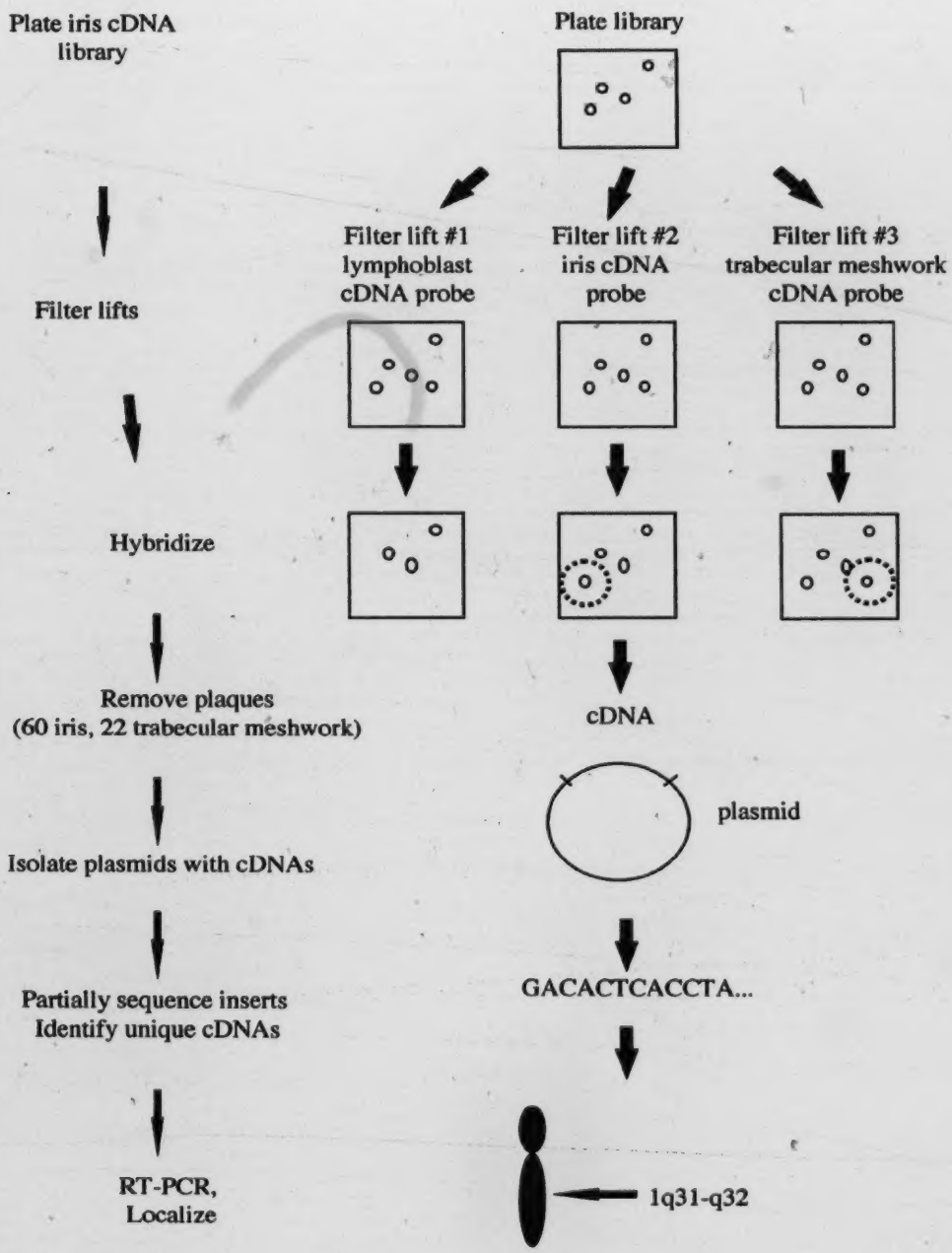
Plate iris cDNA library
Plate library
Filter lifts
Filter lift #1 lymphoblast cDNA probe
Filter lift #2 iris cDNA probe
Filter lift #3 trabecular meshwork cDNA probe
Hybridize
Remove plaques (60 iris, 22 trabecular meshwork)
cDNA
plasmid
Isolate plasmids with cDNAs
GACACTCACCTA...
Partially sequence inserts Identify unique cDNAs
RT-PCR, Localize
1q31-q32

Figure 2-2: Example Autoradiographs from the Iris Differential Screen

Example autoradiographs from the iris differential screen. Left: Filter lift probed with iris cDNA. Right: Filter lift probed with lymphoblast cDNA. The plaque from which the IR185 cDNA was obtained is circled.

Differential Selection Screen

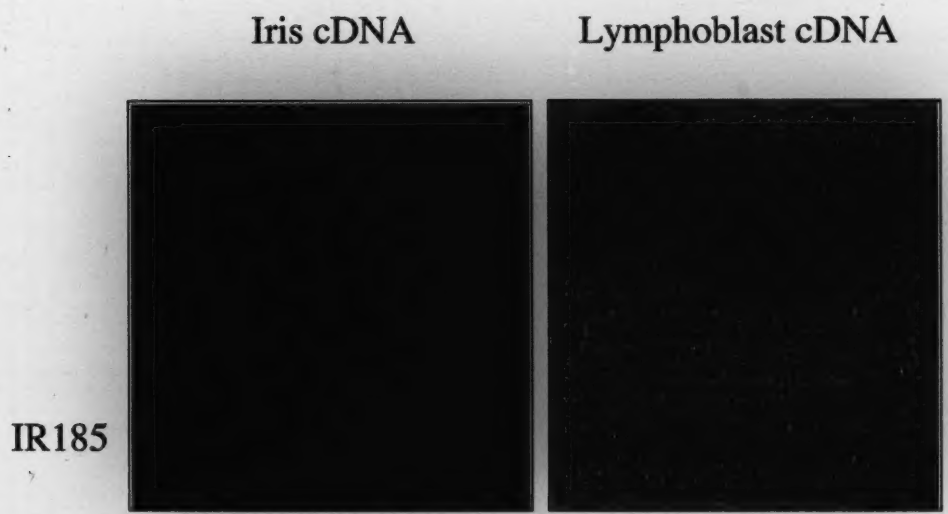

Table 2-1: Chromosomal Localization and *in silico* Expression of Ten Novel Isolated Genes

cDNA No	cDNA size	Location	*Expression
IR42	~870bp	Xq25	Br,Co,FBr,FHe,FK,FLS,FLu,FS,FSp Gb,He,Ll,Mu,Ne,Nr,Pa,Pl,Sk,T,Th,U
IR99	~800bp	20q11.2-q12	Br,FBr,FHe,He,Ll,Lu,O,Pl,Pr,T,U
IR108	~870bp	7p14-7p15	Lv,Sp
IR185	~300bp	1q31-1q32	R
TM257	~500bp	7q31	Br,Bs,Co,E,FHe,FK,FLS,FLu,He,Ll Mu,Pl,Sk,U
TM258	~500bp	5q33-q34	Br,FC,FHe,Ll
TM267	~1kb	19q13	Bs,FHe,FLS,FLu,FSp,Ll,Pa,Pl,Sk
TM305	~700bp	10p12	Br,Co,Ll
TM324	~870bp	11q21-q22	FLS,FHe,FLu,FSp,He,Mu,Pl,Sk,U
IR355	~800bp	10q23-10q24	Br,FHe,Ll,Lv,Pl,Pr,U

* The expression pattern was determined through computer (*in silico*) searches of public databases.
cDNAs beginning with IR were isolated during the screen to detect cDNAs that were more highly expressed in iris than in lymphoblast.
cDNAs beginning with TM were isolated during the screen to detect cDNAs that were more highly expressed in trabecular meshwork than in iris or lymphoblast tissue.
At: Adipose Tissue, Bm: Bone Marrow Stroma, Bn: Bone, Br: Brain, Bs: Breast, Cb: Ciliary,Body, Co: Colon, E: Epididymus, F: Fibroblast, FBr: Fetal Brain, FC: Fetal Cochlea, FHe: Fetal Heart, FK: Fetal Kidney, FLS: Fetal Liver and Spleen, Flu: Fetal Lung, FLv: Fetal Liver, FR: Fetal Retina, FS: Fetal Skin, FSp: Fetal Spleen, Gb: Gall Bladder, Go: Greater Omentum, He: Heart, K: Kidney, Ke: Keratinoctye, Le: Lens, Lu: Lung, Lv: Liver,
Ll: Lymphocytes and Lymphokines, Mu: Muscle, Ne: Neuroepithelium, Nr: Neuron,
O: Ovary, Pa: Pancreas, Pl: Placenta, Pr: Prostate, R: Retina, Si: Small Intestine, Sk: Skin,
Sm: Skeletal Muscle, Sp: Spleen, T: Testis, Th: Thyroid, Ty: Thymus, U: Uterus.

Table 2-2: Identity and Putative Function of Ten Novel Isolated Genes

cDNA No	Gene or ORF Name	Function	References
IR42	Human 16.7 Kd protein	Not characterized	N/A
IR99	Erythrocyte membrane protein band 4.1-like 1 protein (isoform 2)	Putative cytoskeletal protein	(145)
IR108	None characterized	Not characterized	N/A
IR185	Oculoglycan/Opticin (OPTC)	Putative collagen binding protein	(144,146,147)
TM257	CGI-135 putative protein	Not characterized	(148)
TM258	None characterized	Not characterized	N/A
TM267	None characterized	Not characterized	N/A
TM305	Hypothetical protein FLJ13397	Not characterized	N/A
TM324	Hypothetical protein HSPC148	Not characterized	(149)
IR355	Putative ortholog to yeast MSP1	Putative intramitochondrial protein sorter	(150)

Table 2-3: Chromosomal Localization and *in silico* Expression of Known Isolated Genes

cDNA No	Gene Name	Location	**Expression
IR121	*Selenoprotein P	5q31	E,FK,FLu,FLv,FSp,He,K,Lu,Lv, Pl,Pr,T
IR124	Alpha A crystallin	21q22.3	Le,R
IR201	*Phenylalanine hydroxylase	12q24.1	FLS,Gb,Lv
IR212	Metallopanstimulin (MPS1)/Ribosomal protein S27	1q21	At,Br,E,F,FBr,FHe,FLS,FLu,Gb, He,Ll,Lv, Mu,Pa,Pl,Pr,O,R,Si,Sm,Sp,Th
TM229	Rosenthal fiber protein, alphaBcrystallin	11q22.3-q23.1	At,Br,Bs,FC,FHe,FLS,FLu,Go, He Ll,Mu,O,Pl,Pr,R,Sm,U
TM238	*Fatty aldehyde dehydrogenase (ALDH 10)	17p11.2	Br,FLS,He,K,Ke,Lu,Pa,Sk,Sm Pooled Ll,FHe & U
TM244,246	*Very long chain acyl-CoA dehydrogenase	17p11.2-p11.3	Br,Bs,Co,E,F,FHe,FLS,Go,He, Lv,Nr,Pa,Pl,R,Sm,T
IR372	Prostaglandin D2 synthase	9q34.2-q34.3	Br,Cb,E,FBr,FLS,He,Pl,R,Sp,T
IR403	*Cytosolic aldehyde dehydrogenase (ALDH1)	9q21	Br,Co,FC,FLS,FLu,Ll,Lu,Lv, Pa,O
IR404	Mouse adipose differentiation related protein	9p21	At,FHe,FLS,Ll,Lu,Lv,Pa,Pl
TM421	Interleukin BSF-2B cell differentiation factor	7p21	Bn,Ll
IR469	Oryctolagus cuniculus sm. musc. caldesmon	7q33	Bm,Br,FC,FHe,FK,FSp,Gb,He, Ll,Lu, Pl,Pr,Ty,U
IR522	Mouse mRNA SCID complementing gene 2	7q33	At,Br,FLu,FR,Gb,He,Ll,Lu,Ne,Pl R,Si,T,Th,U

* These genes have been associated with genetic disorders

** The expression pattern was determined through computer (*in silico*) searches of public databases. cDNAs beginning with IR were isolated during the screen to detect cDNAs that were more highly expressed in iris than in lymphoblast.

cDNAs beginning with TM were isolated during the screen to detect cDNAs that were more highly expressed in trabecular meshwork than in iris or lymphoblast tissue.

It was decided that IR185, a 300 bp cDNA clone, would be further characterized as radiation hybrid mapping placed it near the locus for retinitis pigmentosa 12 at 1q31-q32 (151) and an age related macular degeneration locus (1q25-q31) (116). In addition, a posterior column ataxia with retinitis pigmentosa locus (1q31-q32) (152) was found to be in the same chromosomal region as IR185. Recently, a study reporting susceptibility loci for age-related macular degeneration (AMD) was published (135). The authors identified a region between markers D1S1660 and D1S1647 with a LOD score of 2.46. Interestingly, these markers overlap with my RH localization of *OPTC* (144). When examined using the NCBI map viewer (http://www.ncbi.nlm.nih.gov/cgi-bin/Entrez/hum_srch), the D1S1660 to D1S1647 region was observed to contain the opticin gene. The chromosomal placement of *OPTC* with the susceptibility locus and other eye disease loci is shown in Figure 2-3.

Reverse transcription (RT) analysis of the novel cDNAs demonstrated that almost all of the cDNAs were expressed in both anterior segment angles and lymphoblasts. IR185 was the only novel cDNA listed in Table 2-1 which was amplified from anterior segment angle cDNA and not amplified from lymphoblast cDNA using RT-PCR (Figure 2-4A). Further RT-PCR experiments demonstrated that IR185 was present in retina cDNA (Figure 2-4B) but was not detected in trabecular meshwork cDNA (data not shown). Northern analysis of IR185 using a Clontech Human Multiple Tissue Northern Blot I, a Clontech Human Multiple Tissue Northern Blot II, and a Clontech Human Fetal

Multiple Tissue Northern Blot II, each containing approximately 2 μg of poly A+ RNA in each lane, identified a 2.7 kb transcript in fetal liver only (Figure 2-5). A northern blot containing 3 μg of human iris, human retina and human lymphocyte total RNA, probed with IR185, showed that IR185 was much more highly expressed in iris than in retina (Figure 2-6).

Figure 2-3: IR185 Locus on Human Chromosome 1

Diagram of the IR185 locus relative to the loci for age related macular degeneration (1q25-q31), retinitis pigmentosa 12 (1q31-1q32), posterior column ataxia with retinitis pigmentosa (1q31-q32) and a susceptibility locus for age-related macular degeneration (1q31). CentiMorgan (cM) distances listed were obtained from the Marshfield Genetic Database (http://www.marshmed.org).

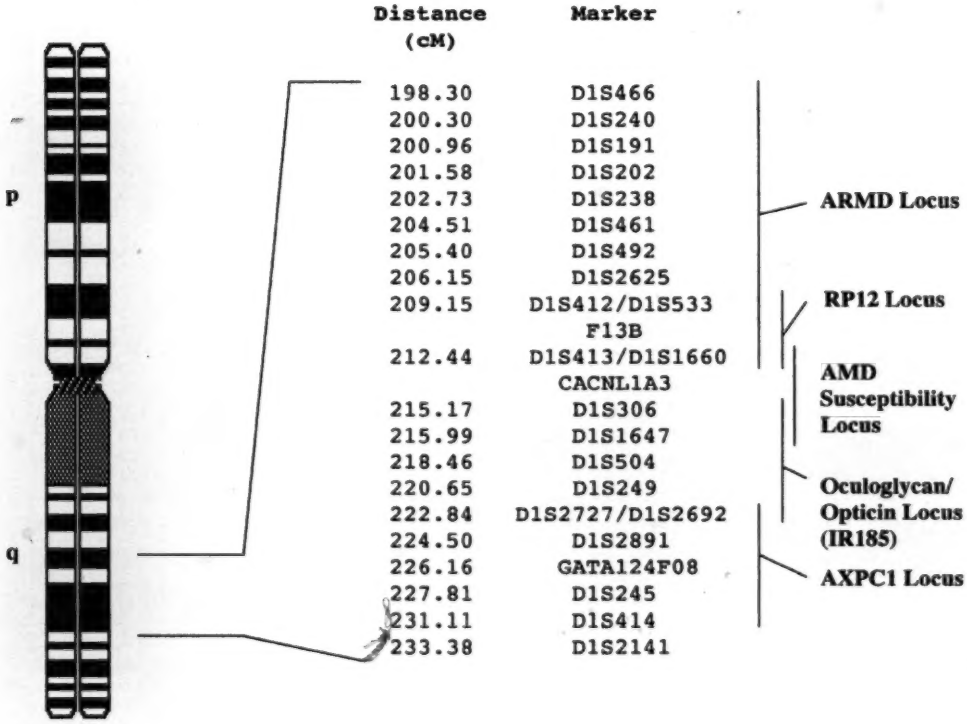
Distance (cM)
Marker
p
q
198.30 D1S466
200.30 D1S240
200.96 D1S191
201.58 D1S202
202.73 D1S238
204.51 D1S461
205.40 D1S492
206.15 D1S2625
209.15 D1S412/D1S533
F13B
212.44 D1S413/D1S1660
CACNL1A3
215.17 D1S306
215.99 D1S1647
218.46 D1S504
220.65 D1S249
222.84 D1S2727/D1S2692
224.50 D1S2891
226.16 GATA124F08
227.81 D1S245
231.11 D1S414
233.38 D1S2141
ARMD Locus
RP12 Locus
AMD Susceptibility Locus
Oculoglycan/ Opticin Locus (IR185)
AXPC1 Locus

Figure 2-4: Reverse Transcriptase PCR Analysis of IR185 (Oculoglycan/Opticin)

A) Reverse Transcriptase analysis using IR185F and IR185R primers on iris cDNA and lymphoblast cDNA. The PCR products were size separated on an agarose gel. Lane 1, 100 bp DNA marker ladder. Lane 2, RT-PCR of anterior segment angle total RNA with reverse transcriptase. Lane 3, RT-PCR of anterior segment angle total RNA without reverse transcriptase. Lane 4, RT-PCR of lymphoblast total RNA with reverse transcriptase. Lane 5, RT-PCR of lymphoblast total RNA without reverse transcriptase. Lane 6, H_20 control. Lane 7, Human genomic DNA control.

B) RT-PCR analysis using the above primers on retina cDNA. Lane 1, 100 bp DNA marker ladder. Lane 2, RT-PCR of retina total RNA with reverse transcriptase. Lane 3, RT-PCR of retina total RNA without reverse transcriptase. Lane 4, H_20 control. Lane 5, Human genomic DNA control.

A)
100 Bp ladder
Anterior Segment Angle +RT
Anterior Segment Angle -RT
Lymphoblast +RT
Lymphoblast -RT
H2O
Human Genomic Control
B)
100 Bp ladder
Retina +RT
Retina -RT
H2O
Human Genomic Control

Figure 2-5: Multiple Tissue Northern Blot Analysis of IR185 (Oculoglycan/Opticin)

Above: Northern blot hybridization analysis of IR185 on a Clontech Human Multiple Tissue Northern blot, a Clontech Human Multiple Tissue Northern blot II and a Clontech Human Fetal Multiple Tissue Northern Blot II. Each lane contains approximately 2 μg of poly A+ RNA in each lane. Tissue sources in each lane are labeled.

Below: β-Actin control probing of the above blots.

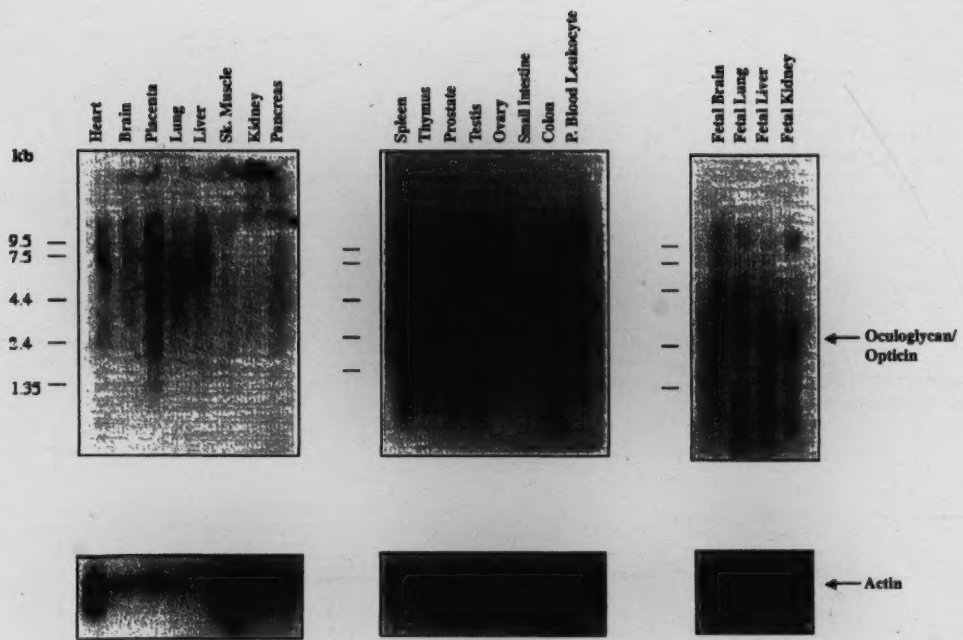
Heart
Brain
Placenta
Lung
Liver
St. Muscle
Kidney
Pancreas
Spleen
Thymus
Prostate
Testis
Ovary
Small Intestine
Colon
P. Blood Leukocyte
Fetal Brain
Fetal Lung
Fetal Liver
Fetal Kidney
kb
9.5
7.5
4.4
2.4
1.35
Oculoglycan/
Opticin
Actin

Figure 2-6: Eye Northern Blot Analysis of IR185 (Oculoglycan/Opticin)

Above: Northern blot hybridization analysis of IR185 on a Northern blot containing 3 μg human total RNA from human iris, human retina and human lymphocyte tissues.

Below: β-Actin control probing of the above blot.

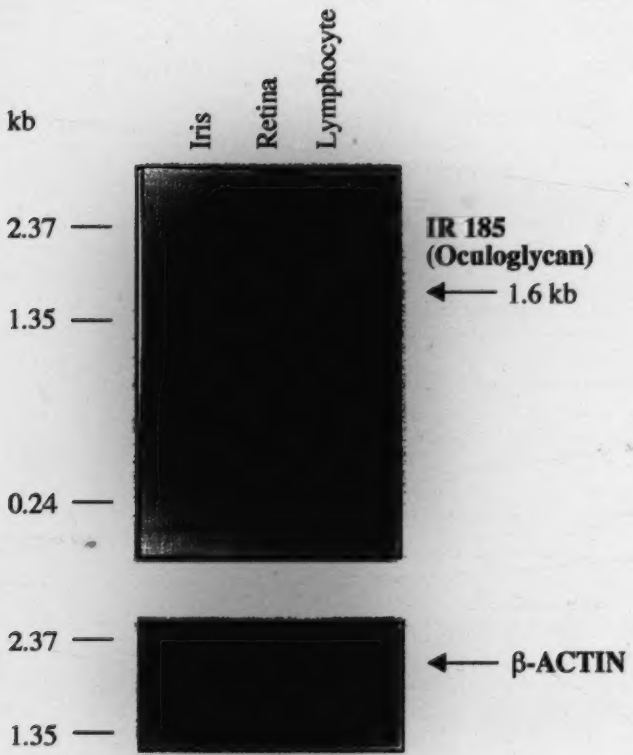
kb
Iris
Retina
Lymphocyte
2.37
1.35
0.24
IR 185
(Oculoglycan)
1.6 kb
2.37
1.35
β-ACTIN

The IR185 transcript size in human iris is approximately 1.6 kb. The 1.6 kb size estimate in iris was based on internal controls used (β-actin, s26 cDNA, 28s RNA and 18s RNA). *In silico* searches of public databases revealed that IR185 has sequence homology to eight ESTs also obtained from retina (EST 112502, EST 112486, EST 112481, EST 112488, aa86a04.s1, aa86a04.r1, EST 19878 and EST 20234). It was therefore determined that IR185 is expressed in three tissues: iris, retina and fetal liver. 5' RACE was used on anterior segment angle cDNA to obtain the entire open reading frame of IR185. Of the estimated 1.6 kb iris transcript of IR185, 1359 bp was sequenced (Figure 2-7). The sequenced transcript appears to represent the entire protein encoding region of IR185 in the eye, as there are two in-frame stop codons upstream of the predicted start site.

Through a combination of techniques including PCR, BAC sequencing and a Rapid Amplification of Genomic Ends (RAGE), I was able to determine the six intron-exon splice junctions for the coding region of IR185. Two other splice sites were obtained through *in silico* methods. Table 2-4 shows the intron-exon splice sites and sizes for IR185.

In order to determine the putative function of IR185, I compared its predicted amino acid sequence to other sequences through *in silico* searches of public databases. IR185 has homologies at the amino acid level with two proteoglycans, Epiphycan and Osteoglycin (47% identity, 60% similarity and 40% identity, 58% similarity

respectively). The amino acid alignment of all three proteins is shown in Figure 2-8. There are six leucine-rich motifs bounded by conserved cysteines in all three proteins. A predicted N-glycosylation site is in the same location in the putative amino acid sequence of IR185 and Epiphycan.

Figure 2-7: DNA Sequence of IR185 (Oculoglycan/Opticin)

DNA sequence of IR185. The hypothesized start methionine is in bold. DNA trinucleotides encoding inframe stop codons are boxed.

```
gacagcctcc accagagtcc ccacctttct ggaagctgca gggctctcca tccaggatcc      60

                                                                  M     1
agaagcattg aaggggacca gccgctgaag ggattctcag tcccatctga ctccccatga     120

R  L  L  A  F  L  S  L  L  A  L  V  L  Q  E  T  G  T  A  S           21
ggctcctggc tttcctgagt ctgctggcct tggtgctgca ggagacaggg acagcttctc     180

L  P  R  K  E  R  K  R  R  E  E  Q  M  P  R  E  G  D  S  F           41
tcccaaggaa ggagaggaag aggagagagg agcagatgcc cagggaaggc gattcctttg     240

E  V  L  P  L  R  N  D  V  L  N  P  D  N  Y  G  E  V  I  D           61
aagttctgcc tctgcggaat gatgtcctga acccagacaa ctatggtgaa gtcattgacc     300

L  S  N  Y  E  E  L  T  D  Y  G  D  Q  L  P  E  V  K  V  T           81
tgagcaacta tgaggagctc acagattatg gggaccaact ccccgaggtt aaggtgacta     360

S  L  A  P  A  T  S  I  S  P  A  K  S  T  T  A  P  G  T  P          101
gcctcgctcc tgcaaccagc atcagtcccg ccaagagcac tacggctcca gggacaccct     420

S  S  N  P  T  M  T  R  P  T  T  A  G  L  L  L  S  S  Q  P          121
cgtcaaaccc cacgatgacc agacctacta cagcagggct gctactgagt tcccagccca     480

N  H  G  L  P  T  C  L  V  C  V  C  L  G  S  S  V  Y  C  D          141
accatggtct gcccacctgc ctggtctgcg tgtgcctcgg ttcctctgtg tattgcgatg     540

D  I  D  L  E  D  I  P  P  L  P  R  R  T  A  Y  L  Y  A  R          161
acattgacct agaggacatt cctcctcttc ctcggaggac tgcctacctg tatgcacgct     600

F  N  R  I  S  R  I  R  A  E  D  F  K  G  L  T  K  L  K  R          181
tcaaccgcat cagccgtatc agggccgaag acttcaaagg gctgacaaag ttgaagagga     660

I  D  L  S  N  N  L  I  S  S  I  D  N  D  A  F  R  L  L  H          201
ttgacctctc caacaacctc atttcctcca tcgataatga tgccttccgc ctgctacatg     720

A  L  Q  D  L  I  L  P  E  N  Q  L  E  A  L  P  V  L  P  S          221
ccctccagga cctcatcctc ccagagaacc agttggaagc tctgcccgtg ctgcccagtg     780

G  I  E  F  L  D  V  R  L  N  R  L  Q  S  S  G  I  Q  P  A          241
gcattgagtt cctggatgtc cgcctaaatc ggctccagag ctcggggata cagcctgcag     840

A  F  R  A  M  E  K  L  Q  F  L  Y  L  S  D  N  L  L  D  S          261
ccttcagggc aatggagaag ctgcagttcc tttacctgtc agacaacctg ctggattcta     900

I  P  G  P  L  P  L  S  L  R  S  V  H  L  Q  N  N  L  I  E          281
tcccggggcc tttgcccctg agcctgcgct ctgtacacct gcagaataac ctgatagaga     960

T  M  Q  R  D  V  F  C  D  P  E  E  H  K  H  T  R  R  Q  L          301
ccatgcagag agacgtcttc tgtgaccccg aggagcacaa acacacccgc aggcagctgg    1020

E  D  I  R  L  D  G  N  P  I  N  L  S  L  F  P  S  A  Y  F          321
aagacatccg cctggatggc aaccccatca acctcagcct cttccccagc gcctacttct    1080

C  L  P  R  L  P  I  G  R  F  T  *                                  332
gcctgcctcg gctccccatc ggccgcttca cgtagctcgg agcccttcca ctcctcccag    1140

gtcatctctt ggaccagcgg gcatcacatt ctccagcagc cgccatctca cacgcctccc    1200
tcctgtggcc gccggcagca tggacaaagg tctccatgca gggggaggag gcctgcttct    1260
ttccccacag ctctcacgtc tcccttctcc ctgcgggtga caaagaagcc caaggaccac    1320
ctccttcctg cctcattgta ataaaattcc ccacactga                           1359
```

Table 2-4: Intron/Exon Boundary Sequences of the IR185 (Oculoglycan/Opticin) Gene

3′ SPLICE ACCEPTOR	EXON	SIZE(bp)	5′ SPLICE DONOR	INTRON	SIZE(bp)
	1	75	AGCATTGAAGGGgtaaggctcaag	1	~1740
cccacttgccagGACCAGCCGCTG	2	272	CAACTCCCCGAGgtgagggacaca	2	~740
ctacatctccagGTTAAGGTGACT	3	139	AGCCCAACCATGgtaagtgcacag	3	~1560
cacctgggccagGTCTGCCCACCT	4	159	TCAAAGGGCTGAgtatgtaatgcc	4	~800
aacctctctcagCAAAGTTGAAGA	5	203	GCAGCCTTCAGGgtgagtcaaggc	5	>4000
ctttctccacagGCAATGGAGAAG	6	96	GTACACCTGCAGgtaaggagcacc	6	~540
tgttcttcccagAATAACCTGATA	7	196	CACTCCTCCCAGgtaagaaccctc	7	>4800
ctctctctcaagGTCATCTCTTGG	8	219			

Invariant bases are underlined

Figure 2-8: Amino Acid Alignment of Opticin with Class III SLRPs

A) Amino acid alignment of the putative IR185 (Oculoglycan/Opticin) protein, Epiphycan, and Osteoglycin. Identical residues among all three proteins are shaded in grey. Conserved cysteine residues are marked with a black circle. Putative O-glycosylation sites are marked by asterisks. A putative N-glycosylation site is underlined. Each leucine-rich repeat between the conserved cysteine residues is boxed. The peptide used to raise an anti-opticin antibody was based on the sequence boxed in yellow.

B) Schematic depiction of the predicted IR185 protein. Conserved cysteine residues are marked by a black circle. Each leucine repeat motif is symbolized by a black rectangle. Putative O-glycosylation sites are shown using arrowheads. The putative N-glycosylation site is shown by a 'tree'.

A)

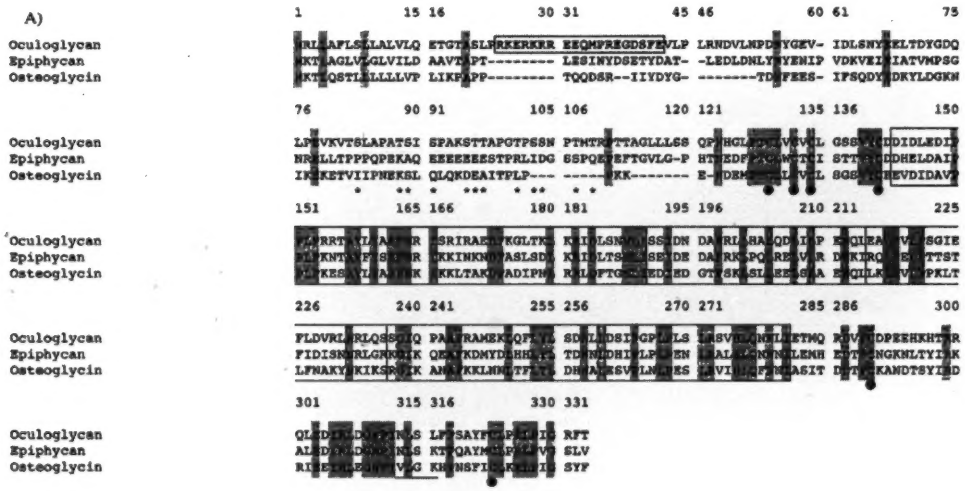

B)

The IR185 sequence was identified by several groups, and the Human Nomenclature Committee determined that opticin (*OPTC*) would be the official name of this gene. In order to identify potentially important residues in the predicted opticin protein, I additionally isolated the mouse and pig orthologs of opticin. The dog ortholog of opticin was also recently determined (153). Residues completely conserved among all orthologs can be considered important for opticin's protein function. A four species amino acid alignment is shown in Figure 2-9. TIGR database and NCBI BLAST searches were performed and identified one mouse EST sequence (AA832880) and one mouse Tentative Consensus sequence (TC207501) with homology to human *OPTC*. PCR was used to amplify the internal *Optc* cDNA from mouse eye cDNA and the fragment was sequenced. A single base pair difference was observed in the coding region between my mouse *Optc* cDNA sequence and the cDNA sequence recently reported (154) (Genbank AF333980). The base pair change is in the first codon position of the encoded amino acid 168, which I predict to be aspartate instead of tyrosine. The difference observed could either be due to a sequencing error or could represent a polymorphism. As the orthologous position of mouse amino acid 168 is aspartate in the three other species, it suggests that the difference is due to a sequencing error. Porcine *OPTC* cDNA was isolated using PCR and RACE methods. The pig *OPTC* cDNA is at least 1364 base pairs in length and encodes a putative protein 333 amino acids in length. The human and dog putative proteins are 76.5% identical and 87.5% similar. The human and pig putative

proteins are 74.2% identical and 88.6% similar, while the human and mouse encoded proteins are 73.5% identical and 88.3% similar.

Figure 2-9: Four Species Amino Acid Alignment of Opticin with its Orthologs

A four species alignment of the predicted opticin protein, and schematic of the human opticin gene.

An amino acid alignment of the putative human opticin protein with mouse pig and dog opticin orthologs. Identical amino acids are boxed in grey. Nonsynonymous amino acid alterations observed in our study are indicated.

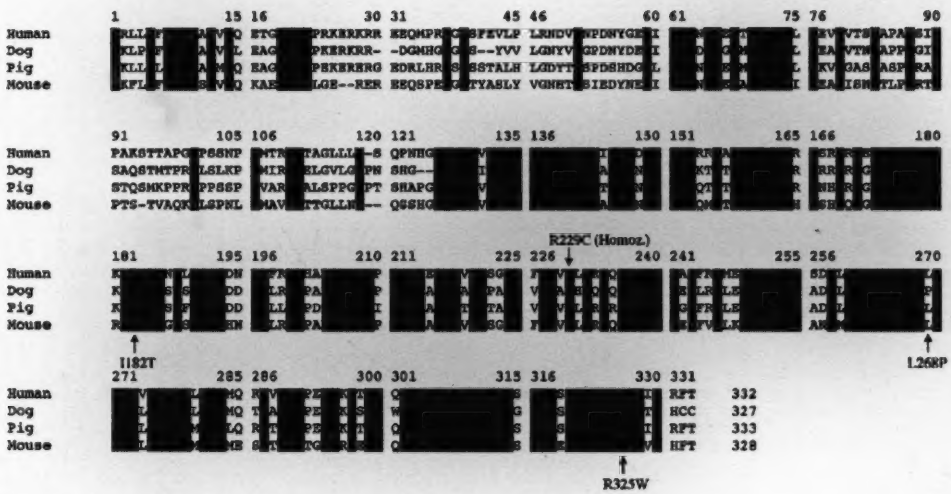
Human
Dog
Pig
Mouse
R229C (Homoz.)
I182T
L268P
R325W

To examine the protein distribution of Opticin, a peptide based on the Opticin protein was used to raise and affinity purify an antibody against Opticin. To test the reactivity of my affinity purified anti-opticin antibody, I first performed immunoblot experiments with a recombinant opticin-GFP protein. Immunoblot analysis of COS-7 cell extracts transfected with and without the *OPTC* cDNA in the pEGFPN1 vector demonstrated two prominent bands. One band, approximately 47.5 kDa, was observed in both transfected and untransfected lanes. The second larger band of about 60 kDa, consistent with the expected size of unmodified opticin (~37 kDa) with GFP (~26 kDa), was seen in transfected lysates (Figure 2-10A). To verify that the 60 kDa band was indeed the opticin-GFP fusion protein, I performed an immunoblot experiment with anti-GFP antibody and detected a single 60 kDa band (Figure 2-10B), confirming that my affinity purified anti-opticin antibody is able to detect human Opticin in mammalian cells.

After these preliminary tests showed that the anti-opticin antibody was able to detect opticin, I expanded my analysis to include human eye tissues. Immunoblot experiments on human eye tissue protein extracts showed a prominent band of approximately 62 kDa in iris, trabecular meshwork/ciliary body, retina, optic nerve and vitreous. Weaker bands were observed at 45 kDa and 38 kDa. The 45 kDa band was seen in iris, trabecular meshwork/ciliary body and optic nerve, while the 38 kDa band was present in iris and retina (Figure 2-10C).

Figure 2-10: Immunoblot Analysis of Opticin

(A) Immunoblot analysis of COS-7 cell extract transfected with and without recombinant Opticin in pEGFP vector. An approximately 47.5 kDa band putatively represents an endogenous form of opticin in COS-7 cells. A band of approximately 60 kDa band corresponds to the expected size of core opticin protein (~37 kDa) with GFP (~26 kDa).

(B) Same immunoblot as in A, examined with anti-GFP antibody. The only band observed corresponds to the expected size of opticin-GFP fusion protein.

(C) Immunoblot analysis using anti-opticin antibody on human eye tissues. An intense band approximately 62 kDa in size was observed in human iris, trabecular meshwork/ciliary body, retina, optic nerve and vitreous. One faint band observed was approximately 47.5 kDa in size and was present in human iris, trabecular meshwork/ciliary body and optic nerve. A second faint signal of 38 kDa was seen in iris and retina.

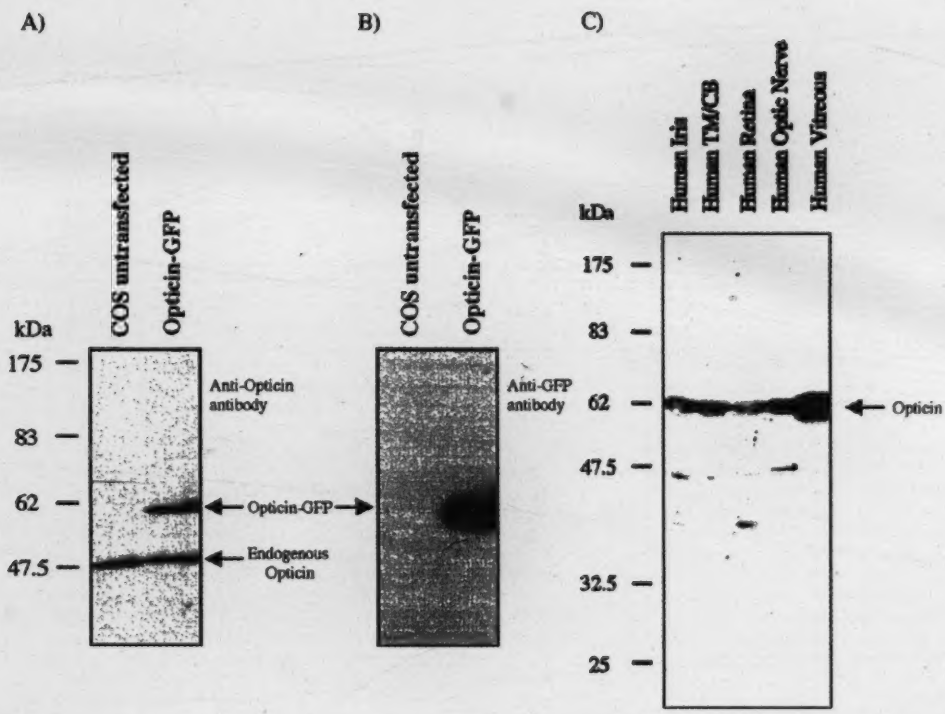
A)
B)
C)
COS untransfected
Opticin-GFP
kDa
175
83
62
47.5
Anti-Opticin antibody
Opticin-GFP
Endogenous Opticin
Anti-GFP antibody
Human Iris
Human TM/CB
Human Retina
Human Optic Nerve
Human Vitreous
32.5
25
Opticin

To further delineate the location of opticin protein in the human eye, I performed immunohistochemistry analysis on eye sections from a human male donor (Figure 2-11). This data was interpreted with the assistance of Dr. Paul Hiscott (Unit of Ophthalmology, University Clinical Departments, Liverpool). Several regions of the eye labeled with the anti-opticin antibody. In the anterior part of the eye, the corneal epithelium basal layer stained heavily (Figure 2-11B), while diffuse staining was observed in the corneal stroma (Figure 2-11B). Within the angle of the eye, the iris vessel walls and stroma around the iris and ciliary body were strongly stained (Figure 2-11D,F). Iris muscles (sphincter and dilator) and ciliary body muscle labeled at background levels (Figure 2-11D,F). The uveal tract labeled, and the trabecular meshwork and sclera showed some staining (Figure 2-11F). Towards the back of the eye, the vitreous and choroid contained the most intense labeling (Figure 2-11H). In the retina, staining was present in the choriocapillaris and where the vitreous attached into the retina. Bruch's membrane had a small amount of staining, while drusen were not labeled. The outer layers of the retina did not label, but the inner retina became increasingly stained towards the optic nerve. Retinal vessel walls also stained. It was not possible to determine whether staining was present in the RPE due to its pigmentation.

Figure 2-11: Immunohistochemistry of the Human Eye with anti-Opticin Antibody

Immunohistochemistry photomicrographs from various parts of the eye stained with the red chromagen AEC (9-amino-3-ethylcarbamazole). A,C,E,G and I are from control sections in which the primary anti-opticin antibody was excluded. B, D, F, H and J are from sections labeled with the affinity purified anti-opticin antibody.

A and B are anterior cornea. Corneal epithelium immunoreactivity is indicated by arrows. diffuse staining in the stroma is noted by stars.

C and D are iris and posterior cornea. No staining was observed in corneal endothelium and Descemet's membrane. However, arrows mark staining in iris vessel walls and a star shows staining in stroma next to one vessel.

E and F are ciliary body. An arrow notes labeling in ciliary body stroma. A star marks ciliary muscle, which did not stain.

G and H are vitreous base, peripheral retina, choroid and sclera. Stars indicate staining in vitreous base. Arrows mark regions where vitreous tufts enter into the retina. Closed circles show staining in the choroid. Sclera did not stain.

I and J are posterior neuroretina. Focal staining was present in neuroretina and arrows note vessel wall staining.

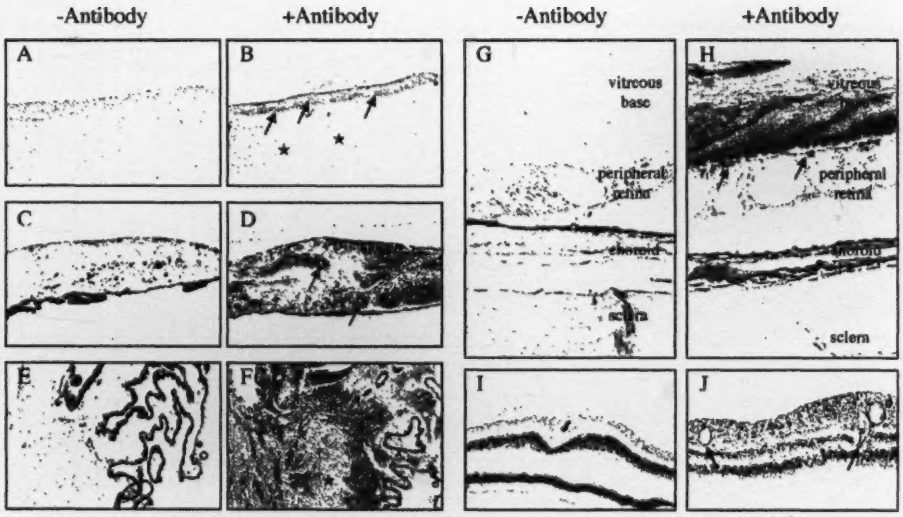
-Antibody
+Antibody
-Antibody
+Antibody
A
B
G
H
vitreous base
peripheral retina
sclera
C
D
E
F
I
J

I decided to perform a genetic screen of *OPTC* in AMD and glaucoma patients, as opticin protein is present in the eye and because of *OPTC*'s location within an AMD locus. Glaucoma patients were also tested as opticin protein was present in tissues associated with this condition, namely the ciliary body and the optic nerve. The genetic screen was carried out in collaboration with Dr. Vincent Raymond's laboratory. More information of this screen as predominantly described by Mathieu Faucher (a Ph.D. student in Dr. Raymond's laboratory) and Dr. Raymond is included in Appendix A.

Four nonsynonymous alterations (Ile182Thr, Arg229Cys, Leu268Pro and Arg325Trp) were detected by our colleagues. These changes are shown in a four species amino acid alignment in Figure 2-9. Three of the four alterations are likely polymorphisms as they were detected in normal controls. The Arg229Cys variation was of interest as it was found in homozygous form in an individual with neovascular AMD and was not observed in any controls. Dr. Raymond recruited the other family members for study (see Appendix A for details). Within this family, four individuals have either AMD or foveomacular dystrophy, while three were clinically normal. It was determined that the Arg229Cys change could not be responsible for the hereditary component of AMD in this family, as the alteration didn't segregate with the disease. Two family members with heterozygous forms of the variation were clinically normal. However, the Arg229Cys homozygous proband had the more severe neovascular form of AMD, while his siblings did not. The proband was originally diagnosed with AMD at 71 years of age.

The presence of the homozygous Arg229Cys variation in our AMD population to our control population was compared through the Fisher's exact test, by using the program created by Dr. David Nash at http://www.zi.ku.dk/personal/drnash/Pages/program.htm (University of Copenhagen, Denmark). Using individuals having only AMD (n=45), and clinically investigated normal subjects (n=55), I determined a non-statistically significant p-value of 0.45. This demonstrates that the association between the homozygous Arg229Cys and AMD is not statistically significant. However, a wider screen of AMD patients may reveal additional patients with *OPTC* alterations.

To examine any biological effect of the Arg229Cys change on Opticin, I expressed normal and mutant forms of OPTC in COS-7 cells. Extracts were size separated under non-reducing, denaturing SDS PAGE gels and examined through immunoblot analysis. No differences in migration were detected between wild-type and Arg229Cys Opticin (data not shown). Similar experiments using media from the transfected cells did not indicate the presence of Opticin (data not shown).

Discussion:

Differential selection is one method that can be used to isolate tissue specific genes. One strength of differential selection is that, unlike a subtracted cDNA library, the differential screen may be repeated with cDNA from different tissues without having to reconstruct the cDNA library. One limitation of a differential screen is that genes important in ocular function but also expressed in lymphoblasts will be missed by this screen. In my differential screen, I chose cDNAs which appeared to be more highly expressed in iris tissue than lymphoblasts or more highly expressed in trabecular meshwork tissue than iris tissue or lymphoblasts. Lymphoblasts were chosen for the screen as lymphoblast RNA was readily available at that time. Although the above limitation still exists for my screen, this strategy will allow the identification of cDNAs with some lymphoblast expression that are highly expressed in iris tissue or trabecular meshwork tissue that would otherwise have been excluded from the screen. In addition, because the iris cDNA library was made using adult human iris mRNA, any developmentally related ocular disease causing genes not expressed in the adult iris would also be missed. These two limitations would however also be present in a subtractive cDNA library screen, depending on the tissues used.

IR185, one novel gene isolated from this differential screen, was selected for further genetic, biochemical and cell biology characterization. Based on IR185's putative

glycosylation site and expression in iris and retinal tissues I have named IR185 Oculoglycan. As portions of this chapter were being published, two other groups reported the finding of the Oculoglycan transcript (146,147). The Human Nomenclature Committee has chosen Opticin (*OPTC*) as the official name for this gene. Opticin is homologous to Osteoglycin (155) and Epiphycan (156), two members of the small leucine-rich proteoglycan (SLRP) family of proteins, which are secreted and associated with the extracellular matrix (157,158). SLRP proteins are characterized by several leucine-rich motifs (158) bounded by conserved cysteine residues that are hypothesized to form internal disulfide bonds (159). The 24 amino acid leucine-rich repeat consensus sequence is: x-x-I/V/L-x-x-x-x-F/P/L-x-x-L/P-x-x-L-x-x-L/I-x-L-x-x-N-x-I/L, where 'x' represents any amino acid (158). Within the consensus sequence, the multiple amino acids listed in positions 3,8,11,17 and 24 are in order of decreasing frequency (158). Leucine-rich repeat consensus amino acids 3-11 and 14-24 are predicted to form a β-sheet and an α-helix respectively (158). The SLRP family is divided into three main classes based on the cysteine spacings on the amino flank of the leucine repeats (158). Osteoglycin and Epiphycan are the sole members of the class 3 SLRPs. Opticin's predicted homology to these proteins at the amino acid level and conservation of cysteine residues among the three proteins strongly suggest that Opticin is also a class 3 SLRP.

Expression of SLRP genes appears to vary depending on their class. Class 1 SLRP genes, Decorin and Biglycan, are expressed in virtually every tissue tested (158),

whereas Class 2 genes, Fibromodulin, Keratocan, Lumican and Proline-arginine-rich and leucine-rich repeat protein (PRELP) are expressed in seven or fewer tissues (160-162). Class 3 genes appear to be expressed in the fewest tissues. Mouse Osteoglycin is expressed in skeletal muscle, lung, kidney and testis (163). Osteoglycin was originally cloned from bovine bone (155). Epiphycan was only seen in placenta in northern blotting experiments (164). Opticin also has a limited tissue expression profile, suggesting that the class 3 SLRP proteins may have a more tissue-specific function than the other SLRP proteins. As other SLRPs are known to bind to collagen (165-167). Opticin may be a novel collagen-associated glycoprotein with a role in eye function.

Two small leucine-rich repeat proteins, keratocan and nyctalopin, have recently been shown to be involved in ocular disease. Keratocan, a class II SLRP, is mutated in individuals with a recessive form of cornea plana, a disorder in which the curvature of the cornea is flattened (168,169). Thirty-five Finnish families and a Chinese-American individual with cornea plana and, recently, a family from Bangladesh with cornea plana and microphthalmia, had either homozygous amino acid substitutions or a homozygous stop mutation in the keratocan gene. These alterations may either eliminate keratocan activity or possibly alter keratocan's binding to collagen (168,169). Nyctalopin, a glycosylphosphatidyl (GPI)-anchored protein, is mutated in an X-linked form of congenital stationary night blindness in a variety of families (170,171). Changes reported

included missense mutations, insertions and deletions in the nyctalopin gene. The mutations observed are thought to affect retinal cell to cell interconnections (170,171).

The size differences between the iris and fetal liver Opticin transcript (Figures 2-5 and 2-6) might be the result of alternative splicing. Alternatively, the increased transcript size might be additional untranslated 3' or 5' sequence or could encode for a larger Opticin protein product in fetal liver. Further studies, such as a screen of a fetal liver library, would be required to determine the nature of the longer Opticin transcript in fetal liver.

OPTC is located near the same chromosomal region as two eye related disorders, age-related macular degeneration (1q25-q31) and retinitis pigmentosa 12 (1q31-1q32) (116,151). *OPTC* was originally localized within the same chromosomal region as posterior column ataxia with retinitis pigmentosa (1q31-q32) (152). Through a collaboration with Dr. J.J. Higgins, (Wadsworth Center, New York State Department of Health) it was determined that *OPTC* was not in the narrowed critical region for AXPC1.

Opticin cDNA has also been isolated from another iris cDNA library and a retinal cDNA library (146,147). Transcripts were observed by RT-PCR in retina, skin and ligament (146). Opticin protein has been isolated from bovine vitreous extracts containing collagen fibrils and has been reported to be glycosylated with sialylated O-linked oligosaccharides in bovine vitreous (146). *In situ* hybridization analysis of opticin in mice showed expression in ciliary body during development from at least 15.5 dpc to

adulthood (154). The canine ortholog was recently examined and excluded as a candidate for canine oculo-skeletal dysplasia (153).

The N-terminal affinity purified antibody used in the immunoblot and immunohistochemistry experiments was initially tested against a recombinant opticin-GFP fusion protein. I determined that the antibody was able to detect the opticin protein as immunoblot experiments identified a band of the expected size in only the transfected COS-7 cells. This finding was confirmed through immunoblot experiments using anti-GFP antibody. The opticin recombinant immunoblot experiment additionally detected an approximate 47.5 kDa band in both the transfected and untransfected lanes. The size observed corresponds to the previously observed size of bovine opticin (146) and suggests that COS-7 cells endogenously express opticin.

In human tissues I observed, through immunoblot blot analysis, a prominent band at 62 kDa in iris, trabecular meshwork/ciliary body, retina, optic nerve and vitreous and weaker bands at 45 kDa and 38 kDa. Previous work using antisera raised against a C-terminal peptide of opticin, in immunoblot experiments, showed major bands in human iris, ciliary body and retina at 48 kDa and other, smaller, heavy bands in retina (147). In rat tissues, the same antisera generated bands in trabecular meshwork/iris, vitreous, retina, optic nerve head and brain (147). In dog, opticin was reported to be present in skeletal muscle, testes, skin, ligament and rib chondrocyte (153). In dog eye, opticin was observed in RPE, retina, iris and vitreous (153). It is possible that the observed

differences in the major protein size of human opticin is due to differences in protein treatment, or differing levels of post-translational modification between individuals examined. The differing sizes of opticin protein seen between species by others and us (data not shown) suggest that levels of post-translational modifications of opticin may vary between species and within species.

Interestingly, I also observed opticin protein in the optic nerve (Figure 2-10). As the optic nerve tissue was extracted prior to eye disruption, there was no possibility for this tissue to be contaminated by other opticin containing tissues. As a secreted extracellular matrix protein, it is possible that opticin protein traveled from the eye to the optic nerve. Alternatively, *OPTC* mRNA may be expressed at some low level in the human optic nerve. Further work, such as RT-PCR experiments, will be required to delineate the presence of *OPTC* mRNA in the optic nerve.

Age-related macular degeneration (AMD) is the leading cause of blindness in North America. AMD incidence ranges depending on age, from 0.2% among those aged 55 to 64 years, to 13% in those over 85 years of age (172). Strongly associated with AMD is the presence of drusen, located between Bruch's membrane and the basal lamina of the retinal pigment epithelium. Drusen may be described as being "hard" or "soft" with "soft" drusen being more strongly associated with exudative AMD. Work using electron microscopy has shown that cell processes from the choroid pass through Bruch's membrane into drusen (173). Studies of carbohydrates within drusen identified a drusen

"core" with O-linked oligosaccharides (174). The presence of O-linked oligosaccharides was observed after neuraminidase digestion of the eye sections used (174). Opticin was previously reported to contain sialylated O-linked oligosaccharides (146). The physical location of opticin in the choroid, the observation that drusen may be choroidally based, and opticin's previously described post-translational modifications make it tempting to hypothesize that opticin protein may be located within the core regions of drusen. An extension of this hypothesis would be that opticin might be involved in drusen biogenesis. Although we did not observe opticin protein within drusen in this study, I did not treat my tissue in the same manner as the aforementioned study (174).

Recently, a whole genome scan for susceptibility loci for AMD was carried out (135). In this paper, the three groups of patients (Models A through C) studied had incidences of neovascularization ranging from 65% to 72%, depending on the clinical stringency applied. In our study, the incidence of neovascularization in our AMD patient pool was at least 70%. In our AMD with glaucoma group, no patients were reported to have neovascularization.

Our collaborators observed a single proband with severe AMD who had a homozygous arginine to cysteine alteration at the encoded amino acid 229 of the opticin protein. The change observed was in an amino acid completely conserved among human, dog, mouse and pig opticin orthologs. The Arg229Cys change is of note because opticin and other SLRPs contain six conserved cysteine residues, of which at least two are

known to form internal disulfide bonds (158). The addition of another cysteine residue to the opticin protein could conceivably cause problems in protein folding. Mutations involving cysteine residues have been observed in nyctalopin. One observed mutation in nyctalopin eliminated a cysteine through alteration to a serine at amino acid 31 (171). A second change inserted the three amino acids "CysLeuArg", while a third mutation removed eight amino acids including two cysteine residues (170). The opticin Arg229Cys alteration was only seen in two other individuals. Both were siblings of the proband with the alteration in heterozygous form and each had a normal phenotype. These findings are consistent with individuals heterozygous with keratocan mutations having no disease phenotype (168,169). The presence of the more severe neovascular form of AMD in the homozygous Arg229Cys proband is consistent with the finding that all keratocan or nyctalopin allele(s) are mutated in their respective diseases. This finding raises the possibility that opticin could be a modifier of the AMD phenotype. However, my statistical analysis has determined that the association between the Arg229Cys variation and AMD is not significant. With the current patient pool, it was estimated that over 860 control individuals would have to be screened to achieve a significant result. Therefore any association between opticin and AMD should currently be considered speculative. I conclude that larger studies would have to be performed to more fully examine the relationship, if any, between opticin and AMD.

I performed additional experiments to try to detect migrational changes of the Arg229Cys opticin variant when compared to the normal protein (data not shown). In another secreted extracellular matrix protein, TIMP3, an additional cysteine residue causes the protein to dimerize (175). This event can be observed in an SDS PAGE gel under denaturing, non-reducing conditions. I was unable to detect any gross changes in migration of the altered opticin protein. Although opticin was able to be expressed in COS-7 cells, there was no evidence to suggest that the protein was folding properly or being secreted into the media. Therefore it is possible that the expected changes in migration would be impossible to observe using the methodologies described herein. A second possibility is that the Arg229Cys alteration does not affect the ability of opticin to migrate and would still not be observed, even if other protein expression techniques were employed. Further work using other protein expression technologies would be required to determine which is the case.

Chapter III: Isolation of a Ubiquitin-Like (UBL5) Gene from a Screen Identifying Highly Expressed and Conserved Iris Genes

Friedman, J.S., Koop, B.F., Raymond, V., Walter, M.A. Isolation of a Ubiquitin-Like (UBL5) Gene From a Screen Identifying Highly Expressed and Conserved Iris Genes. (2001) Genomics. 15;71(2):252-5.

Introduction:

As described in the previous chapter, I used differential selection to search for genes expressed in the iris and trabecular meshwork. Another methodology for selecting genes is to examine genes that are conserved between species and are highly expressed in the tissue of interest. This approach has been used in conjunction with differential selection to identify genes in the retina (140,141), but has not been applied on its own as a selection technique to identify genes highly expressed and conserved in the anterior segment of the eye. This method contrasts with subtractive approaches in that the cDNAs identified can be expressed in more than one tissue type. As retinal disease and glaucoma-causing disease genes can be expressed in a variety of tissues, e.g. *REP-1* (176), *TIMP3* (120), *PITX-2* (177) and *FKHL7* (78), I hypothesized that a conservation-based methodology can be useful in identifying disease-causing genes or genes encoding important tissue related proteins.

This chapter describes the screening of the iris cDNA library that I described in Chapter II to identify highly expressed human iris cDNAs that are conserved between humans and pigs. One novel cDNA, which I will call the Ubiquitin-like 5 gene (*UBL5*), was isolated using this method and analyzed in detail. The *UBL5* gene's chromosomal location and genomic sequence was identified. A *UBL5* pseudogene was also found and its location and genomic structure was determined. The *UBL5* gene was found to be

expressed at varying levels in all tissues examined. Intracellular localization experiments and immunoblot experiments were also performed. Further characterization of the *UBL5* gene will determine the function of the encoded protein and whether it is a candidate for ocular disease.

Materials and Methods:

Identification of Iris cDNAs Which Hybridize at High Stringency to a Porcine Anterior Segment Angle Probe:

The human adult iris cDNA library described in Chapter II was grown in the presence of IPTG (Roche Diagnostics, Laval PQ) and X-gal (Roche Diagnostics). Isolated white plaques, representing a single cDNA containing phage, were picked for screening. Each selected phage was stabbed onto a 20 X 20 grid pattern and grown on 245 mm square bioassay dishes (Fisher Scientific, Nepean ON). I used a total of 4 bioassay dishes to grid out 1568 phage. The phage were allowed to grow until the plaques reached a size of approximately 0.5 cm in diameter. Filter lifts using Hybond-N (Amersham Pharmacia Biotech, Baie d'Urfé, PQ) nylon filters were made of each of the four bioassay dishes as described in Chapter II.

Porcine eyes were obtained from a local abattoir. Anterior segment angle tissue (including iris, trabecular meshwork, and ciliary body tissues) was cut from the eyes and total RNA and mRNA was isolated as described in Chapter II. Oligo-dT primed first strand synthesis of porcine anterior segment angle cDNA was carried out using Superscript I RT (Gibco-BRL).

Each nylon filter was probed with an anterior segment angle porcine single stranded cDNA probe. Porcine cDNA (50 ng) was radiolabeled with ^{32}P dCTP using the

Random Primed Labeling Kit (Gibco-BRL) for each nylon filter. The hybridizations were carried out using Church and Gilbert hybridization solution (142). Each radiolabeled probe was denatured with 50 μg COT-1 DNA at 95°C, cooled rapidly on ice, added to one set of pre-hybridized filter lifts and hybridized at 65°C overnight. The filter lifts were washed under low stringency conditions (2X SSC, 0.05% SDS for 30 minutes at room temperature), followed by high stringency washes (0.1X SSC, 0.1% SDS for 40 minutes at 50°C). The filters were exposed to Biomax film (Kodak, Rochester, NY) at –80°C for 1 week.

Elimination of Elongation factor 1-alpha from selected cDNAs:

cDNA containing plaques observed to be positively hybridizing were cored and grown on a single grid. A filter lift was made of the grid as described above. The filter was probed with one cDNA (Elongation factor 1-alpha) isolated from the grid in an effort to limit the number of cDNAs sequenced. The hybridization and washes were carried out in the same manner as above. The remaining cDNAs were isolated using the *in vivo* excision protocol as supplied by the manufacturer (Stratagene, La Jolla CA) and sequenced using a LI-COR DNA sequencer (LI-COR Inc, Lincon, NE).

Northern Blot hybridization:

50 ng of Iris Grid 5 cDNA (UBL5) was randomly primed and radiolabeled as described in Chapter II. The probe was hybridized to the Clontech Human 12-Lane Multiple Tissue Northern Blot, containing approximately 1 μg of poly A+ RNA per lane, at 68°C for one hour using ExpressHyb hybridization solution (Clontech, Palo Alto CA). The northern blot was washed as above and exposed to Biomax film (Kodak). The northern blot was subsequently probed with β-actin cDNA to control for RNA loading.

A northern blot containing 3 μg of human iris and human lymphoblast total RNA was made using standard methods (178). The northern blot was probed with Iris Grid 5 (UBL5) cDNA and control β-actin cDNA, as described above.

Computer Based (in silico) Searches:

The Iris Grid 5 (UBL5) putative amino acid sequence alignment was performed at the BCM search launcher web site (http://kiwi.imgen.bcm.tmc.edu:8088/search-launcher/launcher.html). The putative protein motifs and predicted cellular localization of the putative Iris Grid 5 (UBL5) protein and other Ubiquitin-like 5 proteins were predicted using software at the ExPASy-Prosite web site (http://www.expasy.ch/). BLAST analysis was performed at the NCBI web site (http://www.ncbi.nlm.nih.gov/).

The Iris Grid 5 (UBL5) genomic sequence and the Iris Grid 5 (UBL5) pseudogene sequence were identified using the BLAST algorithm. The NCBI map viewer (http://www.ncbi.nlm.nih.gov/) was subsequently used to determine the chromosomal location of both the Iris Grid 5 (UBL5) gene and Iris Grid 5 (UBL5) pseudogene.

The three dimensional fold prediction (179) of Iris Grid 5 (UBL5) and the UBL5 homologs were performed at the Bioinbgu web site (http://www.cs.bgu.ac.il/~bioinbgu/).

Intracellular Localization:

The UBL5 cDNA was cloned into the pcDNA4/HisMax C vector (Invitrogen, Carlsbad, CA). The pcDNA4/HisMax C-UBL5 construct was sequenced using a LI-COR DNA sequencer to verify that the UBL5 DNA sequence was in frame with the vector DNA sequence encoding for the N-terminal Xpress™ epitope. Transfection of construct DNA into COS-7 cells on coverslips were performed as described in Chapter II.

The COS-7 cells were fixed with 1% paraformaldehyde for 15 minutes and washed three times with phosphate buffered saline (PBS) solution. A 0.05% TritonX-100 solution was placed on the cells for ten minutes to permeabilize them. The cells were washed three times in PBS and then blocked with 5% bovine serum albumin (BSA) for 30 minutes. Recombinant protein was detected with a 1:400 dilution of Anti-Xpress™ antibody (Invitrogen), followed by a 1:400 dilution of secondary rabbit-anti-mouse antibody linked to Cy3 (Jackson ImmunoResearch, West Grove, PA). Both antibodies

were diluted with 1% BSA. DAPI dye was used to stain nuclei, and the cells were examined by fluorescence microscopy.

Immunoblot Analysis:

Whole cell extracts were isolated 48 hours post transfection as described in Chapter II. Extracts were separated by SDS-PAGE and transferred to nitrocellulose (Trans-Blot Transfer Medium, Bio-Rad Laboratories, Hercules, CA). Recombinant UBL-5 protein was detected with a mouse monoclonal antibody, Anti-Xpress™ (1:5000 dilution), to the plasmid encoded Xpress™ epitope. The secondary antibody, goat-anti-mouse (1:1666 dilution), linked to horseradish peroxidase (Pierce, Rockford, IL), was detected by SuperSignal West Pico Chemiluminescent Substrate (Pierce).

Results:

I performed a screen on 1568 plaques representing 1568 individual cDNAs from an adult iris grid cDNA library. A schematic of the screen is shown in Figure 3-1. An example autoradiograph from the screen is shown in Figure 3-2. 176 cDNAs cross-hybridizing to a porcine anterior segment angle cDNA probe were selected for sequencing. The three largest classes of genes isolated using my screen were ribosomal (96 cDNAs, 54.5%), crystallins (26 cDNAs, 14.8%), and elongation factor 1-alpha (19 cDNAs, 10.8%). Of the remaining genes, the cDNA isolated at the highest frequency encoded the translationally controlled tumor protein (TPT1). I had previously isolated one cDNA, Oculoglycan (144) also named Opticin (146,147) from a differential selection screen of the same iris cDNA library. The isolated genes are listed in Table 3-1.

Figure 3-1: Schematic Diagram of Screen for Highly Expressed and Conserved Genes

Schematic diagram of a screen for genes highly expressed and conserved between species.

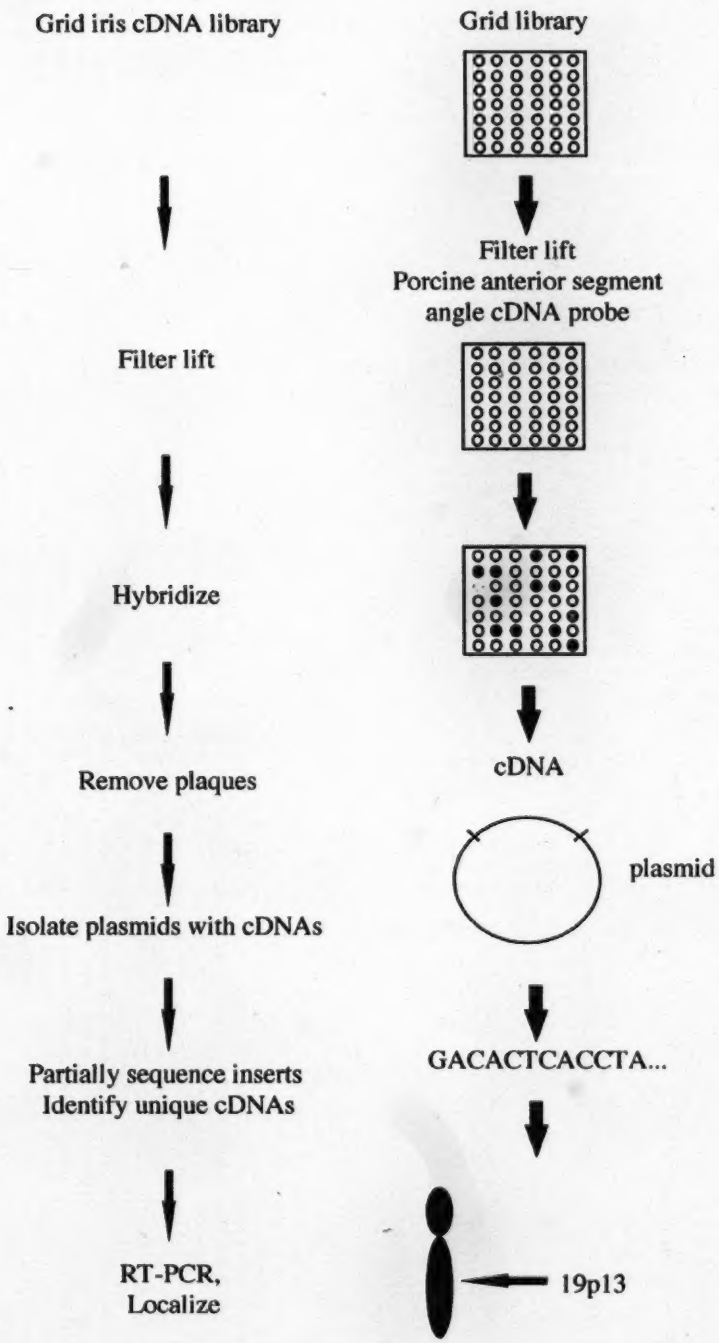
Grid iris cDNA library
Grid library
Filter lift
Porcine anterior segment
angle cDNA probe
Filter lift
Hybridize
Remove plaques
cDNA
plasmid
Isolate plasmids with cDNAs
GACACTCACCTA...
Partially sequence inserts
Identify unique cDNAs
RT-PCR,
Localize
19p13

Figure 3-2: Example Autoradiograph from the Highly Expressed and Conserved Iris Screen

Example autoradiograph from the highly expressed and conserved iris screen. Plaques chosen for further analysis are marked at their center by a small black dot. The plaque containing the UBL5 cDNA is at co-ordinate 20C.

Highly Expressed and Conserved Iris Screen: Plaque 20C contained the UBL5 cDNA

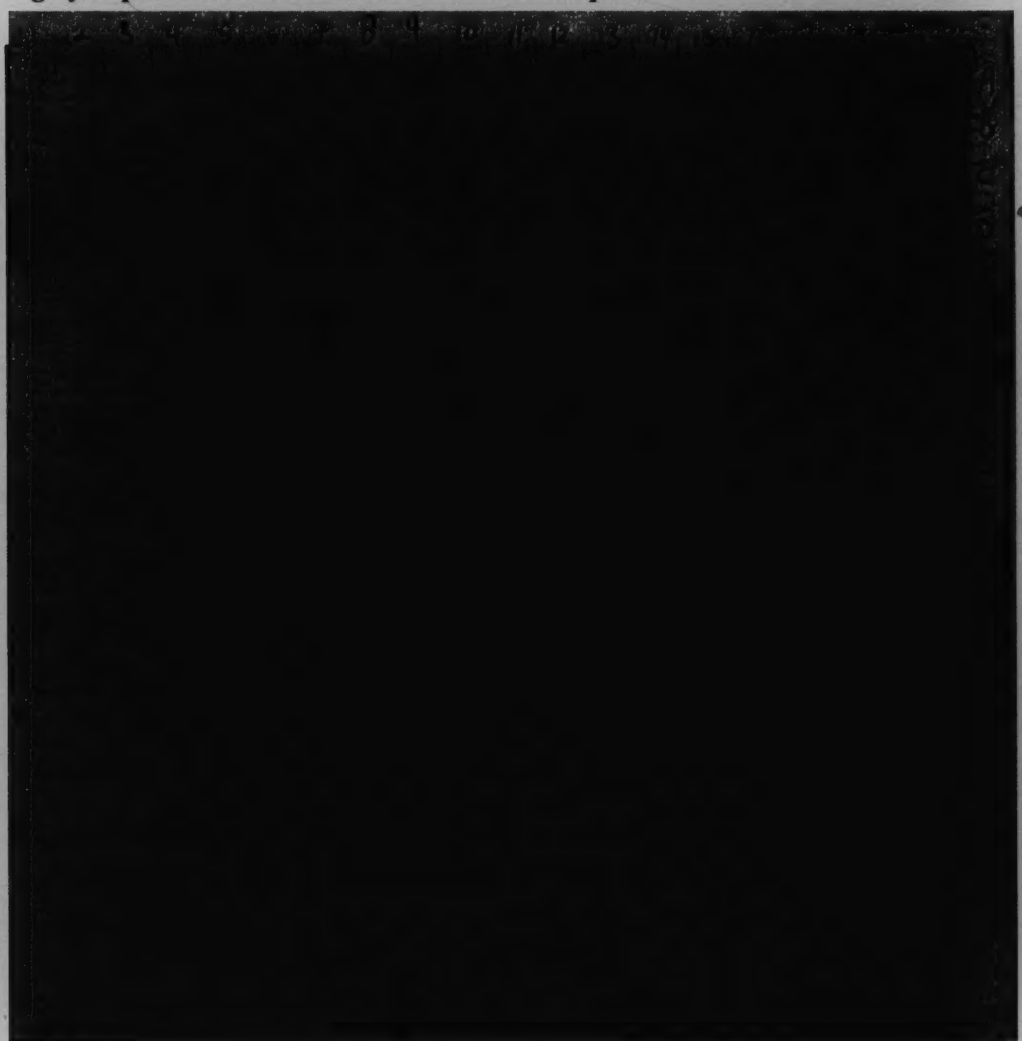

Table 3-1: Genes Isolated From a Human Adult Iris Library

Ribosomal Genes	No. of Clones
Ribo. Protein S3A	19
Ribo. Protein L31	17
Ribo. Protein S27	12
Ribo. Protein L11	5
Ribo. Protein L37	5
Ribo. Protein S7	4
Ribo. Protein S26	4
Ribo. Protein P1	3
Ribo. Protein S3	3
Ribo. Protein S18	3
Ribo. Protein, large	2
Ribo. Protein L9	2
Ribo. Protein L19	2
Ribo. Protein L32	2
Ribo. Protein S11	2
Ribo. Protein L12	1
Ribo. Protein L13a	1
Ribo. Protein L23	1
Ribo. Protein S4	1
Ribo Protein S8	1
Ribo. Protein S10	1
Ribo. Protein S12	1
Ribo. Protein S16	1
Ribo. Protein S24	1
Ribo. Protein S25	1
Ribo. Protien S29	1

Other Genes	No. of Clones
Elongation Factor	19
Translationally Controlled Tumor Protein	7
Mt genome	5
E. coli genomic	4
Ferritin H chain	3
Alpha Tubulin	2
Alkali light chain smooth & non-mucle myosin	1
B cell Translocation protein	1
Beta-tubulin	1
Calmodulin (CALM2)	1
Glutamine Synthase	1
Insulin-like growth factor binding protein 7	1
Nascent polypeptide assoc. complex alpha-polypeptide	1
Oculoglycan/Opticin	1
Poly-ubiquitin/ubiquitin	1
T-cell cyclophillin	1
Thymosin Beta-4	1
Type 2 phosphatidic acid phosphatase alpha-1	1
Vimentin	1

Crystallin Genes	No. of Clones
Beta B2 Crystallin	12
Beta A1/A3 Crystallin	8
Alpha B Crystallin	5
Beta B1 Crystallin	1

Novel Gene	No. of Clones
Iris Grid 5 (UBL5)	1

One novel cDNA, Iris Grid 5, was identified using my screen. This cDNA was 413 nucleotides in length and could encode a 73 amino acid protein (Figure 3-3A). BLAST analysis of the predicted protein determined that it was highly similar to four proteins: a putative protein in *A. thaliana* (Genbank accession no.: CAB72156), a protein named 'weak similarity to *Arabidopsis thaliana* ubiquitin-like protein 8' in *C. elegans* (180) (Genbank accession no.: AAB42266), the ubiquitin-like protein in *S. pombe* (Genbank accession no.: CAB39137), and the protein encoded by open reading frame Ynr032c-ap in *S. cerevisiae* (181,182), (Genbank accession no.: NP014430). As a result of this comparison I have called the Iris Grid 5 cDNA, *Ubiquitin-like 5* (UBL5).

An amino acid alignment of the Ubiquitin-like 5 predicted protein with the above four proteins is shown in Figure 3-3B. Ubiquitin-like 5 is homologous (25.9% identical, 57.5% similar) to the last ubiquitin-like repeat in *Arabidopsis thaliana* ubiquitin-like protein 8 (183) (Genbank accession no.: S55243), and is also homologous (25.9% identical, 57.5% similar) to the last ubiquitin-like repeat in *Arabidopsis thaliana* polyubiquitin (183) (Genbank accession no.: AAA68879).

Figure 3-3: DNA Sequence and Amino Acid Alignment of Ubiquitin-Like 5 (UBL5)

A) DNA sequence of Iris Grid 5 (UBL5). The hypothesized start methionine is in bold. DNA trinucleotides encoding in-frame stop codons are boxed.

B) Amino acid alignment of the putative Iris Grid 5 protein (UBL5) with its homologues in *C. elegans*, *A. thaliana*, *S. pombe* and *S. cerevisiae*. Identical residues among all four proteins are shaded in grey. A putative amidation site is shown by a white rectangle. A potential casein kinase II phosphorylation site is indicated by a black rectangle. Right: Percent identity and percent similarity of the predicted Iris Grid 5 protein (UBL5) to other members of the putative UBL5 sub-family.

A)

```
GGCACGAGCT CGGGTGAGGA GCTGGTGGCG TCGGCAGGTT CGAGGCGATT CGAGCTCCAG      60

     M  I  E  V  V  C  N  D  R  L  G  K  K  V  R  V  K  C              19
CTAGGATGAT CGAGGTTGTT TGCAACGACC GTCTGGGGAA GAAGGTCCGC GTTAAATGCA     120

N  T  D  D  T  I  G  D  L  K  K  L  I  A  A  Q  T  G  T  R           39
ACACGGATGA TACCATCGGG GACCTTAAGA AGCTGATTGC AGCCCAAACT GGTACCCGTT     180

W  N  K  I  V  L  K  K  W  Y  T  I  F  K  D  H  V  S  L  G           59
GGAACAAGAT TGTCCTGAAG AAGTGGTACA CGATTTTTAA GGACCACGTG TCTCTGGGGG     240

D  Y  E  I  H  D  G  M  N  L  E  L  Y  Y  Q                        73
ACTATGAAAT CCACGATGGG ATGAACCTGG AGCTTTATTA TCAATAGATG AGAATCCTCA     300

TCTTCCTGCC CCGCTTTCCT CTCCCATCCT CATCCCCCAC ACTGGGATAG ATGCTTGTTT     360

GTAAAAACTC ACCTTAATAA AGACTTAGAT GTTGAAAAAA AAAAAAAAAA AAA            413
```

B)

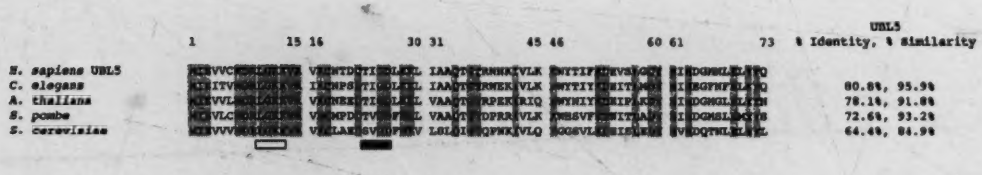

In silico analysis of the Ubiquitin-like 5 predicted protein, using the PROSITE program, predicted two Casein Kinase II phosphorylation sites at amino acids 23-26 and 56-59, one myristylation site at amino acids 36-41 and one amidation site at amino acids 10-13. *In silico* analysis of the Ubiquitin-like 5 putative protein homologues using the PROSITE program revealed that the Casein Kinase II phosphorylation site at amino acids 23-26 and the amidation site at amino acids 10-13 were predicted in all proteins. Using the fold recognition program at the Bioingu web site, the UBL5 putative protein was predicted to fold in a similar manner to ubiquitin. All of the other Ubiquitin-like 5 proteins were also predicted to have a three dimensional fold resembling ubiquitin. Predicted folding consensus scores for all of the ubiquitin-like 5 proteins ranged from 50.3-58.2, well above the threshold consensus score of 12 (179). Further *in silico* analysis using the PSORT II program predicted that the Ubiquitin-like 5 predicted protein was 43.5% likely to be located in the cytoplasm. The Ubiquitin-like 5 homologues were also predicted to be cytoplasmic (39.1%-65.0%) using the PSORT or PSORT II program.

Northern blot analysis of the Ubiquitin-like 5 cDNA was carried out using the Clontech Human 12-Lane Multiple Tissue Northern Blot and a northern blot containing 3 μg total human iris and 3 μg total lymphoblast RNA. The Ubiquitin-like 5 gene produces a transcript of approximately 0.6 kb in size and was expressed at varying levels in all tissues tested. Expression of the Ubiquitin-like 5 gene was highest in heart, muscle, kidney, liver, iris and lymphoblast tissues (Figure 3-4A,B).

The UBL5 genomic sequence was identified using the BLAST algorithm and is located in BAC CTD-2623N2 (Genbank accession no. AC008752.5). BAC CTD-2623N2 was previously mapped to chromosome 19p13.2. The UBL5 gene consists of at least six exons (Table 3-2). The UBL5 processed pseudogene was also identified using *in silico* methods. The pseudogene was present in BACs RP11-474K4 (Genbank accession no. AC021852.4), RP11-443G13 (Genbank accession no. AC026620.2), and RP11-55J8 (Genbank accession no. AC015941.5). All three BACs were previously mapped to chromosome 17 and overlap on chromosome 17p11.2.

Figure 3-4: Northern Blot Analysis of Ubiquitin-like 5 (UBL5)

A) Analysis of the expression pattern of UBL5. Top: Northern blot hybridization analysis of Iris Grid 5 (UBL5) cDNA to a Clontech Human 12 Lane Multiple Tissue Northern Blot. Each lane contains approximately 1 μg of poly A+ RNA. Tissue sources in each lane are labeled. Bottom: β-actin control probing of the above blots.

B) Top: Northern blot hybridization analysis of Iris Grid 5 (UBL5) cDNA on a northern blot containing 3 μg total RNA from human iris and human lymphoblast tissues. Bottom: β-actin control probing of the above blot.

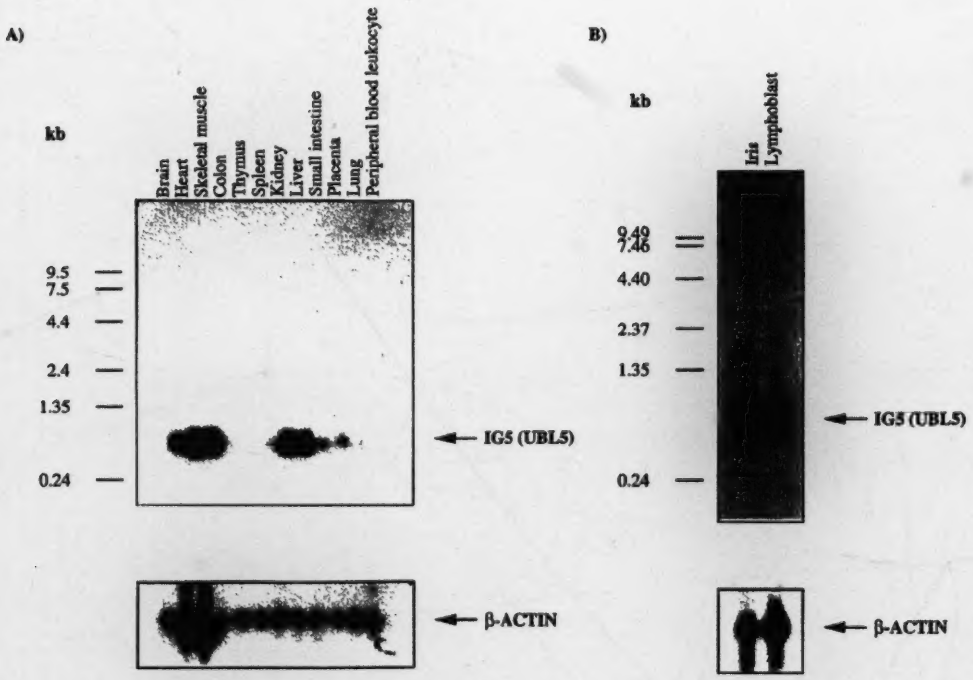
A)
kb
Brain
Heart
Skeletal muscle
Colon
Thymus
Spleen
Kidney
Liver
Small intestine
Placenta
Lung
Peripheral blood leukocyte
9.5
7.5
4.4
2.4
1.35
0.24
IG5 (UBL5)
β-ACTIN
B)
kb
Iris
Lymphoblast
9.49
7.46
4.40
2.37
1.35
0.24
IG5 (UBL5)
β-ACTIN

Table 3-2 Intron/Exon Boundary Sequences of the Ubiquitin-like 5 (UBL5) Gene

3′ SPLICE ACCEPTOR	EXON	SIZE(bp)	5′ SPLICE DONOR	INTRON	SIZE(bp)
	2	47	AGGCGATTCGAG**gt**gaggggtca	2	342
cgctttgtgt**ag**CTCCAGCTAGGA	3	67	CGTTAAATGCAA**gt**atccactggc	3	198
ctctgcgccc**ag**CACGGATGATAC	4	84	CCTGAAGAAGTG**gt**gagtgcagcg	4	161
tcttttttctt**ag**GTACACGATTTT	5	38	CTCTGGGGGACT**gt**atcctttgtg	5	1090
cctttccttc**ag**ATGAAATCCACG	6	151			

Invariant bases are underlined

The pseudogene has several changes relative to the UBL5 gene including: 1) containing no introns, 2) a deletion removing 42 bp of the region corresponding the 5' UTR of the UBL5 gene, 3) A silent G to A transition corresponding to base pair 101 of the UBL5 cDNA, 4) an arginine to histidine alteration corresponding to amino acid 15 of the putative UBL5 protein and 5) a glutamine to stop alteration corresponding to amino acid 34 of the putative UBL5 protein.

Intracellular localization experiments in COS-7 cells determined that the recombinant UBL5 protein is localized to the cytoplasm, as predicted (Figure 3-5A). Immunoblot analysis showed that the recombinant UBL5 protein is of the approximate size predicted (Figure 3-5B). The recombinant UBL5 protein with the 4 kDa Xpress™ epitope tag was estimated to be 12 kDa in size.

Figure 3-5: Intracellular Localization and Immunoblot Analysis of Ubiquitin-like 5 (UBL5)

A) Immunoblot analysis of protein extracts from COS-7 cells transfected with pcDNA vector containing UBL5 cDNA.

B) Intracellular localization of UBL5. COS-7 cells were transfected with pcDNA vector containing UBL5 cDNA.

A)

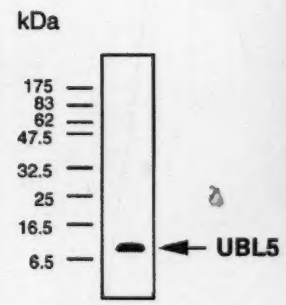

B)

Discussion:

Searching for highly expressed and evolutionarily conserved genes is one method that can be used to isolate genes important for a given tissue. One of the strengths of this approach is that the expression pattern of genes identified is not limited to a single tissue, as in a subtractive method. In my case, this can be an advantage as genes known to be important in eye disease are expressed in multiple tissues (78,120,176,177). One weakness of this approach, using my current method, is the isolation of a high number of highly expressed housekeeping genes. To eliminate the background, it would be necessary to use a subtractive hybridization step using a panel of housekeeping genes to eliminate these cDNAs from the selected pool. I used only one cDNA, Elongation Factor 1-alpha, in a hybridization step to eliminate the cDNA from my pool of interest. It would be possible to use a pool of ribosomal, crystallin and Elongation Factor 1-alpha cDNAs in a single hybridization step to identify these cDNAs early on so they may be eliminated from the screen. This additional step would have removed the high background of housekeeping genes that I encountered in my screen.

I observed a high frequency of the translationally controlled tumor protein (TPT1) cDNA in my screen, suggesting a high level of expression of TPT1 in the iris. TPT1 was originally isolated in growing Ehrlich ascites tumor and was found to be under translational control (184). TPT1 has since been demonstrated to be expressed in other

non-tumorigenic tissues including erythrocytes, liver, keratinocytes and macrophages (185). As I identified TPT1 cDNA in my iris cDNA library, iris can be added to the list of tissues that expresses TPT1. The TPT1 protein is conserved between different species and has been shown to bind to Ca^{++} (185). TPT1 was identified as an immunoglobulin E-dependent histamine releasing factor believed to be involved in human allergic disease (186). The function of TPT1 protein in the eye is yet unknown.

I have identified a novel human cDNA, Iris Grid 5, using my screen. Iris Grid 5 cDNA's predicted protein homologies to a ubiquitin-like protein predicted in *A. thaliana*, C. *elegans*, *S. pombe* and *S. cerevisiae* show that it is highly conserved from humans to yeast. Due to its homology to the other ubiquitin-like protein genes, I am tentatively naming this gene Ubiquitin-like 5 (UBL5). Ubiquitin is a highly conserved 76 amino acid protein involved in protein degradation (187). The high homology of UBL5 predicted protein with its *A. thaliana*, C. *elegans*, *S. pombe* and *S. cerevisiae* equivalents, suggests a conserved protein function, as yet unknown.

The predicted Ubiquitin-like 5 protein, with only 73 amino acids, is the smallest of the ubiquitin-like proteins and is even smaller than Ubiquitin itself. The ubiquitin-like proteins NEDD8 (188), Apg12 (189), Urm1 (190), and Sentrin/SUMO-1 (191,192) also known as UBL1 (193) and PIC1 (194) have been partially characterized, while little is known about UBL3 (195) and UBL4 {OMIM# 312070, (196,197)}. UBL5 is as similar

to ubiquitin as most of the other ubiquitin-like proteins at an amino acid level. UBL5's folding pattern is also similar to ubiquitin. However, as described below, my data suggest that human UBL5 protein behaves in a different manner than ubiquitin, sentrin/SUMO1 or NEDD8.

One characteristic feature of ubiquitin and some of the ubiquitin-like proteins is the diglycine residues at their C-terminus. It is known that these diglycine amino acids are required to allow conjugation of ubiquitin to its target protein (as reviewed in (198)). Ubiquitin-like proteins Sentrin/SUMO-1, 2, and 3, UCRP, NEDD8 and Urm1 all have diglycine residues at their C-terminus. Apg12, Apg12-like, UBL3, UBL4 and UBL5 do not have these C-terminal diglycine residues. Immunoblot analysis of Sentrin, Ubiquitin and NEDD8 (199,200) show high molecular weight bands putatively demonstrating covalent attachment of Sentrin, Ubiquitin or NEDD8, respectively to other proteins. As I did not detect higher molecular weight bands in my immunoblot analysis which could correspond to proteins covalently attached to UBL5, I would predict that if UBL5 binds to other proteins, it would do so non-covalently and would bind in a different manner than the C-terminal diglycine containing Ubiquitin-like proteins. Alternatively, if UBL5 covalently attached to other proteins, it did so at levels lower than I could detect using these methods, which were similar to the methods used in the analysis of Sentrin, Ubiquitin and NEDD8, (199,200).

UBL5 also differs from ubiquitin, NEDD8, and Sentrin-1/SUMO-1 in its subcellular localization. Ubiquitin has been reported to be present in both the cytosol and the nucleus (200). Sentrin-1 and NEDD8 have both been seen primarily in the nucleus (199,200). As UBL5 was seen in the cytoplasm, it supports the suggestion that UBL5 has a function different from ubiquitin, NEDD8 and sentrin-1/SUMO-1. As described below, this has been determined to be the case.

Human UBL5 and its homologs represent a new branch of ubiquitin-like proteins. UBL5 is as relatively similar to ubiquitin as most of the other ubiquitin-like proteins. I have also predicted that its three dimensional folding pattern is similar to Ubiquitin. However, my current evidence suggests that UBL5 does not covalently attach to proteins at significant levels, if at all and lacks the diglycine residues seen in some, but not all, of the ubiquitin-like proteins. UBL5's localization to the cytoplasm also differs from that seen in ubiquitin, NEDD8 and Sentrin-1. Taken together, UBL5 is structurally related to the other Ubiquitin-like proteins yet was not seen to possess the same intracellular location and covalent attachment properties as some of the better characterized ubiquitin-like proteins. The UBL5 gene's current physical location at 19p13.2 does not currently make UBL5 a candidate for ocular disorders. Recent work by Dittmar and co-workers determined that the removal of UBL5's terminal amino acid allowed covalent attachment to occur (201). Examination of the covalently attached proteins revealed that UBL5 (called Hub1 by the authors) was bound to two other proteins, Sph1 and the protein

product of ORF YDL223c, which the author's renamed Hbt1 (201). Sph1 was previously known to be involved in cell polarization, and yeast knockout experiments showed that both Hub1 and Hbt1 were also involved in this process. Futher work will be required to determine the kind of cell polarization, and biological significance of UBL5 in iris tissue. This work could potentially be performed with an anti-UBL5 antibody on sectioned eye tissues or, alternatively, on human eye cell cultures.

Chapter IV: Discussion and Conclusions:

Glaucoma and age-related macular degeneration are two blinding disorders associated with age. Efforts to identify the genes responsible for these diseases will therefore become increasingly important to society as the global population ages. The elucidation of genes causing glaucoma will have an immediate impact, as genetic screening of individuals will identify those at risk. In doing so, these people may be started on currently available treatments hopefully before irreversible damage has occurred. Unfortunately, no such preventative measures currently exist for AMD. However, the characterization of genes responsible for glaucoma and AMD are the first step towards generating new therapies to halt sight loss.

With this in mind, two different approaches, the 'top down' (positional cloning) or 'bottom up' (candidate gene) methods can be used to identify disease causing genes. The former route is advantageous in that there is no preconceived notion on the disease gene's potential function. *CYP1B1*, for example, would probably have been ignored as a housekeeping gene if it were not mapped within a glaucoma locus. A disadvantage of positional cloning is the requirement of at least one large, clinically well defined family. As mentioned above, AMD's late age of onset makes such a collection difficult.

One problem with the candidate gene approach occurs when one is examining a widely expressed gene, such as UBL5. Although it is possible that UBL5 may cause disease, it would be impossible to narrow down likely disorders to test without additional biological data. On the other hand, the 'bottom up' method is advantageous in that one

might immediately have candidate genes for disorders based on expression or other biological information without linkage analysis. For example, the mouse knockout of the proteoglycan perlecan gene, Hspg2, displayed skeletal problems including severe chondrodysplasia. Arikawa-Hirasawa and co-workers noted this biological phenotype and found two siblings and a third patient with a similar phenotype. Further work by this group uncovered the mutations in HSPG2 responsible for the dyssegmental dysplasia seen in these individuals (202). It is possible then, to use a 'bottom up' approach exclusively and find disease causing genes. However, both methods are typically used in combination. In my case, the limited expression of *OPTC* in the retina would not immediately suggest that patients with retinal disease be screened for mutations. However, my immunohistochemistry data coupled with the AMD susceptibility locus information, provided enough biological data to warrant a screen beyond the glaucoma cohort.

During my Ph.D. program, I created an adult iris cDNA library and screened it in two different ways. The first screen was used to identify genes more highly expressed in the iris than lymphoblast or more highly expressed in the trabecular meshwork than iris or lymphoblast. From this screen I isolated the opticin cDNA. I radiation hybrid mapped the gene and determined its expression profile through northern and RT-PCR experiments. I obtained the mRNA transcripts of human, mouse and pig opticin. Additionally, I performed immunoblot and immunohistochemistry experiments to

delineate where the opticin protein is present in the eye. Lastly, I compared the migration of wildtype opticin and an Arg299Cys variant under denaturing, non-reducing conditions.

The second screen was performed to isolate genes highly expressed and conserved between species. Interestingly, I obtained the opticin transcript in both screens. I found a new ubiquitin-like gene, that I called UBL5, and examined its transcript through Northern blot experiments. I additionally performed immunoblot and intracellular localization experiments to further characterize UBL5. Interestingly, UBL5 was recently found to be involved in cell polarization (201). This work suggests that UBL5 performs an important biological role in the human iris, allowing cells to properly orient themselves.

Of these two genes, opticin is currently more likely to be associated with human disease. The preliminary results of the genetic screen performed by our collaborators coupled with my protein localization of opticin may promote the examination of OPTC in AMD patients by other groups. Only through a broader examination of AMD patients will the question of opticin's association with AMD be answered. Overall, both methodologies I used to isolate genes have proven fruitful and have led to a further understanding of iris expressed genes.

The completion of the human genome sequence and the rapid proliferation of EST databases, have greatly expanded the tools available for studying novel or uncharacterized genes. One might consider, if starting this type of project today, that

much of the preliminary work could currently be performed *in silico*. The NEI Bank, for example, contains a wide EST database from a variety of eye tissues such as ciliary body, iris and trabecular meshwork. A student could examine the ESTs present in the Bank and compare them to any other database of interest. Candidate genes could be localized within the human genome, their open reading frames determined or mostly determined and the intron/exon boundaries elucidated through *in silico* means.

With this preliminary work easily available, the biological question "What does my protein do?" is becoming the first question a researcher must face. It is not an easy question to answer. The easiest way to gain an insight on a protein's function is to look for amino acid similarities between one's protein of interest and any well characterized protein. The best situation is if the characterized protein turns out to be a class of proteins that are very well studied, such as transcription factors. The next level is to identify a family of proteins of which the protein of interest is a member. Both opticin and UBL5 may be placed within this category. The most challenging situation is when the protein has uncharacterized orthologs, but no homologies to any other protein. Some of my uncharacterized genes, such as TM324, may be placed in this last group.

The next step to garner biological information on any of these proteins would be to examine their protein-protein interactions with an as yet unknown, but hopefully characterized, protein. Although several methodologies exist for this type of analysis, including immunoprecipitations and column binding experiments, the yeast two hybrid

method is one method currently associated with cDNA libraries. Additionally, given the limited amounts of donated human eye tissue available, the creation of a two hybrid library is likely the most efficient method of determining protein-protein interactions while remaining within a 'human' system.

Future Directions

There are a number of possible experiments which can be performed on either opticin or UBL5. Interacting proteins still need to be discovered, through two hybrid, column binding or immunoprecipitation experiments. As I was unable to determine whether opticin was properly expressed within COS-7 cells, other protein expression systems, such as baculovirus, may have to be developed in the laboratory. I did not have enough time to perform immunoprecipitations using the anti-opticin antibody. However, the laboratory has the materials to test opticin's ability to bind collagen type I with this method. Additionally, the collagen control within the Cyto-Trap kit may also be adjusted for the same purpose.

Knockout mice may also be developed for both Optc and UBL5. It would be interesting to know whether an Optc knockout mouse would have an effect on a mouse knockout without another extracellular matrix protein, like TIMP3. Examining crosses in this manner might reveal important functional relationships between opticin and other proteins.

Although UBL5 did not appear to behave like other diglycine containing ubiquitin-like proteins, it does not negate the possibility that UBL5 covalently attaches to other proteins. Indeed, the work recently performed by Dittmar and colleages suggest that there is a protein that post-translationally modifies UBL5 to remove its terminal amino acid prior to activation (201). The lack of covalent attachment in COS-7 cells may reflect the absence of the modifier protein in this cell type. It would be interesting to transfect UBL5-pcDNA constructs (both wild type and the 'active', deleted form) into human trabecular meshwork cells or COS-7 cells and ask whether the immunoblot will change from my earlier result.

Last Remarks

Although substantial progress has been made towards the goal of finding the genes responsible for eye disease, much remains to be done. Of the glaucoma loci mentioned above, numerous disease causing genes have yet to be discovered. Once identified, figuring out what the proteins do will probably take even more time. For example, *TIGR* was first described in 1995, however myocilin's function is still debated to this day. Where AMD is concerned, few loci are currently associated with this disorder, and family collection will remain a slow affair due to AMD's late onset. Any candidate gene or modifier for this disease will therefore require fairly large numbers to show any association with AMD, as has been the case with ABCR. Ultimately, the

unravelling of the biological puzzles that currently confront us will lead to a better understanding of how the eye works, and will hopefully provide a means to provide better treatments for those afflicted by these debilitating conditions.

References:

(1) West, S. and Sommer, A. (2001) Prevention of blindness and priorities for the future. *Bull World Health Organ.* **79,** 244-248.

(2) Riordan-Eva, P. (1999) Anatomy and Embryology of the Eye. In *General Ophthalmology.* 15th ed. ed. Appleton and Lange, Norwalk, Connecticut, pp. 1-26.

(3) Jakibiec, F.A. (1982) *Ocular anatomy, embryology, and teratology.* Harper & Row, Philadelphia.

(4) Quigley, H.A. (1996) Number of people with glaucoma worldwide. *Br J Ophthalmol.* **80,** 389-393.

(5) Sheffield, V.C., Stone, E.M., Alward, W.L.M., Drack, A.V., Johnson, A.T., Streb, L.M. and Nichols, B.E. (1993) Genetic-linkage of familial open-angle glaucoma to chromosome-1q21-q31. *Nat Genet.* **4,** 47-50.

(6) Sunden, S.L., Alward, W.L., Nichols, B.E., Rokhlina, T.R., Nystuen, A., Stone, E.M. and Sheffield, V.C. (1996) Fine mapping of the autosomal dominant juvenile open angle glaucoma (GLC1A) region and evaluation of candidate genes. *Genome Res.* **6,** 862-869.

(7) Stone, E.M., Fingert, J.H., Alward, W.L.M., Nguyen, T.D., Polansky, J.R., Sunden, S.L.F., Nishmura, D., Clark, A.F., Nystuen, A., Nichols, B.E. *et al.* (1997) Identification of a gene that causes primary open angle glaucoma. *Science.* **275,** 668-670.

(8) Escribano, J., Ortego, J. and Coca-Prados, M. (1995) Isolation and characterization of cell-specific cDNA clones from a subtractive library of the

ocular ciliary body of a single normal human donar: Transcription and synthesis of plasma proteins. *J Biochem.* **118,** 921-931.

(9) Michels-Rautenstrauss, K.G., Mardin, C.Y., Budde, W.M., Liehr, T., Polansky, J., Nguyen, T., Timmerman, V., Van Broeckhoven, C., Naumann, G.O., Pfeiffer, R.A. *et al.* (1998) Juvenile open angle glaucoma: fine mapping of the TIGR gene to 1q24.3-q25.2 and mutation analysis. *Hum Genet.* **102,** 103-106.

(10) Fingert, J.H., Heon, E., Liebmann, J.M., Yamamoto, T., Craig, J.E., Rait, J., Kawase, K., Hoh, S.T., Buys, Y.M., Dickinson, J. *et al.* (1999) Analysis of myocilin mutations in 1703 glaucoma patients from five different populations. *Hum Mol Genet.* **8,** 899-905.

(11) Kubota, R., Kudoh, J., Mashima, Y., Asakawa, S., Minoshima, S., Hejtmancik, J.F., Oguchi, Y. and Shimizu, N. (1998) Genomic organization of the human myocilin gene (MYOC) responsible for primary open angle glaucoma (GLC1A). *Biochem Biophys Res Commun.* **242,** 396-400.

(12) Nguyen, T.D., Chen, P., Huang, W.D., Chen, H., Johnson, D. and Polansky, J.R. (1998) Gene structure and properties of TIGR, an olfactomedin-related glycoprotein cloned from glucocorticoid-induced trabecular meshwork cells. *J Biol Chem.* **273,** 6341-6350.

(13) Yokoe, H. and Anholt, R.R.H. (1993) Molecular cloning of olfactomedin, an extracellular matrix protein specific to the olfactory neuroepithelium. *Proc Natl Acad Sci USA.* **90,** 4655-4659.

(14) Danielson, P.E., Forss-Petter, S., Battenberg, E.L., deLecea, L., Bloom, F.E. and Sutcliffe, J.G. (1994) Four structurally distinct neuron-specific olfactomedin-related glycoproteins produced by differential promoter utilization and alternative mRNA splicing from a single gene. *J Neurosci Res.* **38,** 468-478.

(15) Adam, M.F., Belmouden, A., Binisti, P., Brezin, A.P., Valtot, F., Bechetoille, A., Dascotte, J.C., Copin, B., Gomez, L., Chaventre, A. *et al.* (1997) Recurrent mutations in a single exon encoding the evolutionarily conserved olfactomedin-homology domain of TIGR in familial open-angle glaucoma. *Hum Mol Genet.* **6,** 2091-2097.

(16) Takahashi, H., Noda, S., Mashima, Y., Kubota, R., Ohtake, Y., Tanino, T., Kudoh, J., Minoshima, S., Oguchi, Y. and Shimizu, N. (2000) The myocilin (MYOC) gene expression in the human trabecular meshwork. *Curr Eye Res.* **20,** 81-84.

(17) Swiderski, R.E., Ross, J.L., Fingert, J.H., Clark, A.F., Alward, W.L., Stone, E.M. and Sheffield, V.C. (2000) Localization of MYOC transcripts in human eye and optic nerve by in situ hybridization. *Invest Ophthalmol Vis Sci.* **41,** 3420-3428.

(18) Wang, X. and Johnson, D.H. (2000) mRNA in situ hybridization of TIGR/MYOC in human trabecular meshwork. *Invest Ophthalmol Vis Sci.* **41,** 1724-1729.

(19) Ricard, C.S., Agapova, O.A., Salvador-Silva, M., Kaufman, P.L. and Hernandez, M.R. (2001) Expression of Myocilin/TIGR in Normal and Glaucomatous Primate Optic Nerves. *Exp Eye Res.* **73,** 433-447.

(20) Huang, W., Jaroszewski, J., Ortego, J., Escribano, J. and Coca-Prados, M. (2000) Expression of the TIGR gene in the iris, ciliary body, and trabecular meshwork of the human eye. *Ophthalmic Genet.* **21,** 155-169.

(21) Rao, P.V., Allingham, R.R. and Epstein, D.L. (2000) TIGR/myocilin in human aqueous humor. *Exp Eye Res.* **71,** 637-641.

(22) Noda, S., Mashima, Y., Obazawa, M., Kubota, R., Oguchi, Y., Kudoh, J., Minoshima, S. and Shimizu, N. (2000) Myocilin expression in the astrocytes of the optic nerve head. *Biochem Biophys Res Commun.* **276,** 1129-1135.

(23) Karali, A., Russell, P., Stefani, F.H. and Tamm, E.R. (2000) Localization of myocilin/trabecular meshwork--inducible glucocorticoid response protein in the human eye. *Invest Ophthalmol Vis Sci.* **41,** 729-740.

(24) Russell, P., Tamm, E.R., Grehn, F.J., Picht, G. and Johnson, M. (2001) The Presence and Properties of Myocilin in the Aqueous Humor. *Invest Ophthalmol Vis Sci.* **42,** 983-986.

(25) Ueda, J., Wentz-Hunter, K.K., Cheng, E.L., Fukuchi, T., Abe, H. and Yue, B.Y. (2000) Ultrastructural localization of myocilin in human trabecular meshwork cells and tissues. *J Histochem Cytochem.* **48,** 1321-1330.

(26) O'Brien, E.T., Ren, X. and Wang, Y. (2000) Localization of myocilin to the golgi apparatus in Schlemm's canal cells. *Invest Ophthalmol Vis Sci.* **41,** 3842-3849.

(27) Wentz-Hunter, K., Ueda, J., Shimizu, N. and Yue, B.Y. (2002) Myocilin is associated with mitochondria in human trabecular meshwork cells. *J Cell Physiol.* **190,** 46-53.

(28) Filla, M.S., Liu, X., Nguyen, T.D., Polansky, J.R., Brandt, C.R., Kaufman, P.L. and Peters, D.M. (2002) In vitro localization of TIGR/MYOC in trabecular meshwork extracellular matrix and binding to fibronectin. *Invest Ophthalmol Vis Sci.* **43,** 151-161.

(29) Morissette, J., Clepet, C., Moisan, S., Dubois, S., Winstall, E., Vermeeren, D., Nguyen, T.D., Polansky, J.R., Cote, G., Anctil, J.-L. *et al.* (1998) Homozygotes carrying an autosomal dominant TIGR mutation do not manifest glaucoma. *Nat Genet.* **19,** 319-321.

(30) Caballero, M., Rowlette, L.L. and Borras, T. (2000) Altered secretion of a TIGR/MYOC mutant lacking the olfactomedin domain. *Biochim Biophys Acta.* **1502,** 447-460.

(31) Fautsch, M.P. and Johnson, D.H. (2001) Characterization of myocilin-myocilin interactions. *Invest Ophthalmol Vis Sci.* **42,** 2324-2331.

(32) Wentz-Hunter, K., Ueda, J. and Yue, B.Y. (2002) Protein interactions with myocilin. *Invest Ophthalmol Vis Sci.* **43,** 176-182.

(33) Borras, T., Rowlette, L.L., Tamm, E.R., Gottanka, J. and Epstein, D.L. (2002) Effects of elevated intraocular pressure on outflow facility and TIGR/MYOC expression in perfused human anterior segments. *Invest Ophthalmol Vis Sci.* **43,** 33-40.

(34) Fautsch, M.P., Bahler, C.K., Jewison, D.J. and Johnson, D.H. (2000) Recombinant TIGR/MYOC increases outflow resistance in the human anterior segment. *Invest Ophthalmol Vis Sci.* **41,** 4163-4168.

(35) Jacobson, N., Andrews, M., Shepard, A.R., Nishimura, D., Searby, C., Fingert, J.H., Hageman, G., Mullins, R., Davidson, B.L., Kwon, Y.H. *et al.* (2001) Non-secretion of mutant proteins of the glaucoma gene myocilin in cultured trabecular meshwork cells and in aqueous humor. *Hum Mol Genet.* **10,** 117-125.

(36) Caballero, M. and Borras, T. (2001) Inefficient processing of an olfactomedin-deficient myocilin mutant: potential physiological relevance to glaucoma. *Biochem Biophys Res Commun.* **282,** 662-670.

(37) Johnson, W., G. (1980) Metabolic interference and the + - heterozygote. A hypothetical form of simple inheritance which is neither Dominant nor Recessive. *Am J Hum Genet.* **32,** 374-386.

(38) Morissette, J., Cote, G., Anctil, J.L., Plante, M., Amyot, M., Heon, E., Trope, G.E., Weissenbach, J. and Raymond, V. (1995) A common gene for juvenile and adult-onset primary open-angle glaucomas confined on chromosome 1q. *Am J Hum Genet.* **56,** 1431-1442.

(39) Wiggs, J.L., Damji, K.F., Haines, J.L., Pericak-Vance, M.A. and Allingham, R.R. (1996) The distinction between juvenile and adult-onset primary open-angle glaucoma. *Am J Hum Genet.* **58,** 243-244.

(40) Hanson, I.M., Fletcher, J.M., Jordan, T., Brown, A., Taylor, D., Adams, R.J., Punnett, H.H. and van Heyningen, V. (1994) Mutations at the PAX6 locus are found in heterogeneous anterior segment malformations including Peters anomaly. *Nat Genet.* **6,** 168-173.

(41) Mirzayans, F., Pearce, W.G., MacDonald, I.M. and Walter, M.A. (1995) Mutation of the PAX6 gene in patients with autosomal dominant keratitis. *Am J Hum Genet.* **57,** 539-548.

(42) Glaser, T., Jepeal, L., Edwards, J.G., Young, R., Favor, J. and Maas, R.L. (1994) PAX6 gene dosage effect in a family with congenital cataracts, aniridia, anophthalmia and central nervous system defects. *Nat Genet.* **7,** 463-469.

(43) Azuma, N. and Nishina, S. (1996) PAX6 missense mutation in isolated foveal hypoplasia. *Nat Genet.* **13,** 141-142.

(44) Semina, E.V., Reiter, R., Leysens, N.J., Alward, W.L., Small, K.W., Datson, N.A., Siegel, B.J., Bierke, N.D., Bitoun, P., Zabel, B.U. *et al.* (1996) Cloning and characterization of a novel bicoid-related homeobox transcription factor gene, RIEG, involved in Rieger syndrome. *Nat Genet.* **14,** 392-399.

(45) Alward, W.L., Semina, E.V., Kalenak, W., Heon, E., Sheth, B.P., Stone, E.M. and Murray, J.C. (1998) Autosomal dominant iris hypoplasia is caused by a mutation in the Rieger Syndrome (RIEG/PITX2) gene. *Am J Ophthalmol.* **125,** 98-100.

(46) Kulak, S.C., Kozlowski, K., Semina, E.V., Pearce, W.G. and Walter, M.A. (1998) Mutation in the RIEG1 gene in patients with iridogoniodysgenesis syndrome. *Hum Mol Genet.* **7,** 1113-1117.

(47) Stoilova, D., Child, A., Trifan, O.C., Crick, R.P., Coakes, R.L. and Sarfarazi, M. (1996) Localization of a locus (GLC1B) for adult-onset primary open angle glaucoma to the 2cen-q13 region. *Genomics.* **36,** 142-150.

(48) Wirtz, M.K., Samples, J.R., Kramer, P.L., Rust, K., Topinka, J.R., Yount, J., Koler, R.D. and Acott, T.S. (1997) Mapping a gene for adult-onset primary open-angle glaucoma to chromosome 3q. *Am J Hum Genet.* **60,** 296-304.

(49) Xu, H., Acott, T.S. and Wirtz, M.K. (2000) Identification and expression of a novel type I procollagen C-proteinase enhancer protein gene from the glaucoma candidate region on 3q21-q24. *Genomics.* **66,** 264-273.

(50) Kitsos, G., Eiberg, H., Economou-Petersen, E., Wirtz, M.K., Kramer, P.L., Aspiotis, M., Tommerup, N., Petersen, M.B. and Psilas, K. (2001) Genetic linkage of autosomal dominant primary open angle glaucoma to chromosome 3q in a Greek pedigree. *Eur J Hum Genet.* **9,** 452-457.

(51) Trifan, O.C., Traboulsi, E.I., Stoilova, D., Alozie, I., Nguyen, R., Raja, S. and Sarfarazi, M. (1998) A third locus (GLC1D) for adult-onset primary open-angle glaucoma maps to the 8q23 region. *Am J Ophthalmol.* **126,** 17-28.

(52) Rezaie, T., Child, A., Hitchings, R., Brice, G., Miller, L., Coca-Prados, M., Heon, E., Krupin, T., Ritch, R., Kreutzer, D. *et al.* (2002) Adult-onset primary open-angle glaucoma caused by mutations in optineurin. *Science.* **295,** 1077-1079.

(53) Faber, P.W., Barnes, G.T., Srinidhi, J., Chen, J., Gusella, J.F. and MacDonald, M.E. (1998) Huntingtin interacts with a family of WW domain proteins. *Hum Mol Genet.* **7,** 1463-1474.

(54) Li, Y., Kang, J. and Horwitz, M.S. (1998) Interaction of an adenovirus E3 14.7-kilodalton protein with a novel tumor necrosis factor alpha-inducible cellular protein containing leucine zipper domains. *Mol Cell Biol.* **18,** 1601-1610.

(55) Wirtz, M.K., Samples, J.R., Rust, K., Lie, J., Nordling, L., Schilling, K., Acott, T.S. and Kramer, P.L. (1999) GLC1F, a new primary open-angle glaucoma locus, maps to 7q35-q36. *Arch Ophthalmol.* **117,** 237-241.

(56) Sarfarazi, M., Child, A., Stoilova, D., Brice, G., Desai, T., Trifan, O.C., Poinoosawmy, D. and Crick, R.P. (1998) Localization of the fourth locus (GLC1E) for adult-onset primary open- angle glaucoma to the 10p15-p14 region. *Am J Hum Genet.* **62,** 641-652.

(57) Stoilov, I., Akarsu, A.N., Alozie, I., Child, A., Barsoum-Homsy, M., Turacli, M.E., Or, M., Lewis, R.A., Ozdemir, N., Brice, G. *et al.* (1998) Sequence analysis and homology modeling suggest that primary congenital glaucoma on 2p21 results from mutations disrupting either the hinge region or the conserved core structures of cytochrome P4501B1. *Am J Hum Genet.* **62,** 573-584.

(58) Sutter, T.R., Guzman, K., Dold, K.M. and Greenlee, W.F. (1991) Targets for Dioxin: Genes for Plasminogen Activator Inhibitor-2 and Interleukin-1β. *Science.* **254,** 415-418.

(59) Stoilov, I., Akarsu, A.N. and Sarfarazi, M. (1997) Identification of three different truncating mutations in cytochrome P4501B1 (CYP1B1) as the principal cause of primary congenital glaucoma (Buphthalmos) in families linked to the GLC3A locus on chromosome 2p21. *Hum Mol Genet.* **6,** 641-647.

(60) Bejjani, B.A., Stockton, D.W., Lewis, R.A., Tomey, K.F., Dueker, D.K., Jabak, M., Astle, W.F. and Lupski, J.R. (2000) Multiple CYP1B1 mutations and incomplete penetrance in an inbred population segregating primary congenital glaucoma suggest frequent de novo events and a dominant modifier locus. *Hum Mol Genet.* **9,** 367-374.

(61) Bejjani, B.A., Lewis, R.A., Tomey, K.F., Anderson, K.L., Dueker, D.K., Jabak, M., Astle, W.F., Otterud, B., Leppert, M. and Lupski, J.R. (1998) Mutations in CYP1B1, the gene for cytochrome P4501B1, are the predominant cause of primary congenital glaucoma in Saudi Arabia. *Am J Hum Genet.* **62,** 325-333.

(62) Ohtake, Y., Kubota, R., Tanino, T., Miyata, H. and Mashima, Y. (2000) Novel compound heterozygous mutations in the cytochrome P4501B1 gene (CYP1B1) in a Japanese patient with primary congenital glaucoma. *Ophthalmic Genet.* **21,** 191-193.

(63) Vincent, A., Billingsley, G., Priston, M., Williams-Lyn, D., Sutherland, J., Glaser, T., Oliver, E., Walter, M.A., Heathcote, G., Levin, A. *et al.* (2001) Phenotypic heterogeneity of CYP1B1: mutations in a patient with Peters' anomaly. *J Med Genet.* **38,** 324-326.

(64) Jansson, I., Stoilov, I., Sarfarazi, M. and Schenkman, J.B. (2001) Effect of two mutations of human CYP1B1, G61E and R469W, on stability and endogenous steroid substrate metabolism. *Pharmacogenetics.* **11,** 793-801.

(65) Vincent, A.L., Billingsley, G., Buys, Y., Levin, A.V., Priston, M., Trope, G., Williams-Lyn, D. and Heon, E. (2002) Digenic Inheritance of Early-Onset Glaucoma: CYP1B1, a Potential Modifier Gene. *Am J Hum Genet.* **70,** 448-460.

(66) Akarsu, A.N., Turacli, M.E., Aktan, S.G., M., B.-H., Chevrette, L., Sayli, B.S. and Sarfarazi, M. (1996) A second locus (GLC3B) for primary secondary glaucoma (Buphthalmos) maps to 1p36. *Hum Mol Genet.* **5,** 1199-1203.

(67) Sarfarazi, M., Akarsu, A.N., Hossain, A., Turacli, M.E., Aktan, S.G., Barsoum-Homsy, M., Chevrette, L. and Sayli, B.S. (1995) Assignment of a locus (GLC3A) for primary congenital glaucoma (Buphthalmos) to 2p21 and evidence for genetic heterogeneity. *Genomics.* **30,** 171-177.

(68) Ton, C.C., Hirvonen, H., Miwa, H., Weil, M.M., Monaghan, P., Jordan, T., van, H.V., Hastie, N.D., Meijers, H.H., Drechsler, M. *et al.* (1991) Positional cloning and characterization of a paired box- and homeobox-containing gene from the aniridia region. *Cell.* **67,** 1059-1074.

(69) Favor, J., Neuhauser-Klaus, A. and Ehling, U.H. (1988) The effect of dose fractionation on the frequency of ethylnitrosourea-induced dominant cataract and recessive specific locus mutations in germ cells of the mouse. *Mutat Res.* **198,** 269-275.

(70) Hill, R.E., Favor, J., Hogan, B.L., Ton, C.C., Saunders, G.F., Hanson, I.M., Prosser, J., Jordan, T., Hastie, N.D. and van Heyningen, V. (1991) Mouse small eye results from mutations in a paired-like homeobox-containing gene. *Nature.* **354,** 522-525.

(71) Halder, G., Callaerts, P. and Gehring, W.J. (1995) Induction of ectopic eyes by targeted expression of the eyeless gene in Drosophila. *Science.* **267,** 1788-1792.

(72) Tomarev, S.I., Callaerts, P., Kos, L., Zinovieva, R., Halder, G., Gehring, W. and Piatigorsky, J. (1997) Squid Pax-6 and eye development. *Proc Natl Acad Sci USA.* **94,** 2421-2426.

(73) Munier, F.L., Korvatska, E., Djemai, A., Le Paslier, D., Zografos, L., Pescia, G. and Schorderet, D.F. (1997) Kerato-epithelin mutations in four 5q31-linked corneal dystrophies. *Nat Genet.* **15,** 247-251.

(74) Axenfeld, T. (1920) Embryotoxon corneae posterius. *Ber Deutsch Ophthalmol Ges.* **42,** 381-382.

(75) Rieger, H. (1934) Verlagerung und Schitzform der Pupille mit Hypoplasie des Irisvordblattes. *Z Augenheilk.* **84,** 98-99.

(76) Gould, D.B., Mears, A.J., Pearce, W.G. and Walter, M.A. (1997) Autosomal dominant Axenfeld-Rieger anomaly maps to 6p25. *Am J Hum Genet.* **61,** 765-768.

(77) Nishimura, D.Y., Swiderski, R.E., Alward, W.L., Searby, C.C., Patil, S.R., Bennet, S.R., Kanis, A.B., Gastier, J.M., Stone, E.M. and Sheffield, V.C. (1998) The forkhead transcription factor gene FKHL7 is responsible for glaucoma phenotypes which map to 6p25. *Nat Genet.* **19,** 140-147.

(78) Mears, A.J., Jordan, T., Mirzayans, F., Dubois, S., Kume, T., Parlee, M., Ritch, R., Koop, B., Kuo, W.L., Collins, C. *et al.* (1998) Mutations of the forkhead/winged-helix gene, FKHL7, in patients with Axenfeld-Rieger anomaly. *Am J Hum Genet.* **63,** 1316-1328.

(79) Mirzayans, F., Gould, D.B., Heon, E., Billingsley, G.D., Cheung, J.C., Mears, A.J. and Walter, M.A. (2000) Axenfeld-Rieger syndrome resulting from mutation of the FKHL7 gene on chromosome 6p25. *Eur J Hum Genet.* **8,** 71-74.

(80) Nishimura, D.Y., Searby, C.C., Alward, W.L., Walton, D., Craig, J.E., Mackey, D.A., Kawase, K., Kanis, A.B., Patil, S.R., Stone, E.M. *et al.* (2001) A spectrum of FOXC1 mutations suggests gene dosage as a mechanism for developmental defects of the anterior chamber of the eye. *Am J Hum Genet.* **68,** 364-372.

(81) Lehmann, O.J., Ebenezer, N.D., Jordan, T., Fox, M., Ocaka, L., Payne, A., Leroy, B.P., Clark, B.J., Hitchings, R.A., Povey, S. *et al.* (2000) Chromosomal duplication involving the forkhead transcription factor gene FOXC1 causes iris hypoplasia and glaucoma. *Am J Hum Genet.* **67,** 1129-1135.

(82) Kulharya, A.S., Maberry, M., Kukolich, M.K., Day, D.W., Schneider, N.R., Wilson, G.N. and Tonk, V. (1995) Interstitial deletions 4q21.1q25 and 4q25q27: Phenotype variability and relation to Rieger anomaly. *Am J Med Genet.* **55,** 165-170.

(83) Motegi, T., Nakamura, K., Terakawa, T., Oohira, A., Minoda, K., Kishi, K., Yanagawa, Y. and Hayakawa, H. (1988) Deletion of a single chromosome band 4q26 in a malformed girl: exclusion of Rieger syndrome associated gene(s) from the 4q26 segment. . *J Med Genet.* **25,** 628-633.

(84) Makita, T., Masuno, M., Imaizumi, K., Yamashita, S., Ohba, S., Daizou, I. and Kuroki, Y. (1995) Rieger Syndrome with de novo reciprocal translocation t(1;4) (q23.1;q25). *Am J Med Genet.* **57,** 19-21.

(85) Murray, J.C., Bennett, S.R., Kwitek, A.E., Small, K.W., Schinzel, A., Alward, W.L., Weber, J.L., Bell, G.I. and Buetow, K.H. (1992) Linkage of Rieger syndrome to the region of the epidermal growth factor gene on chromosome 4. *Nat Genet.* **2,** 46-49.

(86) Yoshioka, H., Meno, C., Koshiba, K., Sugihara, M., Itoh, H., Ishimaru, Y., Inoue, T., Ohuchi, H., Semina, E.V., Murray, J.C. *et al.* (1998) Pitx2, a bicoid-type homeobox gene, is involved in a lefty-signalling pathway in determination of left-right asymmetry. *Cell.* **94,** 299-305.

(87) Piedra, M.E., Icardo, J.M., Albajar, M., Rodriguez-Rey, J.C. and Ros, M.A. (1998) Pitx2 participates in the late phase of the pathway controlling left-right asymmetry. *Cell.* **94,** 319-324.

(88) Heon, E., Sheth, B.P., Kalenak, J.W., Sunden, S.L.F., Streb, L.M., Taylor, C.M., Alward, W.L.M., Sheffield, V.C. and Stone, E.M. (1995) Linkage of autosomal dominant iris hypoplasia to the region of the Rieger syndrome locus (4q25). *Hum Mol Genet.* **4,** 1435-1439.

(89) Walter, M.A., Mirzayans, F., Mears, A.J., Hickey, K. and Pearce, W.G. (1996) Autosomal-dominant iridogoniodysgenesis and Axenfeld-Rieger syndrome are genetically distinct. *Ophthalmology.* **103,** 1907-1915.

(90) Doward, W., Perveen, R., Lloyd, I.C., Ridgway, A.E., Wilson, L. and Black, G.C. (1999) A mutation in the RIEG1 gene associated with Peters' anomaly. *J Med Genet.* **36,** 152-155.

(91) Kozlowski, K. and Walter, M.A. (2000) Variation in residual PITX2 activity underlies the phenotypic spectrum of anterior segment developmental disorders. *Hum Mol Genet.* **9,** 2131-2139.

(92) Priston, M., Kozlowski, K., Gill, D., Letwin, K., Buys, Y., Levin, A.V., Walter, M.A. and Heon, E. (2001) Functional analyses of two newly identified PITX2 mutants reveal a novel molecular mechanism for Axenfeld-Rieger syndrome. *Hum Mol Genet.* **10,** 1631-1638.

(93) Phillips, J.C., Del Bono, E.A., Haines, J.L., Pralea, A.M., Cohen, J.S., Greff, L.J. and Wiggs, J.L. (1996) A second locus for Rieger Syndrome maps to chromosome 13q14. *Am J Hum Genet.* **59,** 613-619.

(94) Andersen, J.S., Pralea, A.M., DelBono, E.A., Haines, J.L., Gorin, M.B., Schuman, J.S., Mattox, C.G. and Wiggs, J.L. (1997) A gene responsible for the pigment

dispersion syndrome maps to chromosome 7q35-q36. *Arch Ophthalmol.* **115,** 384-388.

(95) Anderson, J.S., Parrish, R., Greenfield, D., DelBono, E.A., Haines, J.L. and Wiggs, J.L. (1998) A second locus for the pigment dispersion syndrome and pigmentary glaucoma maps to 18q11-q21. *Am J Hum Genet.* **63 Supplement,** A279.

(96) Chang, B., Smith, R.S., Hawes, N.L., Anderson, M.G., Zabaleta, A., Savinova, O., Roderick, T.H., Heckenlively, J.R., Davisson, M.T. and John, S.W. (1999) Interacting loci cause severe iris atrophy and glaucoma in DBA/2J mice. *Nat Genet.* **21,** 405-409.

(97) Anderson, M.G., Smith, R.S., Hawes, N.L., Zabaleta, A., Chang, B., Wiggs, J.L. and John, S.W. (2002) Mutations in genes encoding melanosomal proteins cause pigmentary glaucoma in DBA/2J mice. *Nat Genet.* **30,** 81-85.

(98) Weterman, M.A., Ajubi, N., van Dinter, I.M., Degen, W.G., van Muijen, G.N., Ruitter, D.J. and Bloemers, H.P. (1995) nmb, a novel gene, is expressed in low-metastatic human melanoma cell lines and xenografts. *Int J Cancer.* **60,** 73-81.

(99) Turque, N., Denhez, F., Martin, P., Planque, N., Bailly, M., Begue, A., Stehelin, D. and Saule, S. (1996) Characterization of a new melanocyte-specific gene (QNR-71) expressed in v-myc-transformed quail neuroretina. *Embo J.* **15,** 3338-3350.

(100) Kobayashi, T., Urabe, K., Winder, A., Jimenez-Cervantes, C., Imokawa, G., Brewington, T., Solano, F., Garcia-Borron, J.C. and Hearing, V.J. (1994) Tyrosinase related protein 1 (TRP1) functions as a DHICA oxidase in melanin biosynthesis. *Embo J.* **13,** 5818-5825.

(101) Boissy, R.E., Zhao, H., Oetting, W.S., Austin, L.M., Wildenberg, S.C., Boissy, Y.L., Zhao, Y., Sturm, R.A., Hearing, V.J., King, R.A. *et al.* (1996) Mutation in and lack of expression of tyrosinase-related protein-1 (TRP-1) in melanocytes from an individual with brown oculocutaneous albinism: a new subtype of albinism classified as "OCA3". *Am J Hum Genet.* **58,** 1145-1156.

(102) Manga, P., Kromberg, J.G., Box, N.F., Sturm, R.A., Jenkins, T. and Ramsay, M. (1997) Rufous oculocutaneous albinism in southern African Blacks is caused by mutations in the TYRP1 gene. *Am J Hum Genet.* **61,** 1095-1101.

(103) Dvorak-Theobald, G.M. (1954) Pseudo-Exfoliation of the lens Capsule. *Am J Ophthalmol.* **37,** 1-12.

(104) Stefansson, D.E., Loftsdottir, M., Sverrisson, T., Thorgeirsson, E., Jonasson, F., Gottfredsdottir, M., Bains, H.S. and Allingham, R.R. (1998) Maternal inheritance in pseudoexfoliation syndrome. *Am J Hum Genet.* **63 Supplement,** A324.

(105) Wiggs, J.L., Andersen, J.S., Stefansson, E., Loftsdottir, M., Sverisson, T., Thorgeirsson, E., Jonasson, F., Price, P., Hamilton, J., Lennon-Grahm, F. *et al.* (1998) A genomic screen suggests a locus on chromosome 2p16 for Pseudoexfoliation Syndrome. *Am J Hum Genet.* **63 Supplement,** A314.

(106) Cooper, R.L. (1990) Blind registrations in Western Australia: a five-year study. *Aust N Z J Ophthalmol.* **18,** 421-426.

(107) Chan, C.W. and Billson, F.A. (1991) Visual disability and major causes of blindness in NSW: a study of people aged 50 and over attending the Royal Blind Society 1984 to 1989. *Aust N Z J Ophthalmol.* **19,** 321-325.

(108) Leibowitz, H.M., Krueger, D.E., Maunder, L.R., Milton, R.C., Kini, M.M., Kahn, H.A., Nickerson, R.J., Pool, J., Colton, T.L., Ganley, J.P. *et al.* (1980) The Framingham Eye Study monograph: An ophthalmological and epidemiological

study of cataract, glaucoma, diabetic retinopathy, macular degeneration, and visual acuity in a general population of 2631 adults, 1973-1975. *Surv Ophthalmol.* **24,** 335-610.

(109) Ghafour, I.M., Allan, D. and Foulds, W.S. (1983) Common causes of blindness and visual handicap in the west of Scotland. *Br J Ophthalmol.* **67,** 209-213.

(110) Stone, E.M., Sheffield, V.C. and Hageman, G.S. (2001) Molecular genetics of age-related macular degeneration. *Hum Mol Genet.* **10,** 2285-2292.

(111) Petrukhin, K., Koisti, M.J., Bakall, B., Li, W., Xie, G., Marknell, T., Sandgren, O., Forsman, K., Holmgren, G., Andreasson, S. *et al.* (1998) Identification of the gene responsible for Best macular dystrophy. *Nat Genet.* **19,** 241-247.

(112) Marquardt, A., Stohr, H., Passmore, L.A., Kramer, F., Rivera, A. and Weber, B.H. (1998) Mutations in a novel gene, VMD2, encoding a protein of unknown properties cause juvenile-onset vitelliform macular dystrophy (Best's disease). *Hum Mol Genet.* **7,** 1517-1525.

(113) Kramer, F., White, K., Pauleikhoff, D., Gehrig, A., Passmore, L., Rivera, A., Rudolph, G., Kellner, U., Andrassi, M., Lorenz, B. *et al.* (2000) Mutations in the VMD2 gene are associated with juvenile-onset vitelliform macular dystrophy (Best disease) and adult vitelliform macular dystrophy but not age-related macular degeneration. *Eur J Hum Genet.* **8,** 286-292.

(114) Allikmets, R., Seddon, J.M., Bernstein, P.S., Hutchinson, A., Atkinson, A., Sharma, S., Gerrard, B., Li, W., Metzker, M.L., Wadelius, C. *et al.* (1999) Evaluation of the Best disease gene in patients with age-related macular degeneration and other maculopathies. *Hum Genet.* **104,** 449-453.

(115) Lotery, A.J., Munier, F.L., Fishman, G.A., Weleber, R.G., Jacobson, S.G., Affatigato, L.M., Nichols, B.E., Schorderet, D.F., Sheffield, V.C. and Stone, E.M.

(2000) Allelic variation in the VMD2 gene in best disease and age-related macular degeneration. *Invest Ophthalmol Vis Sci.* **41,** 1291-1296.

(116) Klein, M.L., Schultz, D.W., Edwards, A., Matise, T.C., Rust, K., Berselli, C.B., Trzupek, K., Weleber, R.G., Ott, J., Wirtz, M.K. *et al.* (1998) Age-related Macular Degeneration. *Arch Ophthalmol.* **116,** 1082-1088.

(117) Chen, C.K., Wieland, T. and Simon, M.I. (1996) RGS-r, a retinal specific RGS protein, binds an intermediate conformation of transducin and enhances recycling. *Proc Natl Acad Sci U S A.* **93,** 12885-12889.

(118) Ding, C., Li, X., Griffin, C.A., Jabs, E.W., Hawkins, A.L. and Levine, M.A. (1993) The gene for human phosducin (PDC), a soluble protein that binds G-protein beta gamma dimers, maps to 1q25-q31.1. *Genomics.* **18,** 457-459.

(119) Lee, R.H., Fowler, A., McGinnis, J.F., Lolley, R.N. and Craft, C.M. (1990) Amino acid and cDNA sequence of bovine phosducin, a soluble phosphoprotein from photoreceptor cells. *J Biol Chem.* **265,** 15867-15873.

(120) Weber, B.H., Vogt, G., Pruett, R.C., Stohr, H. and Felbor, U. (1994) Mutations in the tissue inhibitor of metalloproteinases-3 (TIMP3) in patients with Sorsby's fundus dystrophy. *Nat Genet.* **8,** 352-356.

(121) Allikmets, R., Singh, N., Sun, H., Shroyer, N.F., Hutchinson, A., Chidambaram, A., Gerrard, B., Baird, L., Stauffer, D., Peiffer, A. *et al.* (1997) A photoreceptor cell-specific ATP-binding transporter gene (ABCR) is mutated in recessive Stargardt macular dystrophy. *Nat Genet.* **15,** 236-246.

(122) Dean, M., Hamon, Y. and Chimini, G. (2001) The human ATP-binding cassette (ABC) transporter superfamily. *J Lipid Res.* **42,** 1007-1017.

(123) Martinez-Mir, A., Paloma, E., Allikmets, R., Ayuso, C., del Rio, T., Dean, M., Vilageliu, L., Gonzalez-Duarte, R. and Balcells, S. (1998) Retinitis pigmentosa caused by a homozygous mutation in the Stargardt disease gene ABCR. *Nat Genet.* **18,** 11-12.

(124) Cremers, F.P., van de Pol, D.J., van Driel, M., den Hollander, A.I., van Haren, F.J., Knoers, N.V., Tijmes, N., Bergen, A.A., Rohrschneider, K., Blankenagel, A. *et al.* (1998) Autosomal recessive retinitis pigmentosa and cone-rod dystrophy caused by splice site mutations in the Stargardt's disease gene ABCR. *Hum Mol Genet.* **7,** 355-362.

(125) Allikmets, R., Shroyer, N.F., Singh, N., Seddon, J.M., Lewis, R.A., Bernstein, P.S., Peiffer, A., Zabriskie, N.A., Li, Y., Hutchinson, A. *et al.* (1997) Mutation of the Stargardt disease gene (ABCR) in age-related macular degeneration. *Science.* **277,** 1805-1807.

(126) Dryja, T.P., Briggs, C.E., Berson, E.L., Rosenfeld, P.J. and Abitbol, M. (1998) ABCR Gene and Age-Related Macular Degeneration. *Science.* **279,** 1107a.

(127) Stone, E.M., Webster, A.R., Vandenburgh, K., Streb, L.M., Hockey, R.R., Lotery, A.J. and Sheffield, V.C. (1998) Allelic variation in ABCR associated with Stargardt disease but not age-related macular degeneration. *Nat Genet.* **20,** 328-329.

(128) De La Paz, M.A., Guy, V.K., Abou-Donia, S., Heinis, R., Bracken, B., Vance, J.M., Gilbert, J.R., Gass, J.D., Haines, J.L. and Pericak-Vance, M.A. (1999) Analysis of the Stargardt disease gene (ABCR) in age-related macular degeneration. *Ophthalmology.* **106,** 1531-1536.

(129) Webster, A.R., Heon, E., Lotery, A.J., Vandenburgh, K., Casavant, T.L., Oh, K.T., Beck, G., Fishman, G.A., Lam, B.L., Levin, A. *et al.* (2001) An analysis of allelic variation in the ABCA4 gene. *Invest Ophthalmol Vis Sci.* **42,** 1179-1189.

(130) Guymer, R.H., Heon, E., Lotery, A.J., Munier, F.L., Schorderet, D.F., Baird, P.N., McNeil, R.J., Haines, H., Sheffield, V.C. and Stone, E.M. (2001) Variation of codons 1961 and 2177 of the Stargardt disease gene is not associated with age-related macular degeneration. *Arch Ophthalmol.* **119,** 745-751.

(131) Allikmets, R. (2000) Further evidence for an association of ABCR alleles with age-related macular degeneration. The International ABCR Screening Consortium. *Am J Hum Genet.* **67,** 487-491.

(132) Weng, J., Mata, N.L., Azarian, S.M., Tzekov, R.T., Birch, D.G. and Travis, G.H. (1999) Insights into the function of Rim protein in photoreceptors and etiology of Stargardt's disease from the phenotype in abcr knockout mice. *Cell.* **98,** 13-23.

(133) Sun, H., Molday, R.S. and Nathans, J. (1999) Retinal stimulates ATP hydrolysis by purified and reconstituted ABCR, the photoreceptor-specific ATP-binding cassette transporter responsible for Stargardt disease. *J Biol Chem.* **274,** 8269-8281.

(134) Sun, H., Smallwood, P.M. and Nathans, J. (2000) Biochemical defects in ABCR protein variants associated with human retinopathies. *Nat Genet.* **26,** 242-246.

(135) Weeks, D.E., Conley, Y.P., Tsai, H., Mah, T.S., Rosenfeld, P.J., Paul, T.O., Eller, A.W., Morse, L.S., Dailey, J.P., Ferrell, R.E. *et al.* (2001) Age-related maculopathy: an expanded genome-wide scan with evidence of susceptibility loci within the 1q31 and 17q25 regions. *Am J Ophthalmol.* **132,** 682-692.

(136) Collins, F.C. (1995) Positional cloning moves from perditional to traditional. *Nat Genet.* **9,** 347-350.

(137) Swaroop, A., Xu, J.Z., Agarwal, N. and Weissman, S.M. (1991) A simple and efficient cDNA library subtraction procesure: isolation of human retina-specific cDNA clones. *Nucl Acids Res.* **19,** 1954.

(138) Altschul, S.F., Madden, T.L., Schaffer, A.A., Zhang, J., Zhang, Z., Miller, W. and Lipman, D.J. (1997) Gapped BLAST and PSI-BLAST: a new generation of protein database search programs. *Nucl Acid Res.* **25,** 3389-3402.

(139) Hoog, C. (1991) Isolation of a large number of novel mammalian genes by a differential cDNA library screening strategy. *Nucl Acids Res.* **19,** 6123-6127.

(140) Bascom, R.A., Manara, S., Collins, L., Molday, R.S., Kalnins, V.I. and McInnes, R.R. (1992) Cloning of the cDNA for a novel photoreceptor membrane protein (rom-1) identifies a disk rim protein family implicated in human retinopathies. *Neuron.* **8,** 1171-1184.

(141) Liu, I.S., Chen, J.D., Ploder, L., Vidgen, D., van der Kooy, D., Kalnins, V.I. and McInnes, R.R. (1994) Developmental expression of a novel murine homeobox gene (Chx10): evidence for roles in determination of the neuroretina and inner nuclear layer. *Neuron.* **13,** 377-393.

(142) Church, G.M. and Gilbert, W. (1984) Genomic sequencing. *Proc Natl Acad Sci USA.* **81,** 1991-1995.

(143) Deere, M., Dieguez, J.L., Yoon, S.J., Hewett-Emmett, D., de la Chapelle, A. and Hecht, J.T. (1999) Genomic characterization of human DSPG3. *Genome Res.* **9,** 449-456.

(144) Friedman, J.S., Ducharme, R., Raymond, V. and Walter, M.A. (2000) Isolation of a novel iris specific and leucine-rich repeat protein (Oculoglycan) using differential selection. *Invest Opthalmol Vis Sci.* **41,** 2059-2066.

(145) Nagase, T., Ishikawa, K., Nakajima, D., Ohira, M., Seki, N., Miyajima, N., Tanaka, A., Kotani, H., Nomura, N. and Ohara, O. (1997) Prediction of the coding sequences of unidentified human genes. VII. The complete sequences of 100 new cDNA clones from brain which can code for large proteins in vitro. *DNA Res.* **4,** 141-150.

(146) Reardon, A.J., Le Goff, M., Briggs, M.D., McLeod, D., Sheehan, J.K., Thornton, D.J. and Bishop, P.N. (2000) Identification in vitreous and molecular cloning of opticin, a novel member of the family of leucine-rich repeat proteins of the extracellular matrix. *J Biol Chem.* **275,** 2123-2129.

(147) Hobby, P., Wyatt, M.K., Gan, W., Bernstein, S., Tomarev, S., Slingsby, C. and Wistow, G. (2000) Cloning, modeling, and chromosomal localization for a small leucine-rich repeat proteoglycan (SLRP) family member expressed in human eye. *Mol Vis.* **6,** 72-78.

(148) Lai, C.H., Chou, C.Y., Ch'ang, L.Y., Liu, C.S. and Lin, W. (2000) Identification of novel human genes evolutionarily conserved in Caenorhabditis elegans by comparative proteomics. *Genome Res.* **10,** 703-713.

(149) Zhang, Q.H., Ye, M., Wu, X.Y., Ren, S.X., Zhao, M., Zhao, C.J., Fu, G., Shen, Y., Fan, H.Y., Lu, G. *et al.* (2000) Cloning and functional analysis of cDNAs with open reading frames for 300 previously undefined genes expressed in CD34+ hematopoietic stem/progenitor cells. *Genome Res.* **10,** 1546-1560.

(150) Nakai, M., Endo, T., Hase, T. and Matsubara, H. (1993) Intramitochondrial protein sorting. Isolation and characterization of the yeast MSP1 gene which belongs to a novel family of putative ATPases. *J Biol Chem.* **268,** 24262-24269.

(151) van Soest, S., van den Born, L.I., Gal, A., Farrar, G.J., Bleeker-Wagemakers, L.M., Westerveld, A., Humphries, P., Sandkuijl, L.A. and Bergen, A.A.B. (1994) Assignment of a Gene for Autosomal Recessive Retinitis Pigmentosa (RP12) to

Chromosome 1q31-q32.1 in an Inbred and Genetically Heterogeneous Disease Population. *Genomics.* **22,** 499-504.

(152) Higgins, J.J., Morton, D.H. and Loveless, J.M. (1999) Posterior column ataxia with retinitis pigmentosa (AXPC1) maps to chromosome 1q31-q32. *Neurology.* **52,** 146-150.

(153) Pellegrini, B., Acland, G.M. and Ray, J. (2002) Cloning and characterization of opticin cDNA: evaluation as a candidate for canine oculo-skeletal dysplasia. *Gene.* **282,** 121-131.

(154) Takanosu, M., Boyd, T.C., Le Goff, M., Henry, S.P., Zhang, Y., Bishop, P.N. and Mayne, R. (2001) Structure, chromosomal location, and tissue-specific expression of the mouse opticin gene. *Invest Ophthalmol Vis Sci.* **42,** 2202-2210.

(155) Bentz, H., Nathan, R.M., Rosen, D.M., Armstrong, R.M., Thompson, A.Y., Segarini, P.R., Mathews, M.C., Dasch, J.R., Piez, K.A. and Seyedin, S.M. (1989) Purification and characterization of a unique osteoinductive factor from bovine bone. *J Biol Chem.* **264,** 20805-20810.

(156) Shinomura, T. and Kimata, K. (1992) Proteoglycan-Lb, a Small Dermatan Sulfate Proteoglycan Expressed in Embryonic Chick Epiphyseal Cartilage, Is Structurally Related to Oseteoinducive Factor. *J Biol Chem.* **267,** 1265-1270.

(157) Iozzo, R.V. and Murdoch, A.D. (1996) Proteoglycans of the extracellular environment: clues from the gene and protein side offer novel perspectives in molecular diversity and function. *FASEB J.* **10,** 598-614.

(158) Hocking, A.M., Shinomura, T. and McQuillan, D.J. (1998) Leucine-rich repeat glycoproteins of the extracellular matrix. *Matrix Biol.* **17,** 1-19.

(159) Neame, P.J., Choi, H.U. and Rosenberg, L.C. (1989) The Primary Structure of the Core Protein of the Small, Leucine-rich Proteoglycan (PG I) from Bovine Articular Cartilage. *J Biol Chem.* **264,** 8653-8661.

(160) Grover, J., Chen, X., Korenberg, J.R. and Roughley, P.J. (1995) The Human Lumican Gene. *J Biol Chem.* **270,** 21942-21949.

(161) Corpuz, L.M., Funderburgh, J.L., Funderburgh, M.L., Bottomley, G.S., Prakash, S. and Conrad, G.W. (1996) Molecular Cloning and Tissue Distribution of Keratocan. *J Biol Chem.* **16,** 9759-9763.

(162) Bengtsson, E., Neame, P.J., Heinegard, D. and Sommarin, Y. (1995) The Primary Structure of a Basic Leucine-rich Repeat Protein, PRELP, Found in Connective Tissues. *J Biol Chem.* **270,** 25639-25644.

(163) Ujita, M., Shinomura, T. and Kimata, K. (1995) Molecular Cloning of the Mouse Osteoglycin-Encoding Gene. *Gene.* **158,** 237-240.

(164) Deere, M., Johnson, J., Garza, S., Harrison, W.R., Yoon, S.J., Elder, F.F.B., Kucherlapati, R., Hook, M. and Hecht, J.T. (1996) Characterization of Human DSPG3, a Small Dermatan Sulfate Proteoglycan. *Genomics.* **38,** 399-404.

(165) Hedbom, E. and Heinegard, D. (1993) Binding of Fibromodulin and Decorin to Separate Sites on Fibrillar Collagens. *J Biol Chem.* **268,** 27307-27312.

(166) Pringle, G.A. and Dodd, C.M. (1990) Immunoelectron Microscopic Localization of the Core Protein of Decorin Near the d and e Bands of Tendon Collagen Fibrils by Use of Monoclonal Antibodies. *J Histochem Cytochem.* **38,** 1405-1411.

(167) Rada, J.A., Cornuet, P.K. and Hassell, J.R. (1993) Regulation of Corneal Collagen Fibrillogenesis In Vitro by Corneal Proteoglycan (Lumican and Decorin) Core Proteins. *Exp Eye Res.* **56,** 635-648.

(168) Pellegata, N.S., Dieguez-Lucena, J.L., Joensuu, T., Lau, S., Montgomery, K.T., Krahe, R., Kivela, T., Kucherlapati, R., Forsius, H. and de la Chapelle, A. (2000) Mutations in KERA, encoding keratocan, cause cornea plana. *Nat Genet.* **25,** 91-95.

(169) Lehmann, O.J., El-Ashry, M.F., Ebenezer, N.D., Ocaka, L., Francis, P.J., Wilkie, S.E., Patel, R.J., Ficker, L., Jordan, T., Khaw, P.T. *et al.* (2001) A novel keratocan mutation causing autosomal recessive cornea plana. *Invest Ophthalmol Vis Sci.* **42,** 3118-3122.

(170) Bech-Hansen, N.T., Naylor, M.J., Maybaum, T.A., Sparkes, R.L., Koop, B., Birch, D.G., Bergen, A.A., Prinsen, C.F., Polomeno, R.C., Gal, A. *et al.* (2000) Mutations in NYX, encoding the leucine-rich proteoglycan nyctalopin, cause X-linked complete congenital stationary night blindness. *Nat Genet.* **26,** 319-323.

(171) Pusch, C.M., Zeitz, C., Brandau, O., Pesch, K., Achatz, H., Feil, S., Scharfe, C., Maurer, J., Jacobi, F.K., Pinckers, A. *et al.* (2000) The complete form of X-linked congenital stationary night blindness is caused by mutations in a gene encoding a leucine-rich repeat protein. *Nat Genet.* **26,** 324-327.

(172) Smith, W., Assink, J., Klein, R., Mitchell, P., Klaver, C.C., Klein, B.E., Hofman, A., Jensen, S., Wang, J.J. and de Jong, P.T. (2001) Risk factors for age-related macular degeneration: Pooled findings from three continents. *Ophthalmol.* **108,** 697-704.

(173) Mullins, R.F., Aptsiauri, N. and Hageman, G.S. (2000) Dendritic cells and proteins associated with immune-mediated processes are associated with drusen and may play a role in drusen biogenesis. *Invest Ophthalmol Vis Sci.* **41 Supplement,** S24.

(174) Mullins, R.F. and Hageman, G.S. (1999) Human ocular drusen possess novel core domains with a distinct carbohydrate composition. *J Histochem Cytochem.* **47,** 1533-1540.

(175) Langton, K.P., Barker, M.D. and McKie, N. (1998) Localization of the functional domains of human tissue inhibitor of metalloproteinases-3 and the effects of a Sorsby's fundus dystrophy mutation. *J Biol Chem.* **273,** 16778-16781.

(176) Cremers, F.P., van de Pol, D.J., van Kerkhoff, L.P., Wieringa, B. and Ropers, H.H. (1990) Cloning of a gene that is rearranged in patients with choroideraemia. *Nature.* **347,** 674-677.

(177) Gage, P.J. and Camper, S.A. (1997) Pituitary homeobox 2, a novel member of the bicoid-related family of homeobox genes, is a potential regulator of anterior structure formation. *Hum Mol Genet.* **6,** 457-464.

(178) Sambrook, J., Fritsch, E.F. and Maniatis, T. (1989) *Molecular cloning : a laboratory manual.* 2nd ed. Cold Spring Harbor Laboratory, Cold Spring Harbor, N.Y.

(179) Fischer, D. (2000) Hybrid fold recognition: Combining sequence derived properties with evolutionary information. *Pacific Symp. Biocomputing.* Hawaii, pp. 119-130.

(180) Wilson, R., Ainscough, R., Anderson, K., Baynes, C., Berks, M., Bonfield, J., Burton, J., Connell, M., Copsey, T., Cooper, J. *et al.* (1994) 2.2 Mb of contiguous nucleotide sequence from chromosome III of C. elegans. *Nature.* **368,** 32-38.

(181) Goffeau, A., Barrell, B.G., Bussey, H., Davis, R.W., Dujon, B., Feldmann, H., Galibert, F., Hoheisel, J.D., Jacq, C., Johnston, M. *et al.* (1996) Life with 6000 genes. *Science.* **274,** 546, 563-547.

(182) Philippsen, P., Kleine, K., Pohlmann, R., Dusterhoft, A., Hamberg, K., Hegemann, J.H., Obermaier, B., Urrestarazu, L.A., Aert, R., Albermann, K. *et al.* (1997) The nucleotide sequence of Saccharomyces cerevisiae chromosome XIV and its evolutionary implications. *Nature.* **387,** 93-98.

(183) Callis, J., Carpenter, T., Sun, C.W. and Vierstra, R.D. (1995) Structure and evolution of genes encoding polyubiquitin and ubiquitin-like proteins in Arabidopsis thaliana ecotype Columbia. *Genetics.* **139,** 921-939.

(184) Bohm, H., Benndorf, R., Gaestel, M., Gross, B., Nurnberg, P., Kraft, R., Otto, A. and Bielka, H. (1989) The growth-related protein P23 of the Ehrlich ascites tumor: translational control, cloning and primary structure. *Biochem Int.* **19,** 277-286.

(185) Sanchez, J.C., Schaller, D., Ravier, F., Golaz, O., Jaccoud, S., Belet, M., Wilkins, M.R., James, R., Deshusses, J. and Hochstrasser, D. (1997) Translationally controlled tumor protein: a protein identified in several nontumoral cells including erythrocytes. *Electrophoresis.* **18,** 150-155.

(186) MacDonald, S.M., Rafnar, T., Langdon, J. and Lichtenstein, L.M. (1995) Molecular identification of an IgE-dependent histamine-releasing factor. *Science.* **269,** 688-690.

(187) Hochstrasser, M. (1996) Ubiquitin-dependent protein degradation. *Annu Rev Genet.* **30,** 405-439.

(188) Kumar, S., Tomooka, Y. and Noda, M. (1992) Identification of a set of genes with developmentally down-regulated expression in the mouse brain. *Biochem Biophys Res Commun.* **185,** 1155-1161.

(189) Mizushima, N., Sugita, H., Yoshimori, T. and Ohsumi, Y. (1998) A new protein conjugation system in human. The counterpart of the yeast Apg12p conjugation system essential for autophagy. *J Biol Chem.* **273,** 33889-33892.

(190) Furukawa, K., Mizushima, N., Noda, T. and Ohsumi, Y. (2000) A protein conjugation system in yeast with homology to biosynthetic enzyme reaction of prokaryotes. *J Biol Chem.* **275,** 7462-7465.

(191) Okura, T., Gong, L., Kamitani, T., Wada, T., Okura, I., Wei, C.F., Chang, H.M. and Yeh, E.T. (1996) Protection against Fas/APO-1- and tumor necrosis factor-mediated cell death by a novel protein, sentrin. *J Immunol.* **157,** 4277-4281.

(192) Desterro, J.M., Rodriguez, M.S. and Hay, R.T. (1998) SUMO-1 modification of IkappaBalpha inhibits NF-kappaB activation. *Mol Cell.* **2,** 233-239.

(193) Shen, Z., Pardington-Purtymun, P.E., Comeaux, J.C., Moyzis, R.K. and Chen, D.J. (1996) UBL1, a human ubiquitin-like protein associating with human RAD51/RAD52 proteins. *Genomics.* **36,** 271-279.

(194) Boddy, M.N., Howe, K., Etkin, L.D., Solomon, E. and Freemont, P.S. (1996) PIC 1, a novel ubiquitin-like protein which interacts with the PML component of a multiprotein complex that is disrupted in acute promyelocytic leukaemia. *Oncogene.* **13,** 971-982.

(195) Chadwick, B.P., Kidd, T., Sgouros, J., Ish-Horowicz, D. and Frischauf, A.M. (1999) Cloning, mapping and expression of UBL3, a novel ubiquitin-like gene. *Gene.* **233,** 189-195.

(196) Martini, G., Toniolo, D., Vulliamy, T., Luzzatto, L., Dono, R., Viglietto, G., Paonessa, G., D'Urso, M. and Persico, M.G. (1986) Structural analysis of the X-linked gene encoding human glucose 6-phosphate dehydrogenase. *Embo J.* **5,** 1849-1855.

(197) Alcalay, M. and Toniolo, D. (1987) Two new genes of the G6PD cluster on the long arm of the X chromosome (Abstract). *Cytogenet Cell Genet.* **46,** 569.

(198) Yeh, E.T., Gong, L. and Kamitani, T. (2000) Ubiquitin-like proteins: new wines in new bottles. *Gene.* **248,** 1-14.

(199) Kamitani, T., Kito, K., Nguyen, H.P. and Yeh, E.T. (1997) Characterization of NEDD8, a developmentally down-regulated ubiquitin- like protein. *J Biol Chem.* **272,** 28557-28562.

(200) Kamitani, T., Nguyen, H.P. and Yeh, E.T. (1997) Preferential modification of nuclear proteins by a novel ubiquitin-like molecule. *J Biol Chem.* **272,** 14001-14004.

(201) Dittmar, G.A., Wilkinson, C.R., Jedrzejewski, P.T. and Finley, D. (2002) Role of a ubiquitin-like modification in polarized morphogenesis. *Science.* **295,** 2442-2446.

(202) Arikawa-Hirasawa, E., Wilcox, W.R., Le, A.H., Silverman, N., Govindraj, P., Hassell, J.R. and Yamada, Y. (2001) Dyssegmental dysplasia, Silverman-Handmaker type, is caused by functional null mutations of the perlecan gene. *Nat Genet.* **27,** 431-434.

Appendix A: Genetic Screen of Opticin in a French-Canadian Population

Portions of this appendix have been published in:

Friedman, J.S., Faucher, M., Hiscott, P., Biron, V.L., Malenfant, M., Turcotte, P., Raymond, V., and Walter, M.A. Protein Localization in the Human Eye and Genetic Screen of Opticin. (In press) Hum. Mol. Genet.

This work was predominantly performed and written by Mathieu Faucher and Dr. Vincent Raymond. The information within this appendix complements the work described in Chapter 2.

Materials and Methods:

Mutational Screening of OPTC:

This research has been approved by the Centre Hospitalier de l'Université Laval (CHUL) Research Center Ethics Committee. All participants, affected or not, signed an informed consent form before entering the study. A total of 197 individuals were clinically investigated. Clinical assessment comprised a complete ophthalmologic assessment including fluorescein angiography, when indicated.

Individuals recruited for the age-related macular degeneration (AMD) study were investigated at the CHUL or at the Clinique d'ophtalmologie de la Cité, both in Québec City, Canada. Diagnostic criteria for early AMD were: presence of large soft drusen and/or pigmentary abnormalities of the retinal pigment epithelium (RPE). Diagnostic criteria for advanced AMD were: photocoagulation or other treatment for choroidal neovascularization, geographic atrophy involving the center of the macula, nondrusenoid retinal pigment epithelial detachment, serous or hemorrhagic retinal detachment, hemorrhage under the retina or the RPE and/or subretinal fibrosis.

Individuals recruited for the familial and for the sporadic glaucoma studies were investigated by members of the Québec Glaucoma Network, comprising 103 ophthalmologists from different regions of the Province of Québec. Diagnostic criteria for primary open-angle glaucoma (POAG) were: intra-ocular pressures $\geq$ 22 mm Hg in

one or both eyes; characteristic optic disk damage and/or visual field impairment; grade III or IV (open-angle) gonioscopy; and exclusion of secondary causes (e.g. uveitis, steroid-induced glaucoma, trauma). Persons with intra-ocular pressures < 22mm Hg and with visual field impairment as well as characteristic optic disk damage were diagnosed as normal tension glaucoma (NTG). Fifty-five (55) other subjects selected at random had a complete normal ophthalmologic assessment and served as investigated normal individuals. Forty-eight (48) spouses of the individuals investigated in the glaucoma study were considered as randomly selected individuals from the general population.

The ages of the asymptomatic "normal" investigated individuals in this screen ranged from 43 to 83 years old, with one subject 43 years old, 14 subjects between 50-59, 29 subjects between 60-69, ten subjects between 70-79 and one subject 83 years in age. The mean age of the investigated group was 63.2 years. The average age of the 45 patients with only AMD was 72.3 years. All individuals examined in this study were ethnically matched Caucasians of French Canadian ancestry.

Polymerase Chain Reaction and DNA sequencing:

Genomic DNA was obtained from 28 ml of whole blood drawn by venipuncture in four 7 ml EDTA tubes. DNA was extracted using the Puregene DNA Isolation Protocol for Whole Blood. The *OPTC* gene was screened for mutations by amplifying the six coding exons using the polymerase chain reaction (PCR) before sequencing. The

amplicons used for sequencing were obtained by using six primer pairs, each amplifying one exon of the gene. I designed the primers and established the PCR conditions prior to the genetic screen. The primer pairs used are as follows:

Pair A: forward-5'-TCTCAGTCCCATCTGACTCC-3',

reverse-5'-AGGGAATGTAGTTGGTCTGC-3',

Pair B: forward-5'-CCAGAGTCCAAAGTTAAGTCC-3',

reverse-5'-CCTATGACCTAGGGATATTGC-3',

Pair C: forward-5'-CTCCCTTTGTTCTGTCTTCC-3',

reverse-5'-GTTGGTGACTGTCCTAGTGG-3',

Pair D:forward-5'-CTGGTTTCTCTCTTTGTTCTCC-3',

reverse-5'-TGGTGGAGGTGATAGATAGTGG-3',

Pair E: forward-5'-CAGCCTCCTACACTCTTTGC-3',

reverse-5'-GTTTATCACCCTTGCTCTGG-3',

Pair F: forward-5'-CAGCTGATGTGAGCCTTTGG-3',

reverse-5'-AGATGACCTGGGAGGAGTGG-3'.

The initial PCRs were performed on a Hybaid Omnigene Temperature Cycling System in a total volume of 50 µl containing 100 ng of genomic DNA, 20 pmol of each primer, 200 µM dNTPs, 50 mM KCl, 10 mM Tris (pH 9), 1.5 mM $MgCl_2$, 0,01% gelatin, 0.1%Triton X-100, and 1 U *Taq* polymerase (Invitrogen, Burlington, ON).

Amplifications were carried out using a "hot-start" procedure. *Taq* polymerase was added after a 5 minute denaturation step at 95°C. Samples were then processed through 35 cycles of denaturation (95°C for 30 seconds) and annealing (55-60°C for 30 seconds), followed by one last step of elongation (30 seconds at 72°C). PCR products were diluted in 5 volumes of Qiagen PB buffer, transferred on a Whatman GF/C filter plate, washed twice with a 80% ethanol 20 mM Tris pH 7.5 solution and eluted in 50 µl of water. Samples were quantified by the PicoGreen reagent protocol. A second PCR was performed on an Applied Biosystem Gene_Amp PCR System 9700 (96 wells) or 9700 Viper (384 wells) to incorporate the sequencing dyes using a protocol of 25 cycles of denaturation (95°C for 10 seconds) and annealing (55°C for 5 seconds), followed by one last step of elongation (2 minutes at 59°C). PCR products were then purified by the ABI ethanol-EDTA precipitation protocol, collected in a Beckman-Coulter Allegra 6R centrifuge and resuspended in a 50% HiDi-formamide solution. Samples were then run on an Applied Biosystems Prism 3700 DNA Analyser automated sequencer. Sequence data was analysed with the Staden pregGap4 and Gap4 programs.

AciI restriction enzyme test:

A cytosine to thymine transition was detected at base pair 685 of the *OPTC* coding sequence. This transition introduced an Arg229Cys missense variation and I determined that it destroyed an *AciI* restriction site. Screening for additional carriers of the Arg229Cys missense variation was thus performed in the Raymond laboratory using an *AciI* restriction enzyme test on the *OPTC* PCR-amplified fragment of exon 4. The wild type sequence of exon 4 contained three restriction fragments of 89, 93 and 99 base pairs, whereas the altered sequence contained one fragment of 99 bp and one fragment of 182 bp. PCR was conducted according to the conditions previously described for exon 4. The PCR products were purified in a QIAquick PCR Purification Kit spin column from Qiagen. In a total reaction volume of 20 μl, 10 μl of the purified PCR fragments were added to 7 μl of water, 1 μl (5 U/μl) of *AciI* (New England Biolabs, Mississauga, ON) and 2 μl of buffer NEB3 (100 mM NaCl, 50 mM Tris-HCl, 10mM $MgCl_2$, 1mM dithiothreitol). The reaction was incubated at 37°C for 2 hours after which digested DNA samples were separated by electrophoresis on a 2.5% agarose gel. Presence of the Arg229Cys alteration in a heterozygous or homozygous state was confirmed by automated sequencing of the amplified fragment.

Results:

The *OPTC* gene was screened for mutations in a total of 197 individuals. A schematic of the *OPTC* gene with the relative positions of PCR primer pairs used and base pair changes seen is shown in Figure A-1. Table A-1 summarizes the variations observed among the different groups examined.

Figure A-1: A Schematic of the Human Opticin Gene

Schematic diagram of the human *OPTC* gene. 5' and 3' untranslated regions are shaded. Coding regions of *OPTC* are in white boxes. Primers used in the mutational screen are as labeled and locations of sequence alterations are indicated by arrows. Start and stop codons are as indicated.

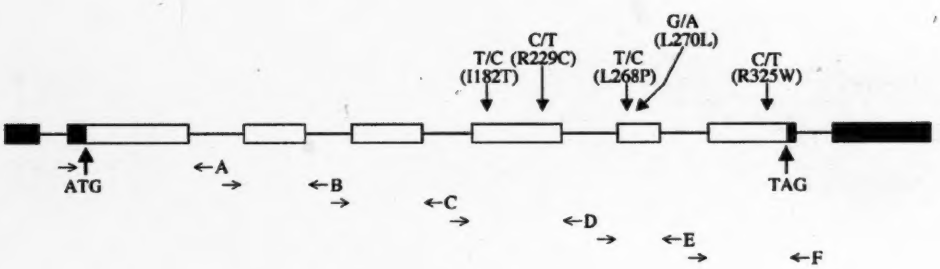
G/A
(L270L)
C/T
T/C (R229C)
(I182T)
T/C
(L268P)
C/T
(R325W)
ATG
TAG
A
B
C
D
E
F

Table A-1: Summary of opticin variations detected among various phenotypic groups.

Variations	Affected Population			Control Population
	Sporadic individuals with AMD[a] (n = 45)	Sporadic individuals with POAG or NTG affected by AMD[b] (n = 10)	Sporadic individuals with POAG or NTG[b] (n = 87)	Clinically investigated normal individuals[c,d] (n = 55)
amino acid alterations				
Ile182Thr	0	0	0	1
Arg229Cys	1[e]	0	0[f]	0
Leu268Pro	3	1	6	8
Arg325Trp	0	0	3	3
synonymous codon and non-coding changes				
Leu270Leu	0	0	0	2
C -> T, 3rd base of Intron 2	1	0	0	0

[a]Sporadic cases of age-related macular degeneration (AMD) recruited at the Centre Hospitalier de l'Université Laval (CHUL) and Clinique d'ophtalmologie de la Cité, Québec City.

[b]Sporadic cases of primary open-angle glaucoma (POAG) and normal tension glaucoma (NTG) recruited by the Québec Glaucoma Network.

[c]Investigated patients normal for glaucoma and AMD seen in the Clinique d'ophtalmologie de la Cité, Québec City.

[d]An additional 48, non-clinically investigated, spouses of glaucoma patients were sequenced. None had the Arg229Cys alteration.

[e]Homozygous variation.

[f]An additional 83 individuals, for a total of 170 sporadic individuals with glaucoma, were tested for this variation

Individuals affected by AMD and/or glaucoma were separated into three "affected" subgroups according to their phenotypes. The affected sporadic group comprised 45 individuals diagnosed with AMD, ten individuals with AMD plus primary open-angle glaucoma (POAG) or normal tension glaucoma (NTG), and 87 individuals with POAG or NTG alone. The control group consisted of 55 clinically investigated individuals asymptomatic for AMD or glaucoma.

A total of five coding and one non-coding sequence variations were found among all the participating subjects. Four of the five coding sequence variations resulted in amino acid change. These changes were Ile182Thr, Arg229Cys, Leu268Pro and Arg325Trp. Nonsynonymous coding changes are shown in a four species (human, dog, mouse and pig) amino acid alignment in Figure 2-9. Nonsynonymous amino acid alterations Ile182Thr, Arg229Cys, and Arg325Trp were at positions completely conserved among human, dog, mouse and pig. The Leu268Pro alteration was at a conserved residue in humans, pigs and mice. However, in canine the orthologous position is a proline. The Ile182Thr substitution and Leu270Leu synonymous codon variation were respectively identified in one and two clinically investigated normal subjects. The Leu268Pro variation was detected in four sporadic individuals with AMD and in six sporadic cases of POAG for a total frequency of 7.0% (10/142) among the affected phenotype groups. The same variation was identified in eight clinically investigated normal subjects for a total frequency of 14.5% (8/55) in the control population.

The Arg325Trp variation was detected in three sporadic individuals with POAG but not in individuals from the other two affected groups. This same variation was detected in three investigated normal subjects. Frequency for the Arg325Trp substitution among sporadic individuals with NTG or POAG was 3.4% (3/87), similar to the 5.5% (3/55) seen in the control population. A variation in the non-coding sequence near an exon-intron junction, causing a cytosine to thymine change at the third base of intron 2, was detected in a sporadic individual affected by AMD. As the orthologous position of Leu268 in canine is proline, it is likely that the Leu268Pro alteration is a polymorphism. Although the Ile182Thr and Arg325Trp alterations were at amino acid positions that were conserved in human, mouse, dog, and pig, there is no current evidence that they are associated with AMD.

Interestingly, the Arg229Cys variation, observed in one of the sporadic patients affected by AMD, was detected as a homozygous change. This individual, BN007, was diagnosed at age 71 with advanced macular degeneration with choroidal neovascularization in his left eye (exudative AMD). The right eye, however, only displayed some rare drusen. Since the Arg229Cys variation was not present in any other subjects from the initial mutational screen, additional individuals were tested for this variation. One group of 83 unrelated individuals with POAG and a second cohort of 48 non-clinically investigated spouses from glaucoma families were tested. None of these individuals harbored the Arg229Cys variation. The close relatives of individual BN007

were recruited to test for co-segregation of the variant with AMD (Figure A-2). Six siblings were investigated and the *OPTC* gene was screened for mutations (Table A-2,A-3). The Arg229Cys change was found in two siblings, BN003 and BN009, in a heterozygous state. BN003 and BN009 both have normal retinas and optic disks at ages 78 and 68 respectively. On the other hand, two other family members (BN004, BN008) harboring the wild-type arginine at position 229 on both opticin alleles, were diagnosed with ocular diseases. One member, BN004, was affected by foveomacular dystrophy while her sister, BN008, was diagnosed with early AMD. Neither sibling displayed as severe a form of retinal disease as the BN007 proband.

Figure A-2: Pedigree of the BN Family Affected with Foveomacular Dystrophy and AMD

Pedigree of the BN family affected with foveomacular dystrophy and AMD. Circles and squares represent females and males, respectively. Diagonal lines indicate deceased individuals. The disease status of each individual is as labeled. The age of each patient at the time of study is indicated below each symbol. Numbers in parenthesis depict age at diagnosis. Individual BN007 has the homozygous opticin Arg229Cys variation.

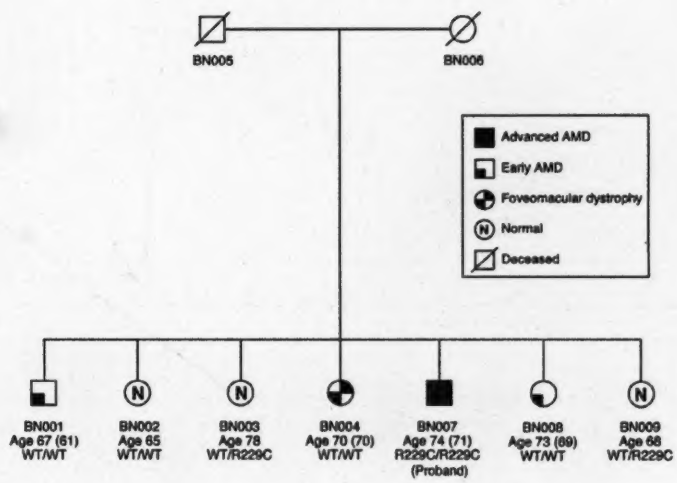
BN005
BN006
Advanced AMD
Early AMD
Foveomacular dystrophy
N Normal
Deceased
BN001
Age 67 (61)
WT/WT
BN002
Age 65
WT/WT
BN003
Age 78
WT/R229C
BN004
Age 70 (70)
WT/WT
BN007
Age 74 (71)
R229C/R229C
(Proband)
BN008
Age 73 (69)
WT/WT
BN009
Age 68
WT/R229C

Table A-2: Genotype/phenotype correlation for opticin Arg229Cys in an AMD-affected family

Individuals	Sex	Opticin Arg229Cys status	Diagnosis	Age at diagnosis	Visual acuity (OD,OS)[a]	Other ocular findings
BN001	M	WT[b]/WT	Early AMD	61	6/7.5-3, 6/9+1	IOPs[c]: 18/18 Small cataract OU
BN002	F	WT/WT	Normal	65	6/7.5, 6/7.5	IOPs: 12/12
BN003	F	WT/R229C	Normal	78	6/9, 6/6	IOPs: 16/16 Small cataract OU
BN004	F	WT/WT	Foveomacular dystrophy	70	6/9+2, 6/7.5	IOPs: 15/15 Small cataract OU
BN007 (proband)	M	R229C/R229C	Advanced AMD	71	6/9, 6/60	IOPs: 14/14 Small cataract OU
BN008	F	WT/WT	Early AMD	69	6/7.5, 6/7.5-1	IOPs: 17/18 Retinal naevus OD Iridotomy OU Small cataract OU
BN009	F	WT/R229C	Normal	68	6/9, 6/7.5	IOPs: 16/15

[a]OD: right eye, OS: left eye, OU: both eyes.
[b]WT: Wild-type
[c]IOP: intra-ocular pressure (in mmHg)

Table A-3: Genotype/phenotype correlation for opticin Arg229Cys in an AMD-affected family con't.

Individuals	Description of diagnosis
BN001	OD: Normal fundus OS: Light RPE detachment, calcified drusen
BN002	OU: Normal fundus
BN003	OU: Normal fundus
BN004	OD: Photo: macular RPE changes and small hard drusen Angiography: fine RPE window defects at macula OS: Photo: zone of hypopigmentation surrounding a zone of foveola hyperpigmentation and small hard drusen Angiography: central zone of blocked choroidal fluroescence secondary to hyperpigmentation, surrounded by a zone of hyperfluorescence
BN007 (proband)	OD: Rare drusen OS: Angiography: choroidal neovascularization with mixture of occult and classic components
BN008	OU: Drusen OS: RPE changes
BN009	OU: Normal fundus

[a]OD: right eye, OS: left eye, OU: both eyes.
[b]WT: Wild-type
[c]IOP: intra-ocular pressure (in mmHg)

Discussion:

The genetic screen results suggested that opticin my have a modifying effect on AMD in this family. However, a statistical analysis of this data demonstrated that the Arg229Cys alteration was not statistically significant (see Chapter II). I examined the data collected by our collaborators and determined using Fisher's exact test that we would require over 860 individuals to achieve a significant result. However, without additional AMD patients showing opticin mutations, there remains the possibility that the Arg229Cys change is a rare variant within the French Canadian population. If this were the case, it would simply be through coincidence that the neovascular AMD affected patient also contained the homozygous variation.

Our current data hint that opticin may be a modifier of AMD. I performed a preliminary biochemical analysis on an Arg229Cys opticin variant protein, but the results were not conclusive (see Chapter II). Without additional patients, one other way to examine the effect of the Arg229Cys change would be after opticin's function was elucidated. An additional approach may be used after an opticin interacting protein was discovered. One might ask if any interaction was affected by the Arg229Cys alteration. These experiments, however, will have to be performed at a later date.

Curriculum Vitae:

Education:

Degree:	Institution:	Department:	Supervisor:	Start and End Date:	
B.Sc.(Hon)	University of Alberta	Genetics	N/A	09/1991	04/1995
M.Sc.	University of Alberta	Ophthalmology	Dr. M.A. Walter	09/1996	05/1999
(Mr. Friedman transferred from a M.Sc. to a Ph.D. program in May 1999.)					
Ph.D.	University of Alberta	Ophthalmology	Dr. M.A. Walter	05/1999	06/2002

Training:

Institution:	Department and Position:	Supervisor:	Start and End Date:	
University of Alberta	Ophthalmology Graduate Student	Dr. Michael Walter	09/1996	06/2002
University of Alberta	Ophthalmology Summer Student	Dr. Michael Walter	05/1996	08/1996
University of Alberta	Ophthalmology Volunteer	Dr. Michael Walter	09/1995	04/1996
University of Alberta	Molec. Oncology Research Project	Dr. Roseline Godbout	09/1994	12/1994
University of Alberta	Molec. Oncology Summer Student	Dr. Roseline Godbout	05/1994	08/1994
University of Alberta	Genetics Summer Student	Dr. Allen Good	05/1993	08/1993
University of Alberta	Genetics Lab Assist.	Dr. Allen Good	09/1992	11/1992
University of Alberta	Med.Micro.And Infect.Dis. Summer Student	Dr. Glen Armstrong	05/1992	08/1992

Awards:

Type:	Awarding Organization:	Year Awarded:
Andrew Stewart Memorial Grad. Prize	University of Alberta	2002
Doctoral Research Award	E.A.Baker Foundation/CIHR	2001
Alcon Research and Education Award	Capital Health Authority	2001
Grant-in-Aid of Research	Sigma Xi	2000
Medical Sciences Graduate Award	University of Alberta	2000
Poster Award	Gordon Research Conference on Proteoglycans	2000
Studentship-75th Anniv. Faculty of Medicine Graduate Student Award	University of Alberta	1997
Travel Award- J. Gordin Kaplan Graduate Student Award	University of Alberta	1997
Studentship-75th Anniv. Faculty of Medicine Graduate Student Award	University of Alberta	1996
Alberta Cancer Board Summer Studentship	Alberta Cancer Board	1994
NSERC Undergraduate Student Res. Award	NSERC	1993
University of Alberta Matriculation Award	University of Alberta	1992

Students Trained:

Name:	Position:	Start and End Date:
Low, Aaron	Summer Student	05/2001 08/2001
Sharp, Michael	4th Year Project Student/Summer Student	09/1999 08/2000
Giordano, Jennifer	Summer Student	05/1999 08/1999
Ray. Kristy	4th Year Project Student	09/1998 04/1999
Ducharme, Ron	Summer Student	05/1998 08/1998

Refereed Publications:

1) Tucker, J.E., Winkfein, R.J., Murthy, S.K., Friedman, J.S., Walter, M.A., Demetrick, D.J., and Schnetkamp, P.P.M. Chromosomal Localization and Genomic Organization of the Human Retinal Rod Na-Ca+K Exchanger. (1998) Hum. Genet. 103:411-414.

2) Friedman, J.S., Ducharme, R., Raymond, V., Walter, M.A. Isolation of a Novel Iris-Specific and Leucine-Rich Repeat Protein (Oculoglycan) Using Differential Selection. (2000) Invest. Ophthal. Vis. Sci. 41(8): 2059-2066.

3) Friedman, J.S., Koop, B., Raymond, V. and Walter, M.A. Isolation of a Ubiquitin-Like (UBL5) Gene from a Screen Identifying Highly Expressed and Conserved Iris Genes. (2001) Genomics Jan 15;71(2): 252-5.

4) Friedman, J.S., Faucher, M., Hiscott, P., Biron, V.L., Malenfant, M., Turcotte, P., Raymond, V. and Walter, M.A. Protein Localization in the Human Eye and Genetic Screen of Opticin. (2002) Hum Mol Genet. 11(11): 1333-1342.

Publications: Chapters/Reviews

1) Friedman, J.S. and Walter, M.A. Glaucoma Genetics, Present and Future. (1999) Clinical Genetics 55:71-79.

2) Friedman, J.S. and Walter, M.A. Use of Radiation Hybrid Panels to Map Genetic Loci. (2001) Molecular Biotechnology 19(2):205-10.

3) Friedman, J.S. and Walter, M.A. Biomedicine: Under Pressure. (2002) Science Feb 8;295(5557):983-4.

Publications: Abstracts

1) Hickey, K., Mirzayans, F., Friedman, J.S., Kulak, S., Pearce, W.G. and Walter, M.A. Progress towards cloning the Axenfeld-Rieger Syndrome gene. Can J Ophthalmol 31 (2): P-6.1996.

2) Friedman, J.S., Raymond, V., and Walter, M.A. Identification of Uniquely of Highly Expressed Genes in the Iris and Trabecular Meshwork: Candidates for Glaucoma. Am J Hum Genet 61 (suppl.): A234 No. 4 Oct 1997.

3) Friedman, J.S., Raymond, V., and Walter, M.A. Identification of Uniquely of Highly Expressed Genes in the Iris and Trabecular Meshwork: Candidates for Glaucoma. Research Revelations, Edmonton, Alberta, Canada. 1998.

4) Friedman, J.S., Raymond, V., and Walter, M.A. Characterization of Genes Highly or Uniquely Expressed in the Iris or Trabecular Meshwork: Candidates for Glaucoma. Candian Genetic Disease Network, Annual Meeting. Montreal, Quebec, Canada. 1998.

5) Friedman, J.S., Raymond, V., and Walter, M.A. Characterization of Genes Highly or Uniquely Expressed in the Iris or Trabecular Meshwork: Candidates for Glaucoma. Can. Fed. Biol. Sci. Annual Meeting. Edmonton, Alberta, Canada. 1998.

6) Friedman, J.S., Raymond, V., and Walter, M.A. Towards Characterization of Genes Highly or Uniquely Expressed in the Iris or Trabecular Meshwork. Am J Hum Genet 63 (suppl.): A249. 1998.

7) Friedman, J.S., Raymond, V., and Walter, M.A. Characterization of a Gene Highly Expressed in the Iris. Candian Genetic Disease Network, Annual Meeting. Toronto, Ontario, Canada. 1999.

8) Friedman, J.S., Koop, B., Raymond, V. and Walter, M.A. Isolation of a Novel Human Homologue to Ubiquitin-like Protein (HHULP) Gene from a Screen Identifying Highly Expressed and Conserved Iris Genes. Canadian Genetic Disease Network, Annual Meeting. Vancouver, British Columbia, Canada. 2000.

Publications: Abstracts con't

9) Friedman, J.S., Koop, B., Raymond, V. and Walter, M.A. Isolation of a Novel Human Homologue to Ubiquitin-like Protein (HHULP) Gene from a Screen Identifying Highly Expressed and Conserved Iris Genes. Human Genome Meeting 2000. Vancouver, British Columbia, Canada. #316. 2000.

10) Friedman, J.S., Ducharme, R., Raymond, V., Walter, M.A. Isolation of a Novel Iris Specific and Leucine-Rich Repeat Protein, "Oculoglycan", Using Differential Selection. Gordon Research Conference on Proteoglycans. Andover, New Hampshire, U.S.A. 2000.

11) Friedman, J.S., Biron, V.L., Raymond, V., Walter, M.A. Further Characterization of the Leucine-Rich Repeat Protein Oculoglycan/Opticin. Invest Ophthal Vis Sci Vol. 42(4): S770 #4125. 2001.

12) Sharp, M.W., Friedman J.S., Raymond, V. and Walter, M.A. Creation of Human Eye cDNA Libraries for Differential Screening and Yeast Two-Hybrid Analysis. (Submitted)